Physiological, morphological and molecular acclimation of *Populus* spp. to high salinity

Dissertation

to attain the degree Doctor of Philosophy (Ph. D.)

of the Faculty of Forest Sciences and Forest Ecology

Georg-August-Universität Göttingen

Submitted by

Shayla Sharmin

born on the 31.05.1988

in Chandpur, Bangladesh

Göttingen, December 2021

Table of contents

Page

List of Abbreviations

ABA	Abscisic acid
ADP	Adenosine diphosphate
ANOVA	Analysis of variance
ATP	Adenosine triphosphate
Bq	Becquerel
CAM	Calmodulin
CBL	Calcineurin B-like
cDNA	Complementary DNA
CDPK	Calcium-dependent protein kinase
CesA	Cellulose synthase
CIPK	CBL-interacting protein kinase
cm	Centimeter
CML	Calmodulin-like
CPM	Counts per minute
Csl	Cellulose synthase-like
CTAB	Hexadecyltrimethylammonium bromide
DA-KORC	Depolarization activated outward-rectifying potassium (K) channel
DA-NSCC	Depolarization activated non-selective cation channel
DEG	Differentially expressed gene
Df	Degrees of freedom
DM	Dry mass
DNA	Deoxyribonucleic acid
dS	Deci Siemens
EC	Electrical conductivity
ECe	Electrical conductivity of the saturation extract
EDXA	Energy dispersive X-ray analysis

EXL	Expansin-like
EXP	Expansin
FLA	Fasciclin-like arabinogalactan
FM	Fresh mass
g	Gram
GLR	Glutamate receptor
GlyT	Glycosyltransferase
GO	Gene ontology
GUS	β-Glucuronidase
HA	Proton (H^+) pumping ATPase
HAK	High-affinity potassium (K) transporter
HKT	High-affinity potassium (K) transporter
HSD	Honestly significant difference
ICP-OES	Inductively coupled plasma-optical emission spectrometry
KEA	Potassium (K) efflux antiporter
KUP	Potassium (K) uptake permease
kV	Kilovolt
L	Liter
LA	Long-Ashton
mg	Milligram
ml	Milliliter
mM	Millimolar
mm	Millimeter
MS	Mean squares
NADPH oxidase	Nicotinamide adenine dinucleotide phosphate oxidase
NhaD	Na^+/H^+ antiporter
NHX	Na^+/H^+ exchanger
P.	*Populus*

PAR	Photosynthetically active radiation
PHT	Phosphate transporter
PME	Pectin methylesterase
RBOH	Respiratory burst oxidase homolog
RNA	Ribonucleic acid
ROS	Reactive oxygen species
SE	Standard error
SEM	Scanning electron microscope
SKOR	Stelar potassium outward rectifier
SOD	Superoxide dismutase
SOS	Salt overly sensitive
SoS	Sum of squares
TEM	Transmission electron microscope
TG	Transgenic
TPK	Two-pore potassium (K) channel
VHA	Vacuolar proton (H^+) pumping ATPase
VI-NSCC	Voltage independent non-selective cation channel
WT	Wild-type
XTH	Xyloglucan endotransglucosylase/hydrolase

Abstract

Salinization of terrestrial land is a global environmental problem, causing loss in soil fertility. Cultivation of salt tolerant species counteracts soil degradation and ensures productive utilization of salt-affected lands. But the tolerance mechanisms of salt-tolerant plants are not entirely understood. Salt tolerance of a plant involves several adaptations at the physiological, morphological and molecular levels. Morphological adaptation via increased tissue thickness and succulence is one of the strategies followed by halophytes (salt tolerant plant) under salinity. Succulent tissues possess larger cell with higher water content. However, little is known about morphological acclimation processes to high salinity in non-halophytic plants such as the salt-tolerant *Populus euphratica*.

Under salinity, the gradual buildup of salt ions in the plant cells causes toxicity and leads the plant to death. In addition, salt ions can greatly affect the uptake and supply of macronutrients like potassium, calcium and magnesium. However, it is not completely known how the root to shoot translocation of macronutrients is affected by sodium under salinity. In addition, it would be interesting to check whether the reduction in translocation processes can reduce salt accumulation in leaves under salinity or not.

In this thesis, I studied the acclimation and tolerance mechanisms in a salt-tolerant, *P. euphratica* and in a salt-susceptible poplar species, *Populus x canescens.* I addressed the following goals: (i) to characterize root morphology and plant gas exchange under salinity and describe the underlying molecular regulation, (ii) to investigate whether root thickening under salinity contributes to enhanced salt tolerance of *P. euphratica*, and (iii) to dissect the influence of the transpirational pull and salinity on the distribution of nutrients in the plant.

To characterize the root morphology of *P. euphratica* under high salinity, I adapted the plants to increased salinity by gradually increasing NaCl concentrations from 50 mM to 150 mM and investigated the changes in root morphology after short- (2 days) and long-term (12 days) high salt (150 mM NaCl) exposure. Gas exchange was measured during the salt exposure period in salt-stressed plants and controls (grown without NaCl) to observe responses of plant under salinity. The molecular regulation induced by short- and long-term salt exposure was studied by transcriptome analysis of roots and leaves. To investigate the impact of auxin in root morphology

under salinity, transgenic *P. euphratica* plants transformed with auxin-inducible promoter reporter GH3::GUS construct were used. With increasing NaCl concentration in the medium from 50 mM to 150 mM, gas exchange significantly declined in stressed plants. However, the stressed plants showed an improved CO_2 assimilation rate after 11 days of exposure to 150 mM NaCl by consuming sub-stomatal CO_2 more efficiently. After long-term salt exposure, main roots showed two-times and lateral roots 1.5 times greater diameters than control roots. Longitudinal sections revealed that an increased number of cortex cells was responsible for the increased thickness of main roots under stress. The dry-to-fresh mass ratio in long-term stressed main and lateral roots did not differ from controls indicating no changes in water content in thick roots compared to control thin roots. In contrast, increased dry-to-fresh mass ratio in leaves after short- and long-term salt exposure suggested that water content decreased in leaves under salinity. Na content increased significantly in main roots and leaves, but not in lateral roots, after long-term salt exposure. Among macronutrients, K and Ca decreased significantly in main and lateral roots under salinity, but nutrient levels were maintained in the leaves. The transgenic plants containing GH3::GUS construct did not show strong noticeable changes in the GUS staining in main and lateral roots after long-term salt exposure. This observation suggested that auxin has no apparent role in the alterations of root morphology under salinity. The salt-induced changes in the regulation of genes for cell wall organization and biogenesis were studied by transcriptome analyses. Pectin methylesterase, expansin, expansin-like, cellulose synthase, cellulose synthase-like, xyloglucan endotransglucosylase/hydrolase, fasciclin-like arabinogalactan, MYB and NAC-type transcription factors were the most abundant differentially expressed gene families. The salt-induced regulation of cell wall associated genes was less affected in leaves than in roots suggesting no stimulation for alteration in leaf morphology. The upregulation of genes involved in the synthesis of cell wall polysaccharides and cell wall extension in the main roots after short-term salt exposure indicated that the reactions to modify cell wall were activated. However, most of these genes were downregulated in thick main roots after long-term salt exposure. The increase in lateral root thickness was likely a result of up- and down-regulation of these cell wall associated genes at both times. Therefore, this study shows that *P. euphratica* adjusted root morphology by increasing root diameter under high salinity. Increased root thickness in response

to salinity was likely induced by salt accumulation in the tissue and regulated by cell wall modifying genes to manage ion toxicity through increased volume for salt deposition.

To investigate the second goal, I studied the contribution of physiological root plasticity of *P. euphratica* to cope with saline conditions and explored the underlying transcriptional regulation. To distinguish between Na^+ present in roots and newly taken up Na^+, $^{22}Na^+$ was used as a tracer. Both Na^+ uptake from and extrusion into the external solution was strongly reduced in salt-acclimated thick roots compared with non-acclimated thin roots. Transcriptome analyses showed high expression of genes required for the control of Na^+ levels (Na^+/H^+ antiporters: *SOS1*, *NHX*, *NhaD* and *ATP*ases) in both salt-acclimated and non-acclimated roots. Significant increases in transcript abundances were found initially (after 2 days of 150 mM NaCl application) for two *NHX* family members and many genes with potential functions in Ca^{2+} signaling. But these responses disappeared in thick, salt-acclimated roots and the majority of differentially expressed genes related to Ca^{2+} signaling were downregulated. Transcriptional upregulation was observed for stress signaling via NADPH oxidases, irrespective of short- or long-term salt exposure. Thick roots showed higher K^+ retention under salt stress than thin roots, presumably as the result of transcriptional downregulation of K^+ transporters and non-selective cation channels. Thick roots contained elevated P concentrations, which corresponded to enhanced transcript levels of P transporters. In conclusion, acclimated thick roots have a high ability to control Na^+ levels without additional transcriptional activation of the SOS pathway. They are relatively resistant toward changes in salt levels and maintain a favorable nutrient balance.

Water flow through the xylem is driven by transpiration and this is thought to be the major driving force for the translocation process. To investigate the third goal, I used the salt-sensitive hybrid poplar, *Populus* × *canescens*. The phytohormone Abscisic acid (ABA) is known to regulate stomatal openings and consequently affects the transpiration rate. To differentiate between the effects of transpiration pull from those of salt, we compared salt-stressed, ABA treated, and combined salt- and ABA treated poplars (*P.* × *canescens*) with untreated controls. The root content of macronutrients like K^+, Ca^{2+} and Mg^{2+} was reduced in response to salinity. Decreased Ca^{2+} levels in roots corresponded to decreased Ca^{2+} levels in leaves. The same was observed for Mg^{2+} levels in roots and leaves. In contrast, K^+ levels in leaves increased under salt stress,

although root K^+ levels were reduced. However, reduced transpiration in response to salinity did not decrease Na^+ accumulation in the leaves. During ABA treatment, leaf Ca^{2+} and leaf Mg^{2+} levels decreased comparably to the salt treatment, while leaf K^+ level was unaffected, although stomatal conductance was reduced by salt or ABA treatment. Thus, these results suggest that Ca^{2+} and Mg^{2+} levels in leaves were predominantly affected by the transpirational pull, while loading and retention of K^+ in leaves are enhanced in response to salt stress, but independently of the transpirational pull.

In summary, the salt-tolerant poplar *P. euphratica* employs a morphological adaptation mechanism in response to high salinity by developing root thickening. Increased root thickness in *P. euphratica* is induced by salt. An increase in the number of cortex cells which leads to enlarged diameter of first order main roots in response to high salinity is likely a strategy to control ion toxicity via increasing the volume for salt deposition. Moreover, salt-induced thick roots contribute to the outstanding salt tolerance of *P. euphratica* by controlling Na^+ influx from and efflux into the outside environment as well as enhancing K^+ retention ability in response to high salinity. Besides, this species is able to maintain the levels of macronutrients K^+, Ca^{2+} and Mg^{2+} in the leaves, even though root contents of K^+ and Ca^{2+} is negatively affected due to salinity. The salt-induced thick roots might be an evolutionary adaptation of *P. euphratica* to salinity, which is associated with constant activation rather than over-expression of stress regulatory pathways. Thus, *P. euphratica* has an improved strategy to maintain a favourable nutrient balance, to control ion toxicity and to continue gas exchange efficiently under high salinity.

Zusammenfassung

Die Versalzung von Ackerland wird immer mehr zum Problem für den Anbau von land- und forstwirtschaftlich genutzten Pflanzen. Erhöhter Salzgehalt im Boden führt zu der Anreicherung toxischer Natrium Ionen im Zellinneren, was ultimativ zum Tod der Pflanze führen kann. Darüber hinaus behindert eine hohe intrazelluläre Natrium-Konzentration die Aufnahme anderer lebenswichtiger Makronährstoffe wie Kalium, Magnesium und Kalzium. Wie genau Natrium bei der Translokation dieser Nährstoffe aus den Wurzeln in den Spross interferiert ist jedoch noch nicht erforscht. Um Salztoleranz auszubilden sind diverse Anpassungen auf molekularer, physiologischer und anatomischer Ebene nötig. Von salztoleranten Pflanzen, auch Halophyten genannt, weiß man, dass sie sukkulente Gewebe ausbilden können. Die Zellen in solchen Geweben sind größer, wodurch das Zell-Lumen und damit der Wasseranteil in den Zellen erhöht wird um die Konzentration an schädlichem Natrium zu verdünnen. Neben den Halophyten, die auf salzige Standorte spezialisiert sind, gibt es auch andere Pflanzen, die erhöhten Salzkonzentrationen standhalten, wie z.B. *Populus euphratica*, die Euphrat Pappel. Warum *P. euphratica* jedoch verglichen mit anderen Pappel Arten eine höhere Salztoleranz zeigt, ist noch nicht verstanden.

In meiner Doktorarbeit habe ich untersucht, welche Mechanismen die salztolerante Pappel Art *Populus euphratica* verwendet um höhere Salzgehalte zu tolerieren und wie die nicht-salztolerante Art *Populus* x *canescens* auf erhöhte Salzkonzentrationen reagiert. Dabei habe ich das Augenmerk auf folgende Schwerpunkte gelegt: (i) Die spezielle Wurzelmorphologie von *P. euphratica* Wurzeln bei Salzexposition zu untersuchen und die molekularen Mechanismen für diese Anpassung zu identifizieren (ii) Zu analysieren, welche Rolle die verdickten Wurzeln von *P. euphratica* bei der Salztoleranz spielen (iii) Herauszufinden, welchen Einfluss der Transpirationssog auf die Translokation von Nährstoffen unter salinen Bedingungen hat.

Um die Wurzelmorphologie von *P. euphratica* bei hoher Salinität zu untersuchen, wurden Pflanzen schrittweise erhöhten NaCl Konzentrationen ausgesetzt. Dazu wurde die Salzkonzentration in der Nährlösung der Pflanzen in 24 h Schritten um je 50 mM NaCl erhöht bis die Zielkonzentration von 150 mM NaCl erreicht war. *P. euphratica* bildet nach etwa 5-6 Tagen bei 150 mM NaCl verdickte Haupt- und Seitenwurzeln. Um die Genese dieser Wurzeln zu

untersuchen wurden nach 2 Tagen bei 150 mM (vor der Verdickung) Proben zur Analyse der Wurzelmorpholgie, sowie zur Transkriptom Analyse genommen. Nach 12 Tagen (nach der Verdickung) wurden erneut Proben genommen. Während des Versuchszeitraums wurde auch kontinuierlich der Gaswechsel (Photosynthese Rate, Transpiration Rate), sowie die stomatäre Leitfähigkeit der Pflanzen bestimmt. Mit zunehmender Salzexposition schlossen die Pflanzen vermehrt ihre Stomata, was sich in verringerter stomatärer Leitfähigkeit und daraus resultierend verringerter CO_2 Assimilation und Transpiration widerspiegelte. Interessanterweise erholte sie die Photosyntheserate aber nach 11 Tagen bei 150 mM NaCl obwohl die stomatäre Leitfähigkeit auf konstant niedrigem Level blieb. Dies deutet darauf hin, dass die Pflanzen einen Weg gefunden haben, das verbleibende CO_2 in den Interzelluarräumen effektiver zu nutzen als zuvor. Die auffälligste Anpassung an Salinität sind die verdickten Wurzeln. Im Vergleich zu den Kontrollpflanzen war die Hauptwurzel salzexponierter Pflanzen doppelt so dick, die Seitenwurzeln 1,5 mal so dick. Die mikroskopische Betrachtung von Längsschnitten der Hauptwurzel zeigte, dass dieser Zuwachs auf eine erhöhte Anzahl an Cortex Zellen zurückzuführen war. Analyse der Trocken- zu Frischgewichtrate ergab keinen Unterschied zwischen den dicken Wurzeln der salzexponierten Pflanzen vergleichen mit den Kontrollen, was darauf schließen lässt, dass die Pflanzen kein zusätzliches Wasser in ihre Zellen eingelagert haben, wie es beispielsweise Halophyten machen. In Blättern hingegen war sogar eine Abnahme des Wassergehalts festzustellen. Lange Salzexposition resultierte in erhöhtem Natrium Gehalt in Hauptwurzeln und Blättern, jedoch nicht in Seitenwurzeln. Der Kalium- und Kalziumgehalt war in beiden Wurzeltypen deutlich reduziert, interessanterweise jedoch nicht in den Blättern. Neben Wildtyp Pflanzen wurden auch Pflanzen, die das Auxin-Reporterkonstrukt GH3:GUS exprimieren, untersucht um festzustellen, ob das Phytohormon Auxin bei der Salzanpassung der Wurzeln eine Rolle spielt. Hier wurden allerdings keine Unterschiede in der Auxinverteilung zwischen salzexponierten und Kontrollwurzeln festgestellt. Analyse der Transkriptionsdaten vor und nach Wurzelverdickung sollten Aufschluss darüber geben welche Gene an diesem morphologischen Akklimatisierungsprozess beteiligt sind. Dabei wurde der Fokus auf folgende Genfamilien gelegt: Pectin Methylesterasen, Expansine, Expansin-like Gene, Cellulose Synthasen, Cellulose Synthase-like Gene, Xyloglucan-Endotransglucosylasen/hydrolasen, Fasciclin-like arabinogalactan Gene,

MYB and NAC-Transcriptionsfaktoren. Zum ersten Zeitpunkt wurde eine erhöhte Transkription aller oben genannter Zellwandsythese Gene festgestellt, was sehr wahrscheinlich zu der erhöhten Bildung von Cortex-Zellen führt. Zum 12 Tage Zeitpunkt waren die Transkription der meisten dieser Gene wieder herunterreguliert, was darauf schließen lässt, dass die Anpassung auf transkriptioneller Ebene zu diesem Zeitpunkt abgeschlossen war. Dies deckt sich auch mit der Beobachtung, dass die Wurzeln sich bei längerer Salzexposition nicht kontinuierlich weiter verdicken. Bei den Seitenwurzeln war zu beiden Zeitpunkten erhöhte Transkription der oben genannten Gene zu beobachten, was darauf hindeutet, dass die Verdickung der Seitenwurzeln langsamer und über einen längeren Zeitraum stattfindet. Zusammenfassend lässt sich sagen, dass *P. euphratica* auf erhöhte Salzkonzentrationen mit einer Verdickung der Wurzeln reagiert, welche auf vermehrte Bildung von Cortex Zellen zurückzuführen ist. Dadurch ist es der Pflanze möglich das Natrium auf mehr Zellen zu verteilen und so die Toxizität zu senken. Das Signal für die Verdickung ist sehr wahrscheinlich eine erhöhte intrazelluläre Natrium Konzentration, die zu erhöhter Transkription von Zellwandsynthese-Genen führt.

Um zu analysieren, wie diese verdickten Wurzeln dazu beitragen, dass *P. euphratica* höhere Salzkonzentrationen als andere Pappeln tolerieren kann, wurde die Aufnahme und Abgabe von NaCl in dicken und dünnen Wurzeln untersucht. Der Einsatz von radioaktiv markiertem Natrium ($^{22}Na^+$) erlaubte es dabei zwischen neu aufgenommenem und bereits in der Pflanze vorhandenem Natrium zu unterscheiden. Verdickte Wurzeln haben deutlich weniger Natrium aufgenommen im Vergleich zu dünnen Wurzeln, die der gleichen Natriumkonzentration ausgesetzt wurden. Umgekehrt mussten dünne Wurzeln mehr Natrium ausschleusen, als das bei dicken Wurzeln der Fall war. Transkriptomanalysen zeigten, dass die Gene, die für die Kontrolle der intrazellulären Natriumkonzentration verantwortlich sind (Na^+/H^+ Antiporter: *NHX, NhaD und ATPasen*), bereits unter Kontrollbedingungen stark exprimiert sind, was darauf schließen lässt, dass die Pflanzen bereits vorangepasst sind an erhöhte Salzkonzentrationen in ihrer Umgebung. Nach kurzer Salzexposition (2 Tage bei 150 mM) werden zusätzlich zwei weitere *NHX* Gene stärker transkribiert sowie Gene, deren Genprodukte essentielle Aufgaben in der Kalzium-Signalübertragung haben. Hier ist insbesondere der SOS Signalweg zu nennen, welcher essentiell für die Regulation das Natrium Gehalts in der Zelle ist. Nach 12 Tagen Salzexposition ist die

Transkription dieser Gene jedoch wieder herunterreguliert, was den Schluss zulässt, dass Kalzium als Signalmolekül besonders in der frühen Anpassung an erhöhte Salzkonzentrationen wichtig ist. Darüber ist auch die Transkription von NADPH Oxidasen, die reaktive Sauerstoffspezies produzieren, die wiederum als Signalmoleküle wirken, über den gesamten Expositionszeitraum hochreguliert. Ein weiterer interessanter Punkt ist, dass dicke Wurzeln dazu in der Lage sind dem Verlust von Kalium Ionen entgegenzuwirken, was auf eine verringerte Expression von Kalium Transportern und nicht-selektiven Kation Kanälen zurückzuführen ist. Es wurde zudem ein erhöhter Phosphor Gehalt in dicken Wurzeln festgestellt. Die Ursache hierfür ist sehr wahrscheinlich eine erhöhte Transkription von Phosphor Transporter Genen im Vergleich zu dünnen Wurzeln. Diese Ergebnisse zeigen, dass *P. euphratica* bereits unter Kontrollbedingungen an das Auftreten höherer Salzkonzentrationen (bis 150 mM NaCl) angepasst ist. Bei Salzexposition sind dann nur noch kleinere Anpassungen im Transkriptom notwendig um den toxischen Effekt des Natriums abzumildern und eine gesunde Nährstoffbalance zu gewährleisten.

Der Transpirationsstrom durch das Xylem ist hauptverantwortlich für die Verteilung von Nährstoffen aus den Wurzeln in alle Bereich der Pflanze. Wie bereits zuvor gezeigt hat NaCl einen Einfluss auf die Verteilung von Nährstoffen in der Pflanze. Um zu analysieren welchen Einfluss einerseits das Salz, andererseits der Transpirationsstrom auf die Verteilung von Nährelementen hat, wurde die salz-sensitive Pappel Art *P.* x *canescens* entweder NaCl, ABA oder einer Kombination aus beiden Substanzen ausgesetzt. ABA ist das zentrale Trockenstress Hormon im pflanzlichen Stoffwechsel und bewirkt bei Ausschüttung das Schließen der Stomata und damit eine Verringerung des Transpirationsstroms. Während für K^+, Ca^{2+} und Mg^{2+} in Wurzeln als auch in Blättern sowohl unter Salz, als auch unter ABA Gabe, geringere Gehalte gemessen wurden verglichen mit dem Kontrollpflanzen, wurde in Blättern unter Salzexposition sogar ein höherer K^+ Gehalt gefunden, was unter ABA Gabe nicht der Fall war. Dies zeigt, dass die Translokation von Ca^{2+} und Mg^{2+} vornehmlich durch den Transpirationsstrom bewerkstelligt wird, während die Regulation des K^+ Gehalt bei Salzexposition in den Blättern weitestgehend unabhängig von diesem ist.

Zusammenfassend lässt sich feststellen, dass die salz-tolerante Spezies *P. euphratica* bei Salzexposition verdickte Wurzeln ausbildet, indem mehr Cortex-Zellen gebildet werden. Dadurch

wird das Gesamtzell-Lumen in der Wurzel erhöht um die Konzentration an Natrium Ionen in der Zelle zu senken. Dicke Wurzeln nehmen auch weniger Natrium auf als dünne Wurzeln, was ebenfalls zu einer geringen intrazellulären Natriumkonzentration beiträgt. Darüber hinaus kann P. euphratica den Kalium Gehalt in den Blättern aufrechterhalten, obwohl in Wurzeln weniger Kalium detektiert wurde als unter Kontrollbedingungen. Diese Anpassungen sind zurückzuführen auf eine konstant hohe Transkription der beteiligten Gene auch in Abwesenheit von NaCl. So ist die Pflanze dauerhaft auf die Erhöhung der Salzkonzentration an ihrem Standort vorbereitet, was ihr einen Vorteil gegenüber Spezies bringt, die unter Salzexposition erst ihre Anpassungsmechanismen aktivieren müssen.

1. General Introduction

1.1 World population and food demand

High temperatures, cold, scarcity of water and salinization of soils are the environmental factors that adversely affect the development and distribution of plants (Ahmad & Prasad, 2012; Khalid et al., 2019; Giordano et al., 2021). Any negative effect on plant growth eventually reduces crop yield production and threatens the supply of food and non-food products worldwide. The world's population was nearly 7.6 billion in the mid-2017 and is projected to reach 9.8 billion by the year 2050 (United Nations, Department of Economic and Social Affairs, Population Division, 2017). Therefore, the demand for food and non-food products is anticipated to increase immensely.

1.2 Soil salinity

Soil salinity is one of the most devastating abiotic stress factors which reduce the area of cultivated lands, degrade the fertility of soil and decrease the growth and productivity of plants (Metternicht & Zinck, 2003; Wicke et al., 2011; Munns & Gilliham, 2015; Sahab et al., 2021). Recent figures on the worldwide extent of saline soils do not available, however, various scientists reported different sizes based on different data sources (Shahid et al., 2018b). According to those reports, between 25% and 30% of irrigated lands are salt-affected and commercially unproductive (Shahid et al., 2018b; Sahab et al., 2021). On a global scale, salinization is causing loss of about 2000 ha arable land per day, contributing to losses of 1 to 2 % agricultural soil every year (Shahid et al., 2018a; Sahab et al., 2021). Therefore, reduction in land available for cultivation and increasing human population are throwing great challenges towards future food safety.

Soil salinity is a measure of all the soluble salts in soil water and is usually expressed as electrical conductivity (EC) or more precisely as the EC of the saturation extract (ECe). The electrical conductivity (EC) of a soil extract collected from a water saturated soil paste refers to the EC of the saturation extract (ECe) (US Salinity Laboratory, 1954; Munns & Tester, 2008; Shahid et al., 2018a). The major cations in salt-affected soils are: sodium (Na^+), calcium (Ca^{2+}), magnesium (Mg^{2+}), potassium (K^+) and the major anions are: chloride (Cl^-), sulfate (SO_4^{2-}), bicarbonate (HCO_3^-), carbonate (CO_3^{2-}), and nitrate (NO_3^-) (US Salinity Laboratory, 1954; Shahid et al., 2018a). The

US Salinity Laboratory (1954) classified the salt-affected soils and termed them as saline, saline-sodic and sodic soils depending on the major ions present in those soils. Saline soils have an ECe ≥ 4 dS m^{-1}, pH values that are usually less than 8.5, and exchangeable sodium percentage (ESP) < 15 (US Salinity Laboratory, 1954; Shahid et al., 2018a). Saline-sodic soils contain high soluble salts (ECe ≥ 4 dS m^{-1}), high ESP (≥ 15) and have pH values less or more than 8.5 (US Salinity Laboratory, 1954; Shahid et al., 2018a). Sodic soils show an ESP ≥ 15, an ECe < 4 dS m^{-1} and pH values generally more than 8.5 (US Salinity Laboratory, 1954; Shahid et al., 2018a).

When the ECe is 4 dS m^{-1} (approximately 40 mM NaCl) or more at 25 °C , this soil is defined as a saline soil (US Salinity Laboratory, 1954; Munns & Tester, 2008; Shahid et al., 2018a). At the ECe 4 to 8 dS m^{-1}, the yield of many crop plants is restricted, though many sensitive crops show yield reduction even at lower ECes (US Salinity Laboratory, 1954; Shahid et al., 2018a).

1.3 Causes of soil salinity

There are many causes of salinization of soils which include both natural and man-made reasons (Polle & Chen, 2015; C. Li et al., 2020). Naturally, salt accumulations in a region can occur due to weathering of rocks, intrusion of seawater, displacement of salts from coastal areas via wind, etc. (Shahid et al., 2018a; C. Li et al., 2020). In arid and semi-arid areas, when evapotranspiration exceeds precipitation, the salt transported deep soil layers to the land surface by water evaporation accumulates and increases the salinity since flushing of the accumulated salts is absent or weak (Polle & Chen, 2015; C. Li et al., 2020). When the drainage of a land is limited due to an impermeable layer, and when annual shallow-rooted crops are grown in the replacement of deep-rooted trees, then the water table of that land can rise and salinity can develop through the evaporation of soil water (Shahid et al., 2018a; Singh, 2018). The salinization of soil due to human activities such as irrigation leads to so-called secondary soil salinization (Polle & Chen, 2015; Shahid et al., 2018a). Irrigation water may reach the stock of minerals in the soil, dissolve the salts and transport them back to the surface by evapotranspiration (Polle & Chen, 2015; Shahid et al., 2018a; C. Li et al., 2020). Therefore, in water-scarce areas, the use of saline water, industrial saline wastewater, or treated sewage waste for irrigation purpose pose a significant

risk for salinization of soil (Shahid et al., 2018a; C. Li et al., 2020). Other human activities such as excessive use of fertilizers can also cause soil salinization (Shahid et al., 2018a).

1.4 Model tree family for research: *Populus*

The species of the genus *Populus*, collectively known as poplars, are fast-growing trees. The genus *Populus* consists of 30 to 35 tree species and they are widely distributed in the Northern Hemisphere from subtropical to boreal forests (Taylor, 2002; Müller et al., 2013; Wang et al., 2020). Poplars are widely cultivated as a source of many economic benefits such as wood, paper pulp and bioenergy, and also for environmental protection e.g. phytoremediation (Hamzeh & Dayanandan, 2004; Peuke & Rennenberg, 2006; Chen & Polle, 2010; Polle et al., 2013). In addition, the genome sequences of several poplar species are available (Tuskan et al., 2006; T. Ma et al., 2013; W. Yang et al., 2017; Z. Zhang et al., 2020). Therefore, *Populus* has become a model organism for basic research in trees.

1.5 Salt-tolerant poplar species: *Populus euphratica*

Populus euphratica is a salt-tolerant poplar species. In comparison with various other poplar species, *P. euphratica* was found to show enhanced tolerance to high salinity (Chen, Li, Fritz, et al., 2002; Chen, Li, Wang, et al., 2002; Chen et al., 2003; Sixto, 2005; Junghans et al., 2006). Being phreatophytic, *P. euphratica* needs access to water for survival in the desert environment and its deep rooting systems support to get access to ground water (Gries et al., 2003; Polle & Chen, 2015). *P. euphratica* is widely spread and can be found in Eurasia, China, Central Asia, Middle East and North Africa (Fig. 1.1) (Gries et al., 2003; Brosché et al., 2005; T. Ma et al., 2013; Polle & Chen, 2015). Some natural habitats of *P. euphratica* are found near water sources that contain up to 130 mM of total salt (Feng et al., 2001; Junghans et al., 2006). The reports on the genome sequence of *P. euphratica* and the genes associated with salt stress adaptation have established this species as an extraordinary natural resource for improving salt tolerance in trees (Ottow, Polle, et al., 2005; Wu et al., 2007; Ye et al., 2009; T. Ma et al., 2013; Y. Ma et al., 2015; Z. Zhang et al., 2020).

1.6 Salt tolerance mechanisms of *P. euphratica*

Salt tolerant plants show a range of adaptations in molecular, physiological, and morphological features to survive in saline environments. In response to high salinity, *P. euphratica* restricts net root uptake and transport of Na^+ to shoot, and shows considerably lower salt accumulation in leaves than other poplars (Chen, Li, Fritz, et al., 2002; Chen et al., 2003). *P. euphratica* is more efficient than salt-sensitive poplars to reduce leaf salt levels by blocking apoplastic ion transport, thus, limiting salt loading into the xylem and restricting subsequent axial transport (Chen, Li, Fritz, et al., 2002; Chen et al., 2003). Besides, *P. euphratica* controls the ion toxicity in cells by depositing salt in the apoplast and the vacuole (Chen, Li, Fritz, et al., 2002; Chen et al., 2003; Ottow, Brinker, et al., 2005; Chen et al., 2014).
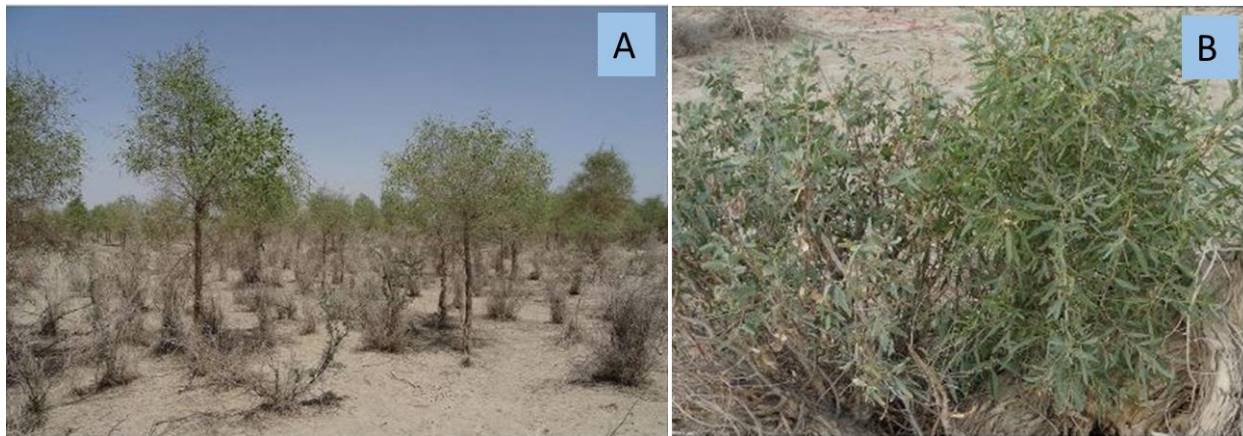
Figure 1.1: The photo of *P. euphratica* forest, located along the upper reaches of the Tarim River at the northern margin of the Tarim Basin of the Xinjiang Uygur Autonomous Region, China, showing juvenile forest (A) and small branches of a plant (B). (The figure and figure legend were obtained from Miao et al. 2020).

In addition, *P. euphratica* exhibits morphological adaptations in leaves in response to increasing high salt exposure by developing leaf succulence (Ottow, Brinker, et al., 2005). The morphological leaf plasticity contributes to the salt tolerance of this species (Ottow, Brinker, et al., 2005). However, adaptations in other tissues such as in the roots of *P. euphratica* in response to salinity are not well known and need to be studied.

Adaptation or tolerance to salt stress involves the regulation of the genes for the proteins which function in the processes of Na^+ uptake, Na^+ compartmentalization into vacuoles, and Na^+ extrusion out of the cell (Tester & Davenport, 2003; Munns & Tester, 2008; Deinlein et al., 2014; van Zelm et al., 2020). A salt stress signalling pathway to mediating K^+/Na^+ homeostasis in *P.*

euphratica cells under salinity was proposed (Chen & Polle, 2010; Polle & Chen, 2015). A schematic model for the stress signaling network in *P. euphratica* adapted from Chen & Polle (2010) and Polle & Chen (2015) is presented in Figure 1.2.
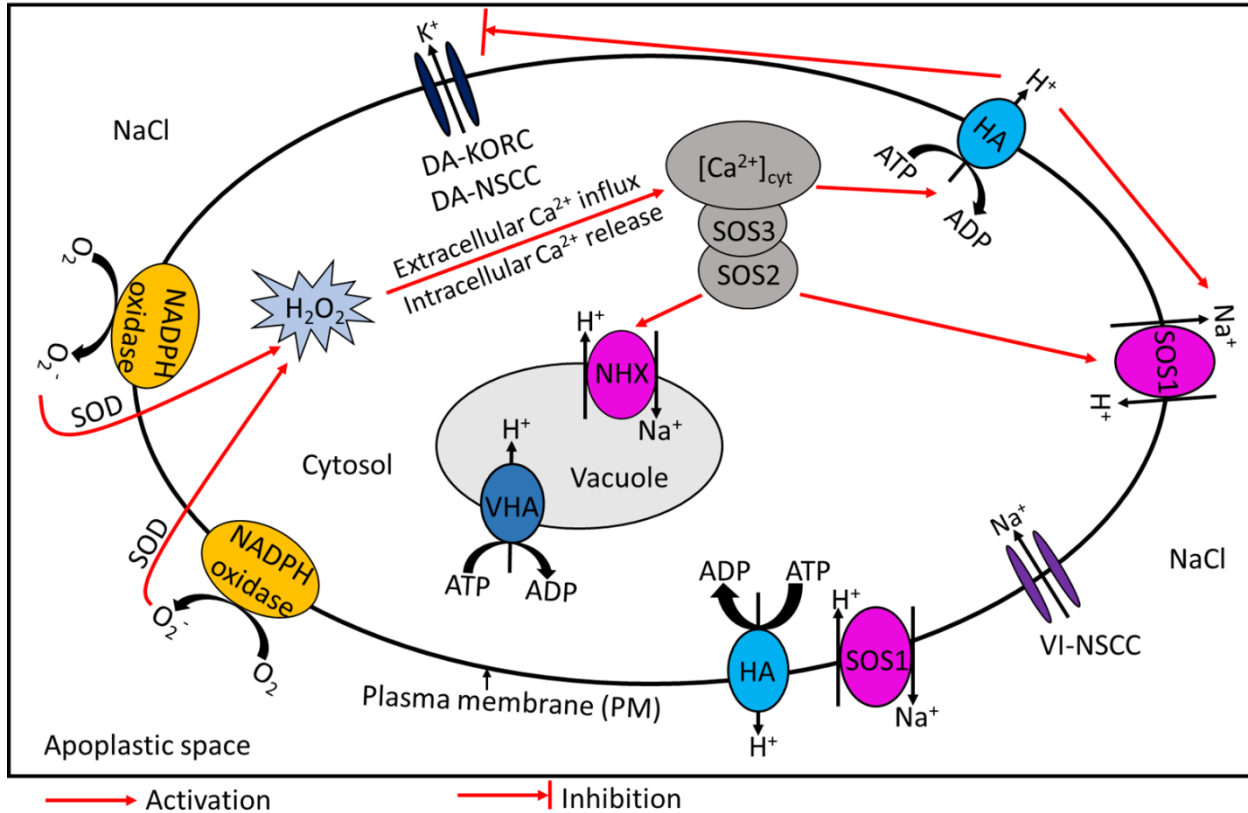
Figure 1.2: A schematic model showing the network of signaling of *P. euphratica* cells in the response to NaCl stress. In brief, NaCl salinity depolarizes the plasma membrane (PM), causing Na$^+$ entry into the cell and K$^+$ loss through depolarization-activated channels such as outward-rectifying K$^+$ channels (KORCs) and non-selective cation channels (NSCCs). The PM H$^+$-coupled ion transporters, for example, an H$^+$-ATPase (HA) and Na$^+$/H$^+$ antiporter (SOS1) sense the ion-specific effect of NaCl and trigger H$^+$ fluxes across the PM. Consequently, the pH at the apoplastic and cytosolic sides alters which activates PM NADPH oxidases and leads to H$_2$O$_2$ production. Superoxide produced by NADPH oxidases is converted to H$_2$O$_2$ by superoxide dismutases (SODs). Increased H$_2$O$_2$ levels stimulates Ca^{2+} entry and elevates cytosolic Ca^{2+} ([Ca^{2+}]$_{cyt}$) concentrations. Elevated [Ca^{2+}]$_{cyt}$ stimulates the PM Na$^+$/H$^+$ antiporters through the salt overly sensitive (SOS) signaling pathway where SOS3 senses the calcium signal and then interacts with SOS2, and finally activates SOS1. Moreover, H$_2$O$_2$ induces a Ca^{2+}-dependent increase in PM H$^+$-ATPase activity. The up-regulated H$^+$-pumps can sustain an H$^+$ gradient to drive the Na$^+$/H$^+$ antiport across the PM and preserve a less-depolarized membrane potential, restricting K$^+$ efflux through depolarization-activated KORCs and NSCCs. As a result, cellular K$^+$/Na$^+$ homeostasis is maintained in salt-stressed *P. euphratica* cells. (This figure was adapted and the figure legend was taken from Chen & Polle (2010) and Polle & Chen (2015)).

In *P. euphratica,* genes encoding putative Na^+/H^+ antiporters, i.e., *PeSOS1, PeNHX1–6,* and *PeNhaD1* have been characterized (Ottow, Polle, et al., 2005; Wu et al., 2007; Ye et al., 2009). Under salinity, increased plasma membrane (PM) H^+-ATPase activity, the driving force for PM Na^+/H^+ antiporters was observed in *P. euphratica* cells (F. Zhang et al., 2007; Y. Yang et al., 2007; X. Ma et al., 2010; Yao et al., 2020). *P. euphratica* induced salt stress signaling via H_2O_2 and $[Ca^{2+}]_{cyt}$ (F. Zhang et al., 2007; Sun et al., 2009; Sun, Li, et al., 2010; Sun, Wang, et al., 2010; Sun et al., 2012). In higher plants, several Ca^{2+} signal sensors i.e. calmodulin (CAM), calmodulin-like proteins (CMLs), calcineurin B-like proteins (CBLs) and calcium-dependent protein kinases (CDPKs) have been identified which function in signal transduction in response to various stimuli (Kudla et al., 1999; Cheng et al., 2002; Luan et al., 2002; McCormack et al., 2005). Some *P. euphratica* members of these Ca^{2+} sensor families have been characterized and were investigated for transcriptional responses under salinity, but information about other members is not available yet (H. Zhang et al., 2013; Lv et al., 2014; H. Zhang et al., 2008; D. Li et al., 2012; Wu et al., 2007). Moreover, the expression of genes forming the molecular network likely involved in salt signaling and ion homeostasis in *P. euphratica* cells under salinity needs to be studied.

1.7 Aim of this study

A better understanding of the mechanisms by which salt-tolerant species cope with high salinity is important for the improvement of the tolerance levels of economically important plants in salt-affected lands. In this thesis, I studied the adaptation mechanisms of *P. euphratica* and the salt susceptible species *Populus* x *canescens* in response to salinity.

In chapter 2, the adaptation of *P. euphratica* roots to enhanced salinity was investigated. The molecular actions likely responsible for morphological modifications were explored by anatomical and transcriptome analysis. The physiological performance and leaf transcriptomes were also investigated. The goal of this study was to characterize the morphological adaptations in *P. euphratica* roots and to investigate the molecular mechanisms regulating the adaptations.

In chapter 3, I investigated whether root morphological flexibility in *P. euphratica* plays a role in salt tolerance. Towards this goal, the uptake of Na^+ by morphologically modified roots under salinity and also a release of Na^+ from them were investigated using radioactive Na tracer. The

regulation of genes involved in ion homeostasis and salt signaling in the roots in response to salinity were studied.

In chapter 4, I experimented with phytohormone applications to improve the salt tolerance of a salt-susceptible poplar species, *P. × canescens.* The phytohormone abscisic acid (ABA) was applied to induce partial stomatal closure and thus to reduce transpiration. The aim was to investigate the effect of reduced transpiration on nutrient accumulation under salinity in comparison with ABA treatment. To differentiate between the effects of transpiration and those of salt, the contents of macronutrients were measured in salt-stressed, ABA treated, and combined salt- and ABA-treated plants and compared with untreated controls.

1.8 References

Ahmad, P., & Prasad, M. N. V. (Eds.). (2012). *Abiotic stress responses in plants*. Springer New York. https://doi.org/10.1007/978-1-4614-0634-1

Brosché, M., Vinocur, B., Alatalo, E. R., Lamminmäki, A., Teichmann, T., Ottow, E. A., Djilianov, D., Afif, D., Bogeat-Triboulot, M.-B., Altman, A., Polle, A., Dreyer, E., Rudd, S., Paulin, L., Auvinen, P., & Kangasjärvi, J. (2005). Gene expression and metabolite profiling of *Populus euphratica* growing in the Negev desert. *Genome Biology*, *6*(12), R101. https://doi.org/10.1186/gb-2005-6-12-r101

Chen, S., Diekmann, H., Janz, D., & Polle, A. (2014). Quantitative x-ray elemental imaging in plant materials at the subcellular level with a transmission electron microscope: Applications and limitations. *Materials*, *7*(4), 3160–3175. https://doi.org/10.3390/ma7043160

Chen, S., Li, J., Fritz, E., Wang, S., & Hüttermann, A. (2002). Sodium and chloride distribution in roots and transport in three poplar genotypes under increasing NaCl stress. *Forest Ecology and Management*, *168*(1–3), 217–230. https://doi.org/10.1016/S0378-1127(01)00743-5

Chen, S., Li, J., Wang, S., Fritz, E., Hüttermann, A., & Altman, A. (2003). Effects of NaCl on shoot growth, transpiration, ion compartmentation, and transport in regenerated plants of *Populus euphratica* and *Populus tomentosa*. *Canadian Journal of Forest Research*, *33*(6), 967–975. https://doi.org/10.1139/x03-066

Chen, S., Li, J., Wang, T., Wang, S., Polle, A., & Hüttermann, A. (2002). Osmotic stress and ion-specific effects on xylem abscisic acid and the relevance to salinity tolerance in poplar. *Journal of Plant Growth Regulation*, *21*(3), 224–233. https://doi.org/10.1007/s00344-002-1001-4

Chen, S., & Polle, A. (2010). Salinity tolerance of *Populus*. *Plant Biology*, *12*(2), 317–333. https://doi.org/10.1111/j.1438-8677.2009.00301.x

Cheng, S.-H., Willmann, M. R., Chen, H.-C., & Sheen, J. (2002). Calcium signaling through protein kinases. The Arabidopsis calcium-dependent protein kinase gene family. *Plant Physiology*, *129*(2), 469–485. https://doi.org/10.1104/pp.005645

Deinlein, U., Stephan, A. B., Horie, T., Luo, W., Xu, G., & Schroeder, J. I. (2014). Plant salt-tolerance mechanisms. *Trends in Plant Science*, *19*(6), 371–379. https://doi.org/10.1016/j.tplants.2014.02.001

Feng, Q., Endo, K. N., & Cheng, G. D. (2001). Towards sustainable development of the environmentally degraded arid rivers of China—A case study from Tarim River. *Environmental Geology*, *41*(1–2), 229–238. https://doi.org/10.1007/s002540100387

Giordano, M., Petropoulos, S. A., & Rouphael, Y. (2021). Response and defence mechanisms of vegetable crops against drought, heat and salinity stress. *Agriculture*, *11*(5), 463. https://doi.org/10.3390/agriculture11050463

Gries, D., Zeng, F., Foetzki, A., Arndt, S. K., Bruelheide, H., Thomas, F. M., Zhang, X., & Runge, M. (2003). Growth and water relations of *Tamarix ramosissima* and *Populus euphratica* on Taklamakan desert dunes in relation to depth to a permanent water table. *Plant, Cell & Environment*, *26*(5), 725–736. https://doi.org/10.1046/j.1365-3040.2003.01009.x

Hamzeh, M., & Dayanandan, S. (2004). Phylogeny of *Populus* (Salicaceae) based on nucleotide sequences of chloroplast *trnT-trnF* region and nuclear rDNA. *American Journal of Botany*, *91*(9), 1398–1408. https://doi.org/10.3732/ajb.91.9.1398

Junghans, U., Polle, A., Düchting, P., Weiler, E., Kuhlman, B., Gruber, F., & Teichmann, T. (2006). Adaptation to high salinity in poplar involves changes in xylem anatomy and auxin physiology. *Plant, Cell & Environment*, *29*(8), 1519–1531. https://doi.org/10.1111/j.1365-3040.2006.01529.x

Khalid, M. F., Hussain, S., Ahmad, S., Ejaz, S., Zakir, I., Ali, M. A., Ahmed, N., & Anjum, M. A. (2019). Impacts of abiotic stresses on growth and development of plants. In M. Hasanuzzaman, M. Fujita, H. Oku, & M. T. Islam (Eds.), *Plant Tolerance to Environmental Stress* (1st ed., pp. 1–8). CRC Press. https://doi.org/10.1201/9780203705315-1

Kudla, J., Xu, Q., Harter, K., Gruissem, W., & Luan, S. (1999). Genes for calcineurin B-like proteins in *Arabidopsis* are differentially regulated by stress signals. *Proceedings of the National Academy of Sciences*, *96*(8), 4718–4723. https://doi.org/10.1073/pnas.96.8.4718

Li, C., Gao, X., Li, S., & Bundschuh, J. (2020). A review of the distribution, sources, genesis, and environmental concerns of salinity in groundwater. *Environmental Science and Pollution Research*, *27*(33), 41157–41174. https://doi.org/10.1007/s11356-020-10354-6

Li, D., Song, S., Xia, X., & Yin, W. (2012). Two CBL genes from *Populus euphratica* confer multiple stress tolerance in transgenic triploid white poplar. *Plant Cell, Tissue and Organ Culture (PCTOC)*, *109*(3), 477–489. https://doi.org/10.1007/s11240-011-0112-7

Luan, S., Kudla, J., Rodriguez-Concepcion, M., Yalovsky, S., & Gruissem, W. (2002). Calmodulins and calcineurin B-like proteins: Calcium sensors for specific signal response coupling in plants. *The Plant Cell*, *14*(suppl 1), S389–S400. https://doi.org/10.1105/tpc.001115

Lv, F., Zhang, H., Xia, X., & Yin, W. (2014). Expression profiling and functional characterization of a CBL-interacting protein kinase gene from *Populus euphratica*. *Plant Cell Reports*, *33*(5), 807–818. https://doi.org/10.1007/s00299-013-1557-4

Ma, T., Wang, J., Zhou, G., Yue, Z., Hu, Q., Chen, Y., Liu, B., Qiu, Q., Wang, Z., Zhang, J., Wang, K., Jiang, D., Gou, C., Yu, L., Zhan, D., Zhou, R., Luo, W., Ma, H., Yang, Y., … Liu, J. (2013). Genomic insights into salt adaptation in a desert poplar. *Nature Communications*, *4*(1), 2797. https://doi.org/10.1038/ncomms3797

Ma, X., Deng, L., Li, J., Zhou, X., Li, N., Zhang, D., Lu, Y., Wang, R., Sun, J., Lu, C., Zheng, X., Fritz, E., Hüttermann, A., & Chen, S. (2010). Effect of NaCl on leaf H^+-ATPase and the relevance to salt tolerance in two contrasting poplar species. *Trees*, *24*(4), 597–607. https://doi.org/10.1007/s00468-010-0430-0

Ma, Y., Xu, T., Wan, D., Ma, T., Shi, S., Liu, J., & Hu, Q. (2015). The salinity tolerant poplar database (STPD): A comprehensive database for studying tree salt-tolerant adaption and poplar genomics. *BMC Genomics*, *16*(1), 205. https://doi.org/10.1186/s12864-015-1414-7

McCormack, E., Tsai, Y.-C., & Braam, J. (2005). Handling calcium signaling: *Arabidopsis* CaMs and CMLs. *Trends in Plant Science*, *10*(8), 383–389. https://doi.org/10.1016/j.tplants.2005.07.001

Metternicht, G. I., & Zinck, J. A. (2003). Remote sensing of soil salinity: Potentials and constraints. *Remote Sensing of Environment*, *85*(1), 1–20. https://doi.org/10.1016/S0034-4257(02)00188-8

Miao, N., Jiao, P., Tao, W., Li, M., Li, Z., Hu, B., & Moermond, T. C. (2020). Structural dynamics of *Populus euphratica* forests in different stages in the upper reaches of the Tarim River in China. *Scientific Reports*, *10*(1), 3196. https://doi.org/10.1038/s41598-020-60139-7

Müller, A., Volmer, K., Mishra-Knyrim, M., & Polle, A. (2013). Growing poplars for research with and without mycorrhizas. *Frontiers in Plant Science*, *4*, 332. https://doi.org/10.3389/fpls.2013.00332

Munns, R., & Gilliham, M. (2015). Salinity tolerance of crops – what is the cost? *New Phytologist*, *208*(3), 668–673. https://doi.org/10.1111/nph.13519

Munns, R., & Tester, M. (2008). Mechanisms of salinity tolerance. *Annual Review of Plant Biology*, *59*(1), 651–681. https://doi.org/10.1146/annurev.arplant.59.032607.092911

Ottow, E. A., Brinker, M., Teichmann, T., Fritz, E., Kaiser, W., Brosché, M., Kangasjärvi, J., Jiang, X., & Polle, A. (2005). *Populus euphratica* displays apoplastic sodium accumulation, osmotic adjustment by decreases in calcium and soluble carbohydrates, and develops leaf succulence under salt stress. *Plant Physiology*, *139*(4), 1762–1772. https://doi.org/10.1104/pp.105.069971

Ottow, E. A., Polle, A., Brosché, M., Kangasjärvi, J., Dibrov, P., Zörb, C., & Teichmann, T. (2005). Molecular characterization of *PeNhaD1*: The first member of the NhaD Na^+/H^+ antiporter family of plant origin. *Plant Molecular Biology*, *58*(1), 75–88. https://doi.org/10.1007/s11103-005-4525-8

Peuke, A. D., & Rennenberg, H. (2006). Heavy metal resistance and phytoremediation with transgenic trees. In M. Fladung & D. Ewald (Eds.), *Tree Transgenesis* (pp. 137–155). Springer Berlin Heidelberg. https://doi.org/10.1007/3-540-32199-3_7

Polle, A., & Chen, S. (2015). On the salty side of life: Molecular, physiological and anatomical adaptation and acclimation of trees to extreme habitats. *Plant, Cell & Environment*, *38*(9), 1794–1816. https://doi.org/10.1111/pce.12440

Polle, A., Janz, D., Teichmann, T., & Lipka, V. (2013). Poplar genetic engineering: Promoting desirable wood characteristics and pest resistance. *Applied Microbiology and Biotechnology*, *97*(13), 5669–5679. https://doi.org/10.1007/s00253-013-4940-8

Sahab, S., Suhani, I., Srivastava, V., Chauhan, P. S., Singh, R. P., & Prasad, V. (2021). Potential risk assessment of soil salinity to agroecosystem sustainability: Current status and management strategies. *Science of The Total Environment*, *764*, 144164. https://doi.org/10.1016/j.scitotenv.2020.144164

Shahid, S. A., Zaman, M., & Heng, L. (2018a). Introduction to soil salinity, sodicity and diagnostics techniques. In M. Zaman, S. A. Shahid, & L. Heng (Eds.), *Guideline for Salinity Assessment, Mitigation and Adaptation Using Nuclear and Related Techniques* (pp. 1–42). Springer International Publishing. https://doi.org/10.1007/978-3-319-96190-3_1

Shahid, S. A., Zaman, M., & Heng, L. (2018b). Soil salinity: Historical perspectives and a world overview of the problem. In M. Zaman, S. A. Shahid, & L. Heng (Eds.), *Guideline for Salinity Assessment, Mitigation and Adaptation Using Nuclear and Related Techniques* (pp. 43–53). Springer International Publishing. https://doi.org/10.1007/978-3-319-96190-3_2

Singh, A. (2018). Salinization of agricultural lands due to poor drainage: A viewpoint. *Ecological Indicators*, *95*, 127–130. https://doi.org/10.1016/j.ecolind.2018.07.037

Sixto, H. (2005). Response to sodium chloride in different species and clones of genus *Populus* L. *Forestry*, *78*(1), 93–104. https://doi.org/10.1093/forestry/cpi009

Sun, J., Dai, S., Wang, R., Chen, S., Li, N., Zhou, X., Lu, C., Shen, X., Zheng, X., Hu, Z., Zhang, Z., Song, J., & Xu, Y. (2009). Calcium mediates root K^+/Na^+ homeostasis in poplar species differing in salt tolerance. *Tree Physiology*, *29*(9), 1175–1186. https://doi.org/10.1093/treephys/tpp048

Sun, J., Li, L., Liu, M., Wang, M., Ding, M., Deng, S., Lu, C., Zhou, X., Shen, X., Zheng, X., & Chen, S. (2010). Hydrogen peroxide and nitric oxide mediate K^+/Na^+ homeostasis and antioxidant defense in NaCl-stressed callus cells of two contrasting poplars. *Plant Cell, Tissue and Organ Culture (PCTOC)*, *103*(2), 205–215. https://doi.org/10.1007/s11240-010-9768-7

Sun, J., Wang, M.-J., Ding, M.-Q., Deng, S.-R., Liu, M.-Q., Lu, C.-F., Zhou, X.-Y., Shen, X., Zheng, X.-J., Zhang, Z.-K., Song, J., Hu, Z.-M., Xu, Y., & Chen, S.-L. (2010). H_2O_2 and cytosolic Ca^{2+} signals triggered by the PM H^+-coupled transport system mediate K^+/Na^+ homeostasis in NaCl-stressed *Populus euphratica* cells. *Plant, Cell & Environment*, *33*(6), 943–958. https://doi.org/10.1111/j.1365-3040.2010.02118.x

Sun, J., Zhang, X., Deng, S., Zhang, C., Wang, M., Ding, M., Zhao, R., Shen, X., Zhou, X., Lu, C., & Chen, S. (2012). Extracellular ATP signaling is mediated by H_2O_2 and cytosolic Ca^{2+} in the salt response of *Populus euphratica* cells. *PLoS ONE*, *7*(12), e53136. https://doi.org/10.1371/journal.pone.0053136

Taylor, G. (2002). *Populus*: Arabidopsis for forestry. Do we need a model tree? *Annals of Botany*, *90*(6), 681–689. https://doi.org/10.1093/aob/mcf255

Tester, M., & Davenport, R. (2003). Na^+ tolerance and Na^+ transport in higher plants. *Annals of Botany*, *91*(5), 503–527. https://doi.org/10.1093/aob/mcg058

Tuskan, G. A., DiFazio, S., Jansson, S., Bohlmann, J., Grigoriev, I., Hellsten, U., Putnam, N., Ralph, S., Rombauts, S., Salamov, A., Schein, J., Sterck, L., Aerts, A., Bhalerao, R. R., Bhalerao, R. P., Blaudez, D., Boerjan, W., Brun, A., Brunner, A., … Rokhsar, D. (2006). The genome of black cottonwood, *Populus Trichocarpa* (Torr. & Gray). *Science*, *313*(5793), 1596–1604. https://doi.org/10.1126/science.1128691

United Nations, Department of Economic and Social Affairs, Population Division. (2017). *World Population Prospects: The 2017 Revision. Key Findings and Advance Tables. Working paper no. ESA/P/WP/248*.

US Salinity Laboratory. (1954). *Diagnosis and improvement of saline and alkali soils* (Agriculture Handbook No. 60). U.S. Government Printing Office.

van Zelm, E., Zhang, Y., & Testerink, C. (2020). Salt tolerance mechanisms of plants. *Annual Review of Plant Biology*, *71*(1), 403–433. https://doi.org/10.1146/annurev-arplant-050718-100005

Wang, M., Zhang, L., Zhang, Z., Li, M., Wang, D., Zhang, X., Xi, Z., Keefover-Ring, K., Smart, L. B., DiFazio, S. P., Olson, M. S., Yin, T., Liu, J., & Ma, T. (2020). Phylogenomics of the genus *Populus* reveals extensive interspecific gene flow and balancing selection. *New Phytologist*, *225*(3), 1370–1382. https://doi.org/10.1111/nph.16215

Wicke, B., Smeets, E., Dornburg, V., Vashev, B., Gaiser, T., Turkenburg, W., & Faaij, A. (2011). The global technical and economic potential of bioenergy from salt-affected soils. *Energy & Environmental Science*, *4*(8), 2669–2681. https://doi.org/10.1039/C1EE01029H

Wu, Y., Ding, N., Zhao, X., Zhao, M., Chang, Z., Liu, J., & Zhang, L. (2007). Molecular characterization of *PeSOS1*: The putative Na$^+$/H$^+$ antiporter of *Populus euphratica*. *Plant Molecular Biology*, *65*(1–2), 1–11. https://doi.org/10.1007/s11103-007-9170-y

Yang, W., Wang, K., Zhang, J., Ma, J., Liu, J., & Ma, T. (2017). The draft genome sequence of a desert tree *Populus pruinosa*. *GigaScience*, *6*(9). https://doi.org/10.1093/gigascience/gix075

Yang, Y., Zhang, F., Zhao, M., An, L., Zhang, L., & Chen, N. (2007). Properties of plasma membrane H$^+$-ATPase in salt-treated *Populus euphratica* callus. *Plant Cell Reports*, *26*(2), 229–235. https://doi.org/10.1007/s00299-006-0220-8

Yao, J., Shen, Z., Zhang, Y., Wu, X., Wang, J., Sa, G., Zhang, Y., Zhang, H., Deng, C., Liu, J., Hou, S., Zhang, Y., Zhang, Y., Zhao, N., Deng, S., Lin, S., Zhao, R., & Chen, S. (2020). *Populus euphratica* WRKY1 binds the promoter of H$^+$-ATPase gene to enhance gene expression and salt tolerance. *Journal of Experimental Botany*, *71*(4), 1527–1539. https://doi.org/10.1093/jxb/erz493

Ye, C.-Y., Zhang, H.-C., Chen, J.-H., Xia, X.-L., & Yin, W.-L. (2009). Molecular characterization of putative vacuolar NHX-type Na$^+$/H$^+$ exchanger genes from the salt-resistant tree *Populus euphratica*. *Physiologia Plantarum*, *137*(2), 166–174. https://doi.org/10.1111/j.1399-3054.2009.01269.x

Zhang, F., Wang, Y., Yang, Y., Wu, H., Wang, D., & Liu, J. (2007). Involvement of hydrogen peroxide and nitric oxide in salt resistance in the calluses from *Populus euphratica*. *Plant, Cell & Environment*, *30*(7), 775–785. https://doi.org/10.1111/j.1365-3040.2007.01667.x

Zhang, H., Lv, F., Han, X., Xia, X., & Yin, W. (2013). The calcium sensor PeCBL1, interacting with PeCIPK24/25 and PeCIPK26, regulates Na^+/K^+ homeostasis in *Populus euphratica*. *Plant Cell Reports*, *32*(5), 611–621. https://doi.org/10.1007/s00299-013-1394-5

Zhang, H., Yin, W., & Xia, X. (2008). Calcineurin B-Like family in *Populus*: Comparative genome analysis and expression pattern under cold, drought and salt stress treatment. *Plant Growth Regulation*, *56*(2), 129–140. https://doi.org/10.1007/s10725-008-9293-4

Zhang, Z., Chen, Y., Zhang, J., Ma, X., Li, Y., Li, M., Wang, D., Kang, M., Wu, H., Yang, Y., Olson, M. S., DiFazio, S. P., Wan, D., Liu, J., & Ma, T. (2020). Improved genome assembly provides new insights into genome evolution in a desert poplar (*Populus euphratica*). *Molecular Ecology Resources*, *20*(3), 781–794. https://doi.org/10.1111/1755-0998.13142

Chapter 2: *Populus euphratica* plant exhibits salt-induced root thickening under high salinity

2.1 Introduction

In nature, plants face various biotic and abiotic stress conditions during their life span. Being sessile organisms, plants, particularly perennials, have to evolve adaptive mechanisms for survival under stress conditions (Polle & Chen, 2015; Lamalakshmi Devi et al., 2017; Estravis-Barcala et al., 2020). Soil salinity is one of the major abiotic stress factors that suppress the normal growth of a plant and will continue to threaten crop yield in the future (Metternicht & Zinck, 2003; Ahmad & Prasad, 2012; Munns & Gilliham, 2015; van Zelm et al., 2020; C. Zhao et al., 2020). Salt tolerance is a manifold phenomenon involving a variety of adjustments in the molecular, physiological, and metabolic processes as well as in the morphological and anatomical features of the plant body (Hameed et al., 2010; C. Zhao et al., 2020; van Zelm et al., 2020). Halophytes, which grow well at extremely high salinities, adopt numerous strategies to control the ion levels in their shoots and leaves (Flowers et al., 1977; Flowers & Colmer, 2008, 2015; Ben Hamed et al., 2018). Halophytes or any salt-tolerant species provide outstanding materials in the progression of understanding and improvement of plant salt tolerance.

Poplars, long-lived woody trees from the genus *Populus*, grow in wild populations with a wide geographic distribution (Polle & Chen, 2015; M. Wang et al., 2020). They provide both economic and ecological benefits (S. Chen & Polle, 2010). A salt-tolerant poplar species, *Populus euphratica*, can withstand up to 450 mM NaCl in hydroponic culture and tolerate high internal concentrations of salt ions in tissues (Gu et al., 2004; Ottow et al., 2005; Zeng et al., 2009; Brinker et al., 2010). Therefore, *P. euphratica* has already gained scientific attention as a model for the research on the adaptation strategies of trees under salinity.

P. euphratica´s strategies to maintain Na^+ levels include restricted root uptake, transport, apoplastic and vacuolar Na^+ deposition (S. Chen et al., 2002, 2003; Ottow et al., 2005; Sun et al., 2009). In addition, the development of leaf succulence via anatomical modification in response to long-term salt exposure was reported (Ottow et al., 2005). After adaptation to increasing salt, *P. euphratica* shows a significant increase in the leaf thickness due to increase in the number and

size of cells that were tightly packed (Ottow et al., 2005). This saline-induced alteration leads to the enlarged cell volume in leaves of *P. euphratica* available for salt deposition (Ottow et al., 2005; S. Chen & Polle, 2010). Larger cells with higher water contents result in leaf succulence, which is defined as water content per unit leaf area (Mantovani, 1999; Suárez & Sobrado, 2000). Succulence is one of the common adaptative features of halophytes in response to salinity (Flowers et al., 1977; Flowers & Colmer, 2008, 2015; Ben Hamed et al., 2018). An increase in succulence under salinity is likely a countermeasure to mitigate the toxic effects of salt through dilution (Albert, 1975). Increased leaf thickness as a consequence of increasing salinity was also reported in non-halophytes such as Arabidopsis, mulberry, etc. (Burssens et al., 2000; Vijayan et al., 2008). In halophytes, the thickness and succulence of leaf or stem tissues were found to increase with growing salinity (Ayala & O'Leary, 1995; Debez et al., 2006; Akcin et al., 2017; Nguyen et al., 2017; Kherraze et al., 2018). Tissue thickening and succulence are likely induced by the internal accumulation of salts (Debez et al., 2006; D. Wang et al., 2012).

The molecular basis for the modification in leaves of *P. euphratica* under salinity needs to be studied. The understanding of the molecular mechanisms underlying the morphological and anatomical modifications upon salt exposure is limited. In plants, cell shape and tissue morphogenesis are regulated by the chemical properties of the cell wall (Chebli & Geitmann, 2017). Besides, the phytohormone auxin is known as a key regulator for many developmental processes in plants and also plays an important role in abiotic stress response (Woodward & Bartel, 2005; Korver et al., 2018; van Zelm et al., 2020). Salt-induced anatomical modifications in tissues are accompanied by the changes in auxin levels (Junghans et al., 2006). Further, the regulation of cell wall related genes was reported for many different plant species under salt stress (Janz et al., 2012; H. Li et al., 2014; Byrt et al., 2018; Eckert et al., 2019; Hori et al., 2020). Notably, not only above-ground tissues but also roots of some species showed thickening in response to salt (Burssens et al., 2000; H. Li et al., 2014; Tan et al., 2020).

In the present study, we aimed to investigate the morphological adjustment in tissues of *P. euphratica* under salinity and to explore the possible molecular network responsible for the alterations. Toward this goal, we gradually acclimated *P. euphratica* to high salt concentrations and studied transcriptomes after short- and long-term acclimation to saline conditions. We

observed greater thickening of the main roots under long-term salt but not of the lateral roots. Therefore, both root types were included in our study. The dry to fresh mass ratio of the tissues was used as an indication of succulence. The tissue accumulation of Na^+ and essential nutrients were compared at time points before and after thickening. We report that cell wall modifications were among the major transcriptional pathways regulated in thickened roots, whereas auxin signaling reported in transgenic GH3::GUS lines of *P. euphratica* was not drastically modified.

2.2 Materials and methods

2.2.1 Propagation and cultivation of plant

Plantlets of *P. euphratica* were multiplied by *in vitro* micropropagation according to Leplé et al. (1992). Wild type (clone B2 from Ein Avdat valley in Israel) and transgenic lines transformed with GH3::GUS construct by Robert Hänsch, Technische Universität Braunschweig, Braunschweig, Germany (according to the same protocol published by Paul et al. (2016)) were cultivated. The stem cuttings (approximately 1 to 2 cm long), each having at least one leaf, were transferred onto Woody Plant Medium (Lloyd & McCown, 1980) under sterile conditions. Then, they were incubated in a culture room maintaining controlled conditions [16 h light / 8 h dark, 150 µmol m^{-2} s^{-1} photosynthetically active radiation (PAR) (Lamp: Osram L 18W/840 cool white, Osram, Munich, Germany), 22 to 25 °C, 40 to 50 % relative air humidity] for six weeks as described by Müller et al. (2013). Afterwards, rooted plants were shifted into aerated hydroponic culture system providing Long-Ashton (LA) nutrient solution (Hewitt & Smith, 1975) which was exchanged weekly. Plants were raised in a greenhouse (Department of Forest Botany and Tree Physiology, University of Göttingen, Germany). A 16 h photoperiod providing additional light of 150 µmol m^{-2} s^{-1} PAR (Lamp: 3071/400 HI-I, Adolf Schuch GmbH, Worms, Germany), 21 to 23 °C air temperature and 60 to 70 % relative air humidity were maintained for growing the plants.

2.2.2 Salt treatment

For the salt treatments, LA solution was prepared with NaCl (with the concentrations indicated below) and the plants were transferred into the salt-containing solution. Controls were transferred into LA without additional NaCl. Salt treatments started when plants had mean

heights of 52 ± 11 cm. Plants were adapted to salt by exposing them to 50 mM NaCl for 1 day followed by 100 mM NaCl for 2 days, and finally to 150 mM NaCl (Fig. 2.1A). The plants were kept in LA solution with or without 150 mM NaCl until harvest, exchanging the nutrient solution weekly (Fig. 2.1A, B).
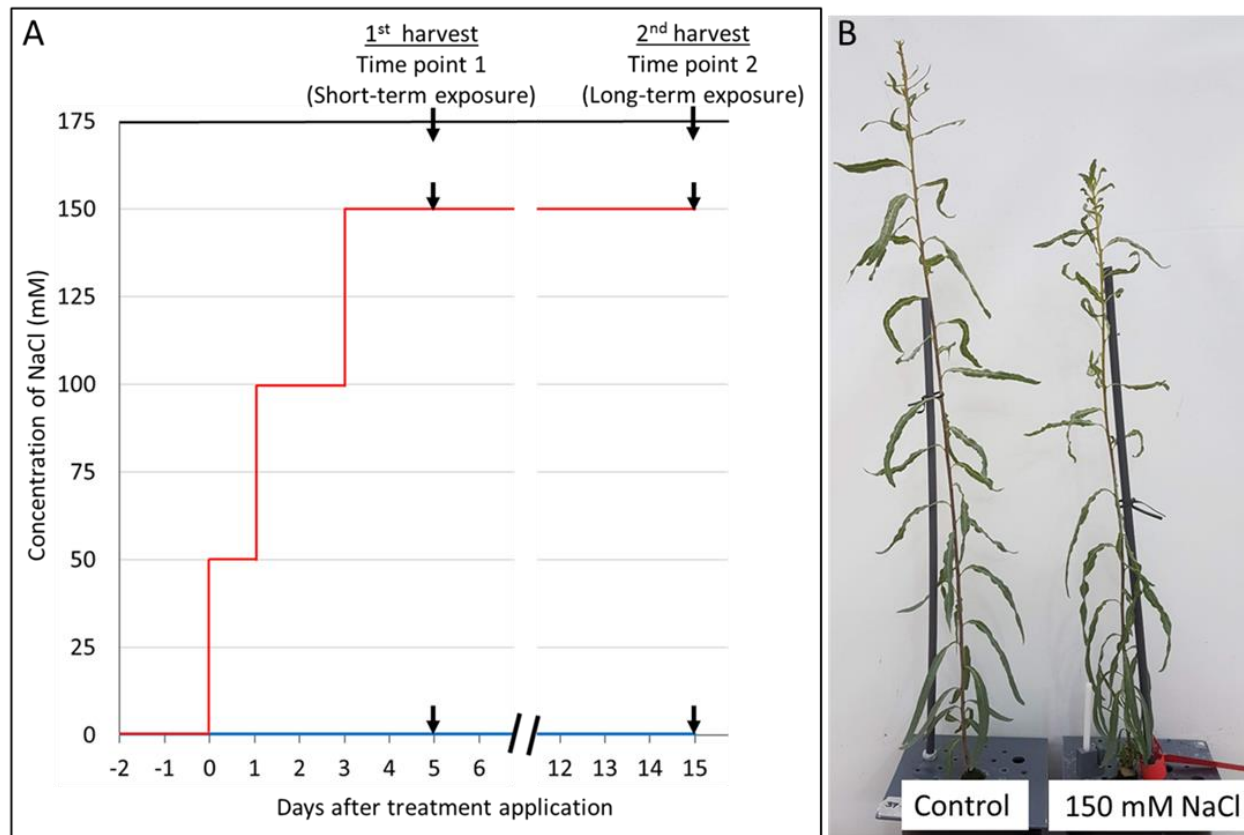
Figure 2.1: Schematic presentation of the salt adaptation steps and sample harvests on *P. euphratica* plants (A), and control and salt-treated plants on day 14 after salt application (B). During salt treatment application (A), salt-treated plants (red line) were gradually adapted to 150 mM NaCl by exposing them to 50 mM NaCl Long-Ashton (LA) solution for 1 day followed by 100 mM NaCl LA solution for 2 days and finally to 150 mM NaCl LA solution. Control plants (blue line) were grown in LA solution (no NaCl) simultaneously. After salt adaptation, plants were maintained in LA solution without NaCl (Control: blue line) or with 150 mM NaCl (Salt: red line) by exchanging the solutions weekly. The leaves, main and lateral roots were harvested from the plants at two time points. The first harvest was done after 5 days of salt adaptation, i.e., after 2 days of 150 mM NaCl exposure (time point 1 = short-term salt exposure). The second harvest was conducted after 15 days of salt adaptation, i.e., after 12 days of 150 mM NaCl exposure (time point 2 = long-term salt exposure).

2.2.3 Gas exchange measurements

Net photosynthesis, transpiration, stomatal conductance, and sub-stomatal CO_2 concentration of mature leaves (8th to 11th leaf from the shoot apex) were measured between 9:00 h to 16:00 h using LI-6800 portable photosynthesis system (Li-COR Ltd., UK). Measurements were conducted with a leaf temperature of 25 ± 1 ^{o}C, at 397 ± 0.8 µmol mol^{-1} ambient atmospheric CO_2 concentration and with a photosynthetic photon flux density of 800 µmol PAR m^{-2} s^{-1}. Gas exchange measurements were carried out daily at the beginning of salt adaptation starting from the day before (d-1) until day 4 (d4) of NaCl application and then once a week. On d0, d1 and d3 when NaCl concentrations were increased from 50 mM to 150 mM (Fig. 2.1A), gas exchange was measured after 5 h of salt exposure.

2.2.4 Harvest of samples

Samples were harvested after 2 days (time point 1: Tp1 = short-term exposure) and 12 days (time point 2: Tp2 = long-term exposure) of 150 mM NaCl exposure (Fig. 2.1A). At each harvest time point, the main root tips, lateral roots, and leaf tissues were collected from wild-type plants (n = 10 per treatment and time point). The roots were cut off and submerged immediately in RNAlater solution (Sigma-Aldrich Chemie GmbH, Steinheim, Germany) to prevent any loss due to RNase activity. Thereafter, main root tips (approx. 5 cm long starting at the apex) and lateral roots were separated and RNAlater was washed off using distilled water. Excessive water was removed with a paper towel and samples were stored in the plastic tubes (Tube 5 ml, Sarstedt, Nümbrecht, Germany) and frozen immediately in liquid nitrogen. After short-term salt exposure (Tp1), three leaves (4th, 6th and 8th leaf from the apex) per plant were pooled in an aluminum bag and frozen in liquid nitrogen. After long-term salt exposure (Tp2), leaves of the same age were harvested. For this purpose, we marked the height at the time point when the salt application started and harvested leaves which were at the apex at this time point. The collection of leaves at Tp2 was done that way since controls had many new leaves at the apex but salt-treated plants did not form many leaves during salt exposure. The harvested tissues were stored at -80 °C until use for either RNA analyses or elements measurement. To perform GUS staining, the main and lateral

roots were harvested from the transgenic lines (n = 5 per treatment and time point) and placed immediately in the GUS buffer (according to Teichmann et al. 2008).

2.2.5 Measurement of biomass and element content of the tissues

Fresh and dry mass of main root tips, lateral roots and leaf tissues (n = 4 to 5 per treatment and time point) were measured on a microbalance (Cubis MCA225S-2S00-I, Sartorius Lab Instruments GmbH & Co. KG, Göttingen, Germany). Samples were dried at 60 $^{\circ}$C for 7 days before measuring the dry mass. The dry-to-fresh mass ratio of the tissue was calculated by dividing the dry mass by fresh mass of the tissue. The dry samples were used to quantify elements (Na, K, Ca, Mg, S, Mn, Fe, and P) in the tissue. The dried root and leaf samples (in the range of 6 to 50 mg) were crushed manually into small parts and then digested with 2 ml of 65 % HNO_3 in a microwave digestion system (ETHOS.start, MLS GmbH, Leutkirch, Germany). The microwave program used for the digestion was as follows: 2.5 min at 90 °C (power 1000 W), 5 min at 150 °C (power 1000 W), 2.5 min at 210 °C (power 1400 W) and 20 min at 210 °C (power 1600 W) (Sharmin et al., 2021). The resulting suspension was cooled and adjusted to 25 ml with ultrapure water obtained from a Sartorius Arium Pro Ultrapure Water System (Sartorius, Göttingen, Germany). The diluted suspension was filtered (MN 280 ¼, Macherey-Nagel GmbH & Co. KG, Düren, Germany) and the elements were measured in the filtered extracts by inductively coupled plasma-optical emission spectrometry (ICP-OES) (iCAP 7000 series ICP-OES, Thermo Fisher Scientific, Dreieich, Germany). The element concentrations (mg g^{-1} dry mass) were calculated using calibration standards (Single-element standards, Bernd Kraft GmbH, Duisburg, Germany) and the sample weight used for extraction.

2.2.6 GUS staining

GUS staining procedure was performed according to Jefferson et al. (1987) as modified by Teichmann et al. (2008). During harvest, the main and lateral root tissues were kept in freshly prepared GUS buffer (100 mM Na-phosphate buffer, pH 7.0, 10 mM Na_4EDTA, 0.05% Triton X-100) containing 1 mM 5-bromo-4-chloro-3-indolyl-β-D-glucuronic acid (Duchefa, Haarlem, The Netherlands) immediately after collection. Plastic tubes (Tube 10 ml, Sarstedt, Nümbrecht,

Germany) containing harvested tissues in GUS buffer were stored inside a styrofoam box filled with ice to keep the samples cool and in darkness until the harvest was done (approximately 1h). Afterwards, vacuum-infiltration of tissues was peformed twice for 15 min each and then the samples were incubated in the dark at 37 °C for 24 h. After incubation, destaining was performed in 50 % (v/v) ethanol for 2 hours followed by several steps of washing in 70 % (v/v) ethanol. Finally, tissues were fixed in FAE solution consisting of 2% formaldehyde, 5% acetic acid and 63% ethanol. Stained root samples were viewed and their images were taken at 8x magnification with the aid of a stereo microscope Stemi 305 (Carl Zeiss Microscopy GmbH, Jena, Germany) equipped with an integrated camera (Stemi 305 cam, Carl Zeiss Microscopy GmbH, Jena, Germany). The diameter of root tips (main and lateral roots) was measured from their images using ImageJ software.

2.2.7 Anatomy

To observe the changes in root anatomy due to salt exposure, main root tip tissues (n = 3 per treatment and time point) were embedded in plastic and thin sections were prepared. For this purpose, main root tip tissues (already fixed in FAE after GUS staining) were dehydrated in a series of ethanol solutions [70, 80, 90 and 96 % (v/v) ethanol] for 2 h each at room temperature. The embedding of tissues in Technovit 7100 resin (Heraeus Kulzer GmbH & Co. KG, Hanau, Germany) was done according to instructions from the manufacturer as modified by Paul et al. (2016). Dehydrated samples were infiltrated in 1:1, 1:2 and 1:3 (v/v) solutions of 96 % ethanol and Technovit 7100 basic solution for 5 h, 12 h and 5 h, respectively. Then, the samples were kept for 24 h in Technovit 7100 infiltration medium comprising 1 g Hardner I in 100 ml Technovit 7100 basic solution (Heraeus Kulzer GmbH & Co. KG, Hanau, Germany). A vacuum (-90 kPa) for 15 min was applied during each step of infiltration. Finally, the tissues were embedded in the embedding medium prepared by mixing 15 ml infiltration medium and 1 ml Hardner II (Heraeus Kulzer GmbH & Co. KG, Hanau, Germany). A special embedding form called histoform (Histoform S, Heraeus Kulzer GmbH & Co. KG, Hanau, Germany) made of Teflon with a stainless steel bottom was used for embedding. Firstly, the embedding cavities of the histoform were filled halfway with the embedding medium, the tissues were positioned therein and then the cavities were filled up. The tissues were kept in embedding medium in the histoform for 2 h at room temperature and

thereafter they were ready to cut. The embedded tissues were sliced at 10 µm thickness with a rotary microtome (Leica RM 2265, Leica Biosystems Nussloch GmbH, Nussloch, Germany). The sections were stained with 0.05 % toluidine blue O (Merck, Darmstadt, Germany) solution and mounted on gelatine-coated glass slides by DePex medium (Serva Electrophoresis GmbH, Heidelberg, Germany). Sections were viewed under a microscope (Axioplan Observer.Z1, Carl Zeiss GmbH, Oberkochen, Germany) and photographs were taken at 100x magnification with a digital camera (AxioCam MRC, Carl Zeiss MicroImaging GmbH, Göttingen, Germany) attached to the microscope.

2.2.8 RNA extraction and analyses

The RNA was extracted from the tissues of main root tips, lateral roots and leaves of the plants (n = 5 per treatment and time point). RNA extraction and library construction were conducted at Beijing Genomics Institute (BGI, Shenzhen, China). Total RNA was extracted with hexadecyltrimethylammonium bromide (CTAB)-pBIOZOL reagent and purified by ethanol steps according to the protocol of Mu et al. (2017). Total RNA was quantified using a NanoDrop (Thermo Fisher Scientific, Waltham, USA) and Agilent 2100 bioanalyzer (Agilent, Santa Clara, USA).

Oligo(dT)-attached magnetic beads were used to purify mRNA. Purified mRNA was fragmented, then first-strand cDNA was generated using random hexamer-primed reverse transcription, followed by a second-strand cDNA synthesis. After A-Tailing and RNA Index adapter addition, cDNA fragments were amplified by PCR and purified via Ampure XP Beads (Beckman Coulter). The products were validated on the Agilent 2100 Bioanalyzer for quality control. The double stranded PCR products from the previous step were heated, denatured and circularized to get the final strand circle DNA library. Paired-end reads with a length of 100 bases were sequenced on a BGIseq-500 (BGI-Shenzhen, China) according to manufacturer's instructions.

Raw sequence data have been deposited in the ArrayExpress database at EMBL-EBI (accession number E-MTAB-8988). Processing of raw sequence data was performed with fastp (S. Chen et al., 2018) using default parameters. The processed sequences were mapped against the transcriptome of *Populus euphratica* (GCF_000495115.1_PopEup_1.0_rna.fna.gz, https://www.ncbi.nlm.nih.gov/genome/13265) using Bowtie 2 (Langmead & Salzberg, 2012).

Depending on the sample, 88 to 92 % of all filtered reads could be mapped to a gene model. Bowtie mapping files were summarized to count tables of the gene models in R (R Core Team 2018). Identification of differentially expressed transcripts was conducted using the DESeq2 package (Love et al., 2014), using a generalized linear model with Benjamini and Hochberg correction to adjust p-values.

2.2.9 Statistical analyses

Statistical analyses were performed with free statistical software R (version 3.5.2) (R Core Team, 2018). The two-way or three-way analysis of variance (ANOVA) followed by Tukey's multiple comparison test was performed. In the case of element contents in roots, three-way ANOVA was done with treatment, time and root type as the main factors. In the other cases, two-way ANOVA was done with treatment and time or day as the main factors. Normal distribution of data was tested by plotting residuals and square root or log transformation was used, when necessary. Data shown are means ± SE. If not indicated otherwise, 5 biological replicates were investigated. Means are considered to be significantly different with p-value <0.05.

2.3 Results

2.3.1 Gas exchange declined in response to high salinity, but a significant recovery was observed only in photosynthetic rate after adaptation

Changes in the gas exchange process in the leaves of *P. euphratica* under high salinity were observed (Fig. 2.2A-D). Gas exchange measurements showed that photosynthetic rate, stomatal conductance and transpiration rate declined significantly in response to salinity and increasing exposure time (Fig. 2.2A-C, Table 2.1). Compared to controls, a significant decrease in stomatal conductance under salinity was found after 5 h exposure to 100 mM NaCl (d1, Fig. 2.2B), while photosynthesis and transpiration rate significantly decreased later, i.e., after 24 h exposure to 100 mM NaCl (d2, Fig 2.2A, C). Sub-stomatal CO_2 concentration in salt-stressed plants also decreased significantly compared to controls on d1 after 100 mM NaCl application (Fig 2.2D). Exposure to higher salinity (150 mM NaCl) on d3 did not cause an additional significant reduction in gas exchange and sub-stomatal CO_2 (Fig. 2.2A-D). After 11 days in LA solution with 150 mM

NaCl (d14), salt-stressed plants showed significant recovery in photosynthetic rate, but not in stomatal conductance and transpiration (Fig. 2.2A-C). On the contrary, sub-stomatal CO_2 level further decreased significantly on d14 (Fig. 2.2D).
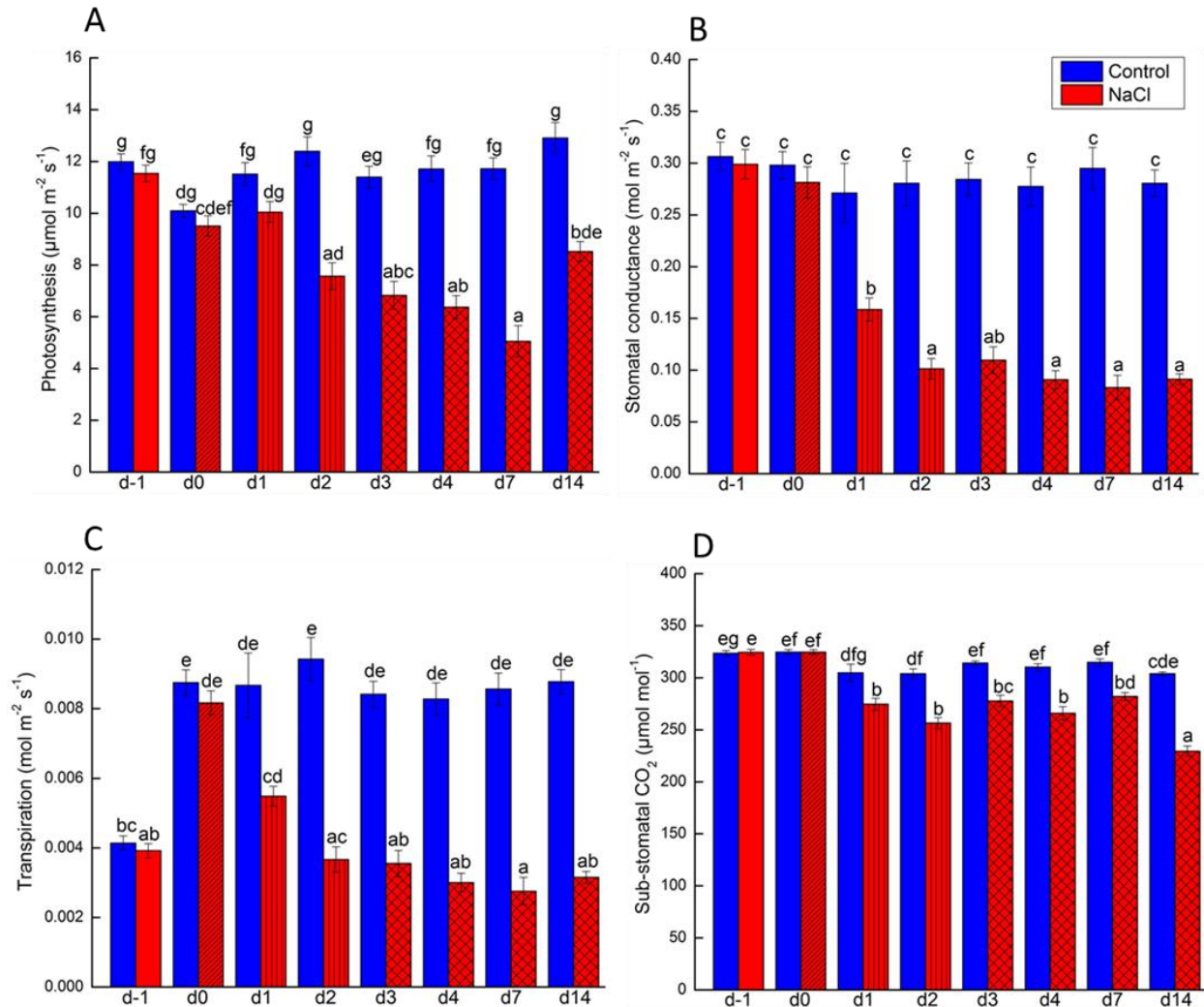
Figure 2.2: Photosynthetic rate (A), stomatal conductance (B), transpiration (C) and sub-stomatal CO_2 concentration (D) in *P. euphratica* leaves in response to salinity. On the day before the start of the treatments (d-1), plants in the control group (blue open bar) and in the NaCl group (red open bar) were grown in Long-Ashton (LA) solution without NaCl. On day 0 (d0), plants in the NaCl group (red hatched bar) were exposed to 50 mM NaCl LA solution. On day 1 (d1), the salt level in NaCl-treated plants (red striped bar) was increased to 100 mM NaCl and plants were kept in this solution until day 3 (d3). On day 3 (d3), NaCl-treated plants (red crossed bar) were exposed to 150 mM NaCl LA solution and continued to grow in this solution until end of the experiment. The solutions were exchanged each time with increase in NaCl concentration and later once a week. Bars indicate means ± SE (n = 5 or 7 plants per treatment;

only on the d-1, n= 26 or 28 plants per treatment). Two-way analysis of variance (ANOVA) was done with treatment and day as the main factors. Normal distribution of data was tested by plotting residuals and log transformation was used for stomatal conductance and transpiration data. Different letters obtained from Tukey's multiple comparison test indicate significant differences at p <0.05.

2.3.2 The diameter of main and lateral roots enlarged significantly after long-term salt exposure but dry-to-fresh mass ratio did not differ from controls

The diameter of main and lateral roots from salt-treated plants was compared with that of controls after short-term (= Tp1) and long-term (= Tp2) salt exposure (Table 2.2). The diameter of main roots (MRs) and lateral roots (LRs) were measured at a distance of 12 mm and 4 mm from the apex, respectively, where approximately maximum radial swelling was noticed in long-Term salt-treated roots. Salt-treated MRs showed no significant difference in diameter in response to short-term but almost twofold increase after long-term exposure compared with controls (Fig. 2.3, Table 2.2). Similarly, LRs of salt-treated plants were significantly thicker than control LRs after long-term exposure, whereas no significant difference in LR diameter was

Table 2.1: Two-way analysis of variance (ANOVA) of photosynthesis, stomatal conductance, transpiration and sub-stomatal CO_2 concentration in the leaves of *P. euphratica* under control and NaCl treatments measured on several days after treatment application. Two-way ANOVA was done with treatment and day as the main factors. Normal distribution of data was tested by plotting residuals and log transformation was used for the stomatal conductance and transpiration data to meet the criteria.

p-value	Photosynthesis	Stomatal conductance	Transpiration	Sub-stomatal CO_2
p(treatment)	<0.001	<0.001	<0.001	<0.001
p(day)	<0.001	<0.001	<0.001	<0.001
p(treatment × day)	<0.001	<0.001	<0.001	<0.001

observed between the treatments after short-term exposure (Table 2.2). However, the diameter increment in LRs after long-term salt exposure was less pronounced (1.48 fold) than that of MRs (Table 2.2).

To get an overview on the alteration in anatomy which led to increased root diameter under salt stress, longitudinal sections of MRs of salt-stressed and control plants were observed (Fig. 2.3A-D). The thin sections revealed that apparently there was no difference in the root anatomy under

salinity in comparison with control after short-term salt exposure (Fig. 2.3A, B). However, there were more cell layers in the cortex tissue of salt-stressed MR than that in controls after long-term salt exposure (Fig. 2.3C, D).

Table 2.2: Diameter (mm) of main and lateral roots of *P. euphratica* under control and 150 mM NaCl treatments at the time points after short-term (Tp1 = after 2 days of 150 mM NaCl exposure) and long-term (Tp2 = after 12 days of 150 mM NaCl exposure) salt exposure. The diameter of main root tips and lateral roots was measured at a distance of 12 mm and 4 mm from the apex, respectively. Data represent means ± SE (n = 5 or 6 plants per treatment and time). Two-way ANOVA was conducted with treatment and time as the main factors. Normal distribution of data was tested by plotting residuals and log transformation was used for the main roots to meet the criteria. Homogeneous subsets were obtained using Post-hoc Tukey's HSD test. Different lower case letters in a column indicate significant differences at $p < 0.05$.

Treatment	Time	Main root	Lateral root
Control	Tp1	1.11 ± 0.10 a	0.55 ± 0.05 a
150 mM NaCl	Tp1	1.36 ± 0.11 a	0.73 ± 0.08 ab
Control	Tp2	1.10 ± 0.06 a	0.56 ± 0.06 a
150 mM NaCl	Tp2	2.09 ± 0.24 b	0.83 ± 0.05 b
p(treatment)		<0.001	0.002
p(time)		0.04	0.377
p(treatment × time)		0.028	0.461

The dry-to-fresh mass ratios (DM/FM) of roots as well as of foliar tissues were measured to check the occurrence of succulence. Neither MRs nor LRs showed a significant difference in DM/FM under salinity compared with control conditions (Table 2.3). MRs, irrespective of salt treatment, had significantly lower DM/FM after long-term than short-term salt exposure (Table 2.3). On the other hand, DM/FM of leaves of salt-treated plants increased significantly compared to controls after short-term salt exposure (Table 2.3). There was a trend of increase in DM/FM in salt-stressed leaves compared to controls after long-term salt exposure but not significant (Table 2.3).

2.3.3 Na content of main roots and leaves, but not of lateral roots, increased significantly after long-term salt exposure, while the nutrient contents were mostly unaffected only in leaves

We measured the contents of Na and nutrient elements (K, Ca, Mg, Mn, Fe, S and P) in the root and leaf tissues. Na content increased significantly in MRs with increasing salt exposure but did

not increase significantly in salt-stressed LRs compared to controls at any time point (Fig. 2.4A). Between the root types, MRs had significantly higher Na content than LRs after long-term salt
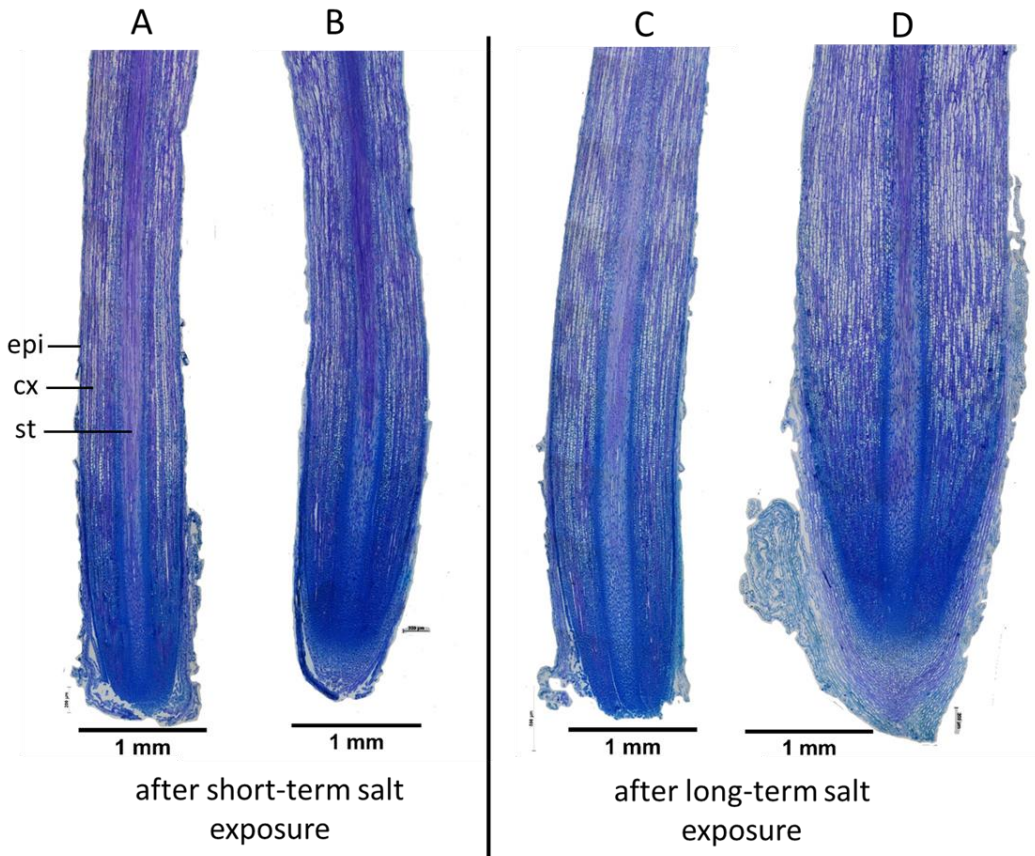
Figure 2.3: Longitudinal sections of main root tips of *P. euphratica*. Main root tips from control (A) and NaCl-treated plant (B) were collected after short-term salt exposure (i.e. after 2 days of 150 mM NaCl exposure). Similarly, main root tips from control (C) and NaCl-treated plant (D) were collected after long-term salt exposure (i.e. after 12 days of 150 mM NaCl exposure). Sections were stained with toluidine blue. Representative main root tip sections from n = 3 plants per treatment and time point are shown. The thickness of the root sections: 10 μm. Scale bar: 1 mm. Abbreviations: ep, epidermis; cx, cortex; st, stele.

exposure (Fig. 2.4A). In the foliar tissues, Na content increased significantly in response to salinity and extending exposure time (Fig. 2.4B).

The contents of K, Ca and Mn decreased significantly in roots in response to salt compared to controls (Table 2.4). Mg and S contents did not differ significantly, but Fe and P contents were increased under salinity compared to controls in the roots. On the contrary, the leaf contents of nutrients mostly did not fluctuate significantly under salinity (Table 2.5).

Table 2.3 Dry-to-fresh mass ratio of main root tips, lateral roots and leaf tissues of *P. euphratica* under control and 150 mM NaCl treatments at the time points after short-term (Tp1 = after 2 days of 150 mM NaCl exposure) and long-term (Tp2 = after 12 days of 150 mM NaCl exposure) salt exposure. Data represent means ± SE (n = 4 or 5 plants per treatment and time). Two-way ANOVA was conducted with treatment and time as the main factors. Normal distribution of data was tested by plotting residuals. Homogeneous subsets were obtained using Post-hoc Tukey's HSD test. Different lower case letters in a column indicate significant differences at $p < 0.05$.

Treatment	Time	Main root	Lateral root	Leaf
Control	TP1	0.19 ± 0.01 b	0.21 ± 0.01 a	0.16 ± 0.00 a
150 mM NaCl	TP1	0.19 ± 0.01 b	0.23 ± 0.01 a	0.19 ± 0.01 b
Control	TP2	0.15 ± 0.00 a	0.18 ± 0.05 a	0.18 ± 0.01 ab
150 mM NaCl	TP2	0.13 ± 0.01 a	0.21 ± 0.04 a	0.21 ± 0.00 b
p(treatment)		0.586	0.442	0.002
p(time)		<0.001	0.448	0.005
P (treatment × time)		0.265	0.945	0.750

2.3.4 GUS staining was observed mainly near the root's apex with no visible difference in response to salt stress

To evaluate the changes in auxin distribution of roots under short- and long-term salt exposure, the localization of GUS staining was observed in the main and lateral roots (Fig. 2.5). Transgenic lines with GH3::GUS construct showed strong GUS staining only in the root apex region in both root types and mild staining in the young portion of roots, especially of the lateral roots (Fig. 2.5C-F, I-L). The staining pattern did not show any apparent difference between control and salt-stressed roots and also between short- and long-term salt-stressed roots (Fig. 2.5C-F, I-L).

2.3.5 Transcriptome analysis exhibited more fluctuations in the regulation of cell wall-associated genes in the root tissues than in leaves in response to short- and long-term salt exposure

To get insight into the molecular event associated with the alteration in tissue morphology under salinity, transcriptome analysis of the roots and leaf tissues from salt treatment as well as control after short- and long-term salt exposure was performed. Genes that changed transcript abundances significantly (differentially expressed genes, DEGs) under salinity compared to
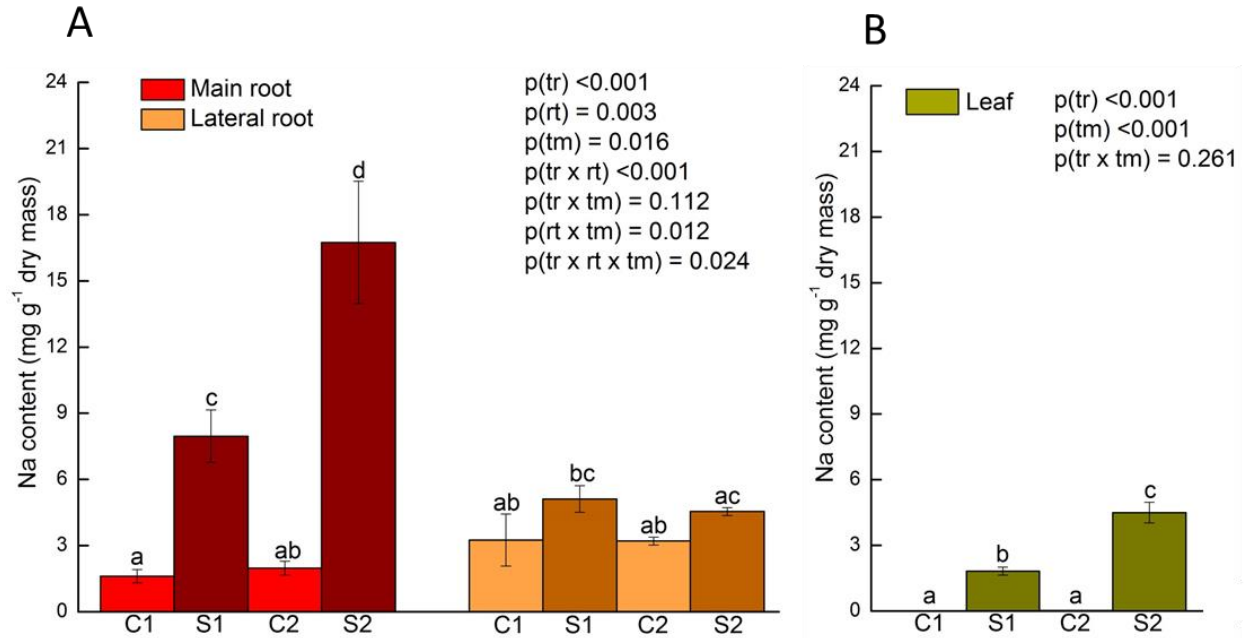
Figure 2.4: The content of Na (mg g^{-1} dry mass) in the main and lateral roots (A) and leaves (B) of *P. euphratica* under control (C1 & C2) condition and salt (S) treatment after short-term (S1: after 2 days of 150 mM NaCl exposure) and long-term (S2: after 12 days of 150 mM NaCl exposure) salt exposure. Bars represent means ± SE (n = 4 or 5 plants per treatment and time). Three-way ANOVA was conducted for roots with treatment (tr), time (tm) and root type (rt) as the main factors. Two-way ANOVA was conducted for leaves with treatment (tr) and time (tm) as the main factors. Normal distribution of data was tested by plotting residuals and square root (for roots) and log transformation (for leaves) were used to meet the criteria. Homogeneous subsets were obtained using Post-hoc Tukey's HSD test. Different lower case letters in a graph indicate significant differences at p <0.05.

control conditions were determined for each time point (Supplement table S2.1). Since cell and tissue morphogenesis in plants are regulated by the chemical properties of cell walls (Chebli & Geitmann, 2017), the study of the regulation of cell wall related genes was of particular interest. Therefore, the list of *Arabidopsis* genes annotated to GO (Gene Ontology) category "Cell wall organization or biogenesis (GO:0071554)" which contains 558 genes, was obtained from GO database (http://www. geneontology.org/, accessed 8 August, 2021, (Gene Ontology Consortium, 2004)). Then our transcriptome data (Supplement table S2.1) were screened based on this gene list and we got a total of 536 *P. euphratica* genes expressed in different tissues (Supplement table S2.2). After short-term salt exposure, 84, 78 and 23 cell wall related genes out of 536 were differentially expressed in LRs, MRs and leaves, respectively, (Supplement table
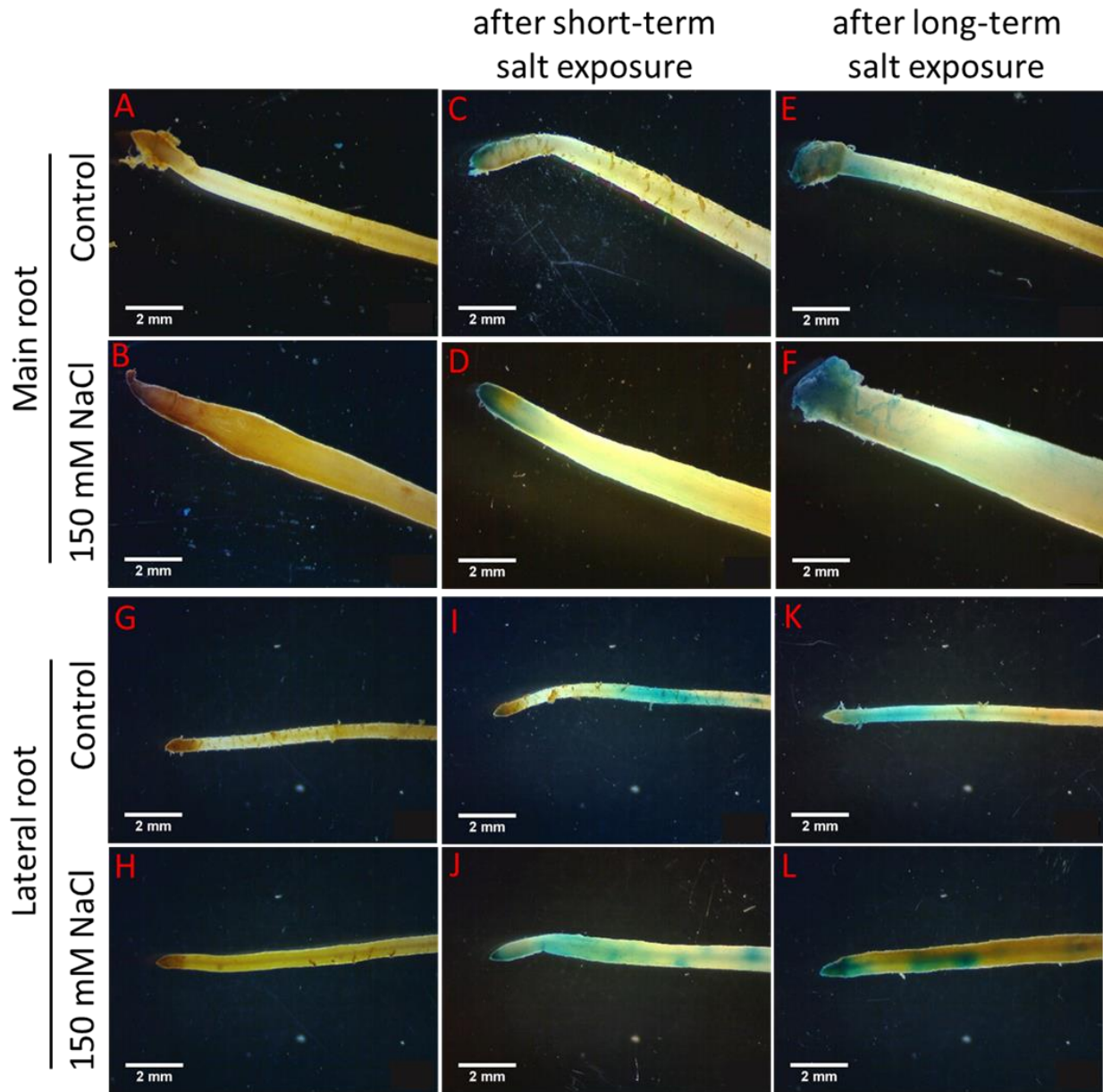
Figure 2.5: GUS staining in the main root tips (A-F) and lateral roots (G-L) of transgenic GH3::GUS lines (TG) and wild-type (WT) plants of *P. euphratica* after short- and long-term salt (150 mM NaCl) exposure and under control condition. Panels (A-B) and (G-H) represent main root tips and lateral roots of WT plants, respectively. Panels (C-F) and (I-L) represent main root tips and lateral roots of GH3::GUS transformed lines (TG), respectively. Panels (C-D) represent main root tips and (I-J) represent lateral roots under control condition and 150 mM NaCl treatment after short-term exposure (i.e. after 2 days of 150 mM NaCl exposure). Panels (E-F) represent main root tips and (K-L) represent lateral roots under control condition and 150 mM NaCl treatment after long-term exposure (i.e. after 12 days of 150 mM NaCl exposure). Representative pictures of n= 5 transgenic plants per treatment and time are shown. Scale bar: 2 mm.

S2.3). After long-term salt exposure, the number of DEGs related to cell wall reactions in LRs, MRs and leaves were 205, 66 and 8, respectively (Supplement table S2.4).

Among the DEGs in a particular tissue, members of the following gene families were abundant: pectin methylesterase (PME), expansin (EXP), expansin-like (EXL), cellulose synthase (CesA), cellulose synthase-like (Csl), xyloglucan endotransglucosylase/hydrolase (XTH), fasciclin-like arabinogalactan (FLA), MYB and NAC-type transcription factor (TF). Therefore, the regulation of these gene families in different tissues in response to salt stress was summarized (Fig. 2.6, 2.7 and 2.8). In MRs, out of DEGs encoding PME, EXP & EXL, CesA & Csl, FLA, XTH, MYB and NAC-type TFs after short-term salt exposure, the majority were upregulated (Fig. 2.6, Supplement table S2.3). However, differentially expressed members of these gene families after long-time salt exposure largely showed downregulation except for some genes encoding PME, EXP, EXL and TFs (Fig. 2.6, Supplement table S2.4).

In LRs, after short-term salt exposure, almost all DEGs from PME, EXP, EXL, MYB and NAC-type TF families showed upregulation, while DEGs from CesA, Csl, FLA and XTH families mostly exhibited downregulation (Fig. 2.7, Supplement table S2.3). More members of these gene families were differentially regulated after long-term than short-term salt exposure in the LRs (Fig. 2.7, Supplement tables S2.3 & S2.4). After long-term salt exposure, in LRs, all DEGs from MYB TF and many DEGs from PME, EXP, EXL, XTH and NAC-type TF families were upregulated, but the majority of DEGs encoding PME, EXP, EXL, CesA, Csl and FLA and many from XTH and NAC-type TF family showed downregulation (Fig. 2.7, Supplement table S2.4).

In the leaf tissues, only a few out of these gene families showed regulation in response to salt (Fig. 2.8, Supplement tables S2.3 & S2.4). After short-term salt exposure, DEGs for MYB TF showed upregulation, while DEGs from PME, CesA & Csl gene families showed both up- and down regulation in the leaf tissues (Fig. 2.8, Supplement table S2.3). After long-term salt exposure, one member from PME, Csl and FLA gene families each was downregulated in the leaves, but members from any of these gene families did not show significant upregulation (Fig. 2.8, Supplement table S2.4).

Table 2. 4: The content of elements (mg g^{-1} dry mass) in the main and lateral roots of *P. euphratica* under control and 150 mM NaCl treatments at the time points after short-term (Tp1 = after 2 days of 150 mM NaCl exposure) and long-term (Tp2 = after 12 days of 150 mM NaCl exposure) salt exposure. Data represent means ± SE (n = 4 or 5 plants per treatment and time). Three-way ANOVA was conducted with treatment, time and root type as the main factors. Normal distribution of data was tested by plotting residuals. To meet the criteria, square root (for Ca, Mg, Fe, S and P) and log transformation (for K and Mn) were used. Homogeneous subsets were obtained using Post-hoc Tukey's HSD test. Different lower case letters in a column indicate significant differences at p <0.05.

Treatment	Time	Root type	K	Ca	Mg	Mn	Fe	S	P
Control	Tp1	Main root	4.45 ± 0.97 c	0.36 ± 0.03 bc	0.31 ± 0.04 b	0.03 ± 0.01 ac	0.02 ± 0.03 a	66.58 ± 10.92 a	1.84 ± 0.48 ab
150 mM NaCl	Tp1	Main root	1.68 ± 0.26 bc	0.18 ± 0.03 ac	0.29 ± 0.03 b	0.06 ± 0.02 bc	0.13 ± 0.06 ac	64.10 ± 5.10 a	2.04 ± 0.15 ab
Control	Tp2	Main root	4.22 ± 0.74 c	0.36 ± 0.03 c	0.37 ± 0.05 b	0.05 ± 0.01 bc	0.03 ± 0.01 ab	72.60 ± 9.18 a	1.66 ± 0.34 ab
150 mM NaCl	Tp2	Main root	2.18 ± 0.39 bc	0.22 ± 0.03 ac	0.31 ± 0.05 b	0.01 ± 0.00 a	0.04 ± 0.01 ab	65.21 ± 6.35 a	2.93 ± 0.48 b
Control	Tp1	Lateral root	2.10 ± 0.71 bc	0.26 ± 0.08 ac	0.27 ± 0.09 ab	0.16 ± 0.08 bc	0.23 ± 0.09 bc	118.25 ± 44.28 a	1.62 ± 0.51 ab
150 mM NaCl	Tp1	Lateral root	1.02 ± 0.15 ab	0.17 ± 0.02 ab	0.22 ± 0.03 ab	0.11 ± 0.01 c	0.30 ± 0.09 c	101.51 ± 5.86 a	1.94 ± 0.27 ab
Control	Tp2	Lateral root	1.03 ± 0.15 ab	0.23 ± 0.06 ac	0.17 ± 0.02 ab	0.09 ± 0.02 bc	0.07 ± 0.01 ac	114.50 ± 5.08 a	0.89 ± 0.13 a
150 mM NaCl	Tp2	Lateral root	0.45 ± 0.08 a	0.16 ± 0.03 a	0.10 ± 0.02 a	0.03 ± 0.01 ab	0.25 ± 0.05 bc	104.81 ± 3.82 a	0.97 ± 0.17 a
p(treatment)			<0.001	<0.001	0.149	0.011	0.012	0.570	0.037
p(root type)			<0.001	0.011	<0.001	<0.001	<0.001	<0.001	0.001
p(time)			0.102	0.877	0.160	0.002	0.199	0.612	0.193
p(treatment × root type)			0.631	0.179	0.777	0.778	0.479	0.967	0.376
p(treatment × time)			0.856	0.741	0.472	<0.001	0.958	0.758	0.608
p(root type × time)			0.022	0.524	0.017	0.894	0.311	0.911	0.013
p(treatment × root type × time)			0.311	0.727	0.722	0.491	0.086	0.997	0.211

Table 2.5: The content of elements (mg g^{-1} dry mass) in the leaves of *P. euphratica* under control and 150 mM NaCl treatments at the time points after short-term (Tp1 = after 2 days of 150 mM NaCl exposure) and long-term (Tp2 = after 12 days of 150 mM NaCl exposure) salt exposure. Data represent means ± SE (n = 4 or 5 plants per treatment and time). Two-way ANOVA was conducted with treatment and time as the main factors. Normal distribution of data was tested by plotting residuals and log transformation (for Mg) was used. Homogeneous subsets were obtained using Post-hoc Tukey's HSD test. Different lower case letters in a column indicate significant differences at p <0.05.

Treatment	Time	K	Ca	Mg	Mn	Fe	S	P
Control	Tp1	16.92 ± 0.96 a	13.16 ± 0.80 ab	4.71 ± 0.26 a	0.12 ± 0.01 a	0.06 ± 0.01 a	10.77 ± 0.66 a	5.55 ± 0.26 a
150 mM NaCl	Tp1	18.65 ± 0.75 a	13.63 ± 0.27 ab	4.98 ± 0.13 a	0.14 ± 0.01 a	0.04 ± 0.00 a	12.16 ± 0.33 a	5.71 ± 0.46 a
Control	Tp2	17.80 ± 0.63 a	16.03 ± 1.08 b	5.72 ± 0.32 a	0.16 ± 0.01 a	0.06 ± 0.01 a	12.13 ± 0.95 a	5.71 ± 0.40 a
150 mM NaCl	Tp2	17.51 ± 1.38 a	11.64 ± 1.51 a	4.74 ± 0.39 a	0.13 ± 0.01 a	0.04 ± 0.00 a	10.76 ± 1.12 a	5.93 ± 0.32 a
p(treatment)		0.506	0.062	0.204	0.428	0.004	0.939	0.636
p(time)		0.853	0.782	0.343	0.431	0.888	0.906	0.618
p(treatment × time)		0.322	0.036	0.048	0.070	0.838	0.125	0.942

2.4 Discussion

2.4.1 *P. euphratica* restores carbon dioxide assimilation under high salinity

Stomatal opening is required for CO_2 to enter the leaf for assimilation and at the same time results in water loss due to transpiration (Farquhar & Sharkey, 1982). After 5 hours of exposure to 100 mM NaCl LA solution (d1), salt-stressed *P. euphratica* significantly reduced the opening of stomata which resulted in a reduction in transpirational water loss (Fig. 2.2B, C). At that time, the uptake rate of CO_2 was not reduced greatly (d1, Fig 2.2A), but the sub-stomatal CO_2 level decreased significantly (d1, Fig. 2.2D). The concentration of CO_2 outside the leaf and stomatal conductance control the supply of CO_2 to the leaf intercellular air spaces (Moss & Rawlins, 1963; Farquhar & Sharkey, 1982; Tominaga et al., 2018). After 5 hours of exposure to 100 mM NaCl, *P. euphratica* maintained a high assimilation rate by consuming intercellular CO_2, whose replenishment was decreased because of reduced stomatal conductance. This ultimately resulted in decreased sub-stomatal CO_2 levels. After one day of exposure to 100 mM NaCl, CO_2 assimilation rate was significantly decreased due to less available CO_2 inside the leaves (d2, Fig. 2.2A, D). *P. euphratica* was then able to maintain a steady level of stomatal conductance and and gas exchanges (150 mM NaCl) (Fig. 2.2B, C). However, after 12 days of exposure to 150 mM NaCl (d14), salt-stressed plants recovered photosynthetic rates, even though stomatal conductance was low, by utilizing more CO_2 from the intercellular air spaces. Consequently, CO_2 concentrations in the sub-stomatal spaces further decreased (d14, Fig. 2.2D). The recovery in the net photosynthesis rate of *P. euphratica* under higher salinity (200 mM NaCl) was also reported earlier (Ma et al., 1997). Therefore, *P. euphratica* has ability to maintain gas exchange efficiently under extended exposure to salinity.

2.4.2 *P. euphratica* shows a morphological modification in roots in response to high salt exposure

The characteristic morphological adaptations in leaves or stems of numerous halophytes under increasing salinity are associated with an increase in cell size, or increase in cell size and numbers,
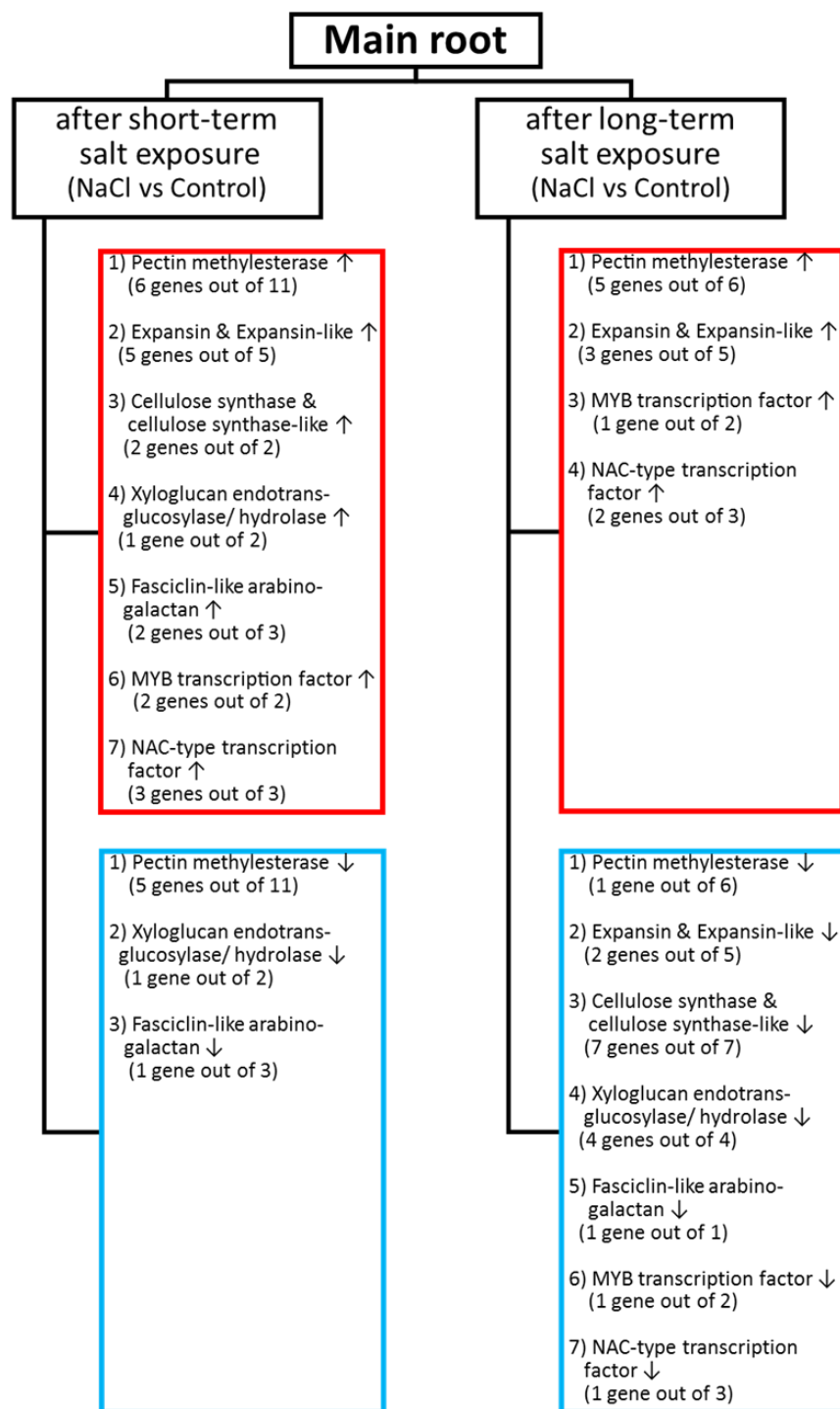
Main root

after short-term salt exposure (NaCl vs Control)

1) Pectin methylesterase ↑
   (6 genes out of 11)

2) Expansin & Expansin-like ↑
   (5 genes out of 5)

3) Cellulose synthase & cellulose synthase-like ↑
   (2 genes out of 2)

4) Xyloglucan endotrans-glucosylase/ hydrolase ↑
   (1 gene out of 2)

5) Fasciclin-like arabino-galactan ↑
   (2 genes out of 3)

6) MYB transcription factor ↑
   (2 genes out of 2)

7) NAC-type transcription factor ↑
   (3 genes out of 3)

1) Pectin methylesterase ↓
   (5 genes out of 11)

2) Xyloglucan endotrans-glucosylase/ hydrolase ↓
   (1 gene out of 2)

3) Fasciclin-like arabino-galactan ↓
   (1 gene out of 3)

after long-term salt exposure (NaCl vs Control)

1) Pectin methylesterase ↑
   (5 genes out of 6)

2) Expansin & Expansin-like ↑
   (3 genes out of 5)

3) MYB transcription factor ↑
   (1 gene out of 2)

4) NAC-type transcription factor ↑
   (2 genes out of 3)

1) Pectin methylesterase ↓
   (1 gene out of 6)

2) Expansin & Expansin-like ↓
   (2 genes out of 5)

3) Cellulose synthase & cellulose synthase-like ↓
   (7 genes out of 7)

4) Xyloglucan endotrans-glucosylase/ hydrolase ↓
   (4 genes out of 4)

5) Fasciclin-like arabino-galactan ↓
   (1 gene out of 1)

6) MYB transcription factor ↓
   (1 gene out of 2)

7) NAC-type transcription factor ↓
   (1 gene out of 3)

Figure 2.6: A schematic chart showing the regulation of few gene families, annotated to GO term "cell wall organization or biogenesis", in the main root tissues of *P. euphratica* after short-term (i.e. 2 days of 150 mM NaCl exposure) and long-term (i.e. after 12 days of 150 mM NaCl exposure) salt exposure. Red lined box includes upregulated and blue lined box includes downregulated gene families. The number indicates the number of genes out of total number of DEGs from the respective gene family at that time. ↑ indicates upregulation and ↓ indicates downregulation.
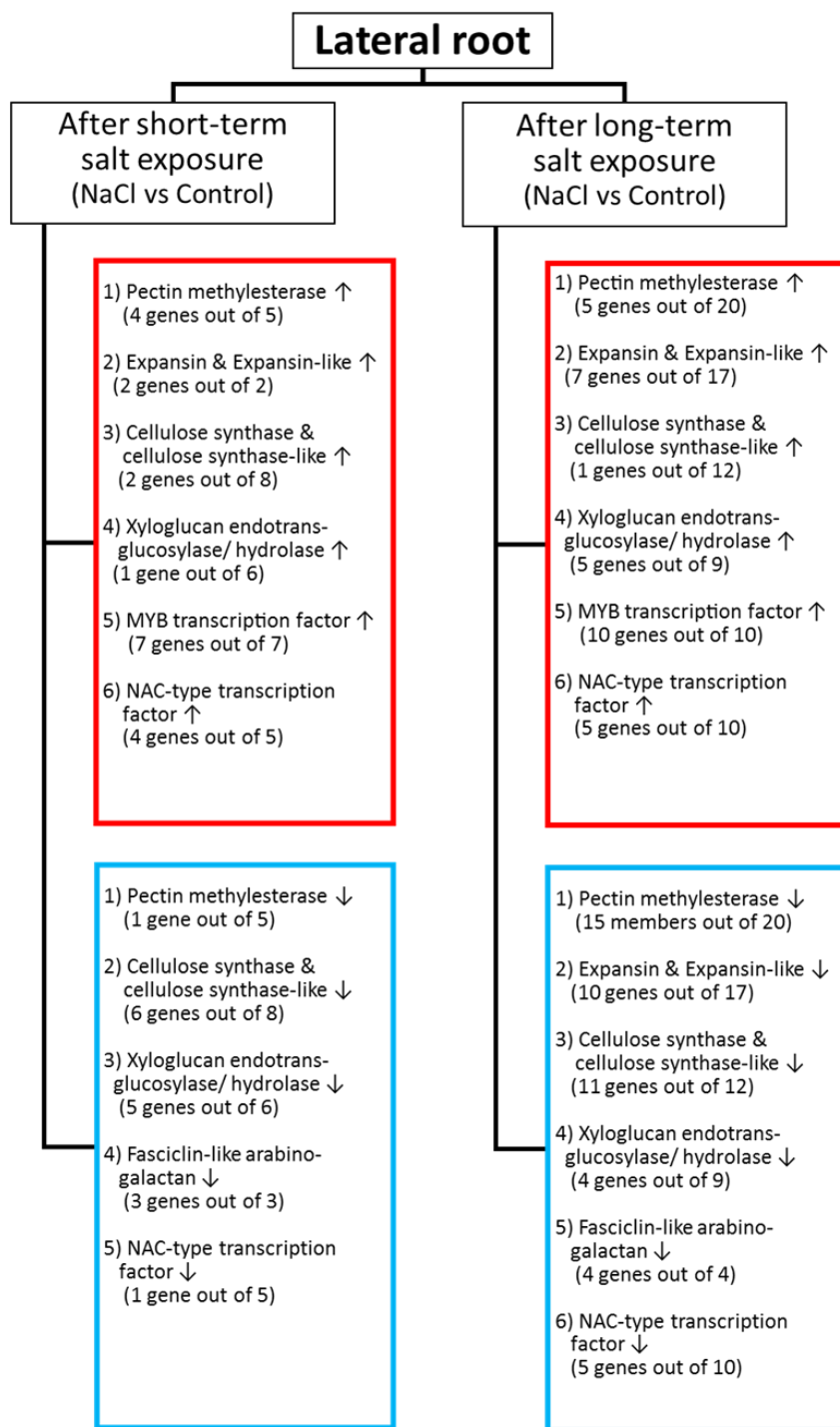
Lateral root

After short-term salt exposure (NaCl vs Control)

Red box (upregulated):
1) Pectin methylesterase ↑ (4 genes out of 5)
2) Expansin & Expansin-like ↑ (2 genes out of 2)
3) Cellulose synthase & cellulose synthase-like ↑ (2 genes out of 8)
4) Xyloglucan endotrans-glucosylase/ hydrolase ↑ (1 gene out of 6)
5) MYB transcription factor ↑ (7 genes out of 7)
6) NAC-type transcription factor ↑ (4 genes out of 5)

Blue box (downregulated):
1) Pectin methylesterase ↓ (1 gene out of 5)
2) Cellulose synthase & cellulose synthase-like ↓ (6 genes out of 8)
3) Xyloglucan endotrans-glucosylase/ hydrolase ↓ (5 genes out of 6)
4) Fasciclin-like arabino-galactan ↓ (3 genes out of 3)
5) NAC-type transcription factor ↓ (1 gene out of 5)

After long-term salt exposure (NaCl vs Control)

Red box (upregulated):
1) Pectin methylesterase ↑ (5 genes out of 20)
2) Expansin & Expansin-like ↑ (7 genes out of 17)
3) Cellulose synthase & cellulose synthase-like ↑ (1 genes out of 12)
4) Xyloglucan endotrans-glucosylase/ hydrolase ↑ (5 genes out of 9)
5) MYB transcription factor ↑ (10 genes out of 10)
6) NAC-type transcription factor ↑ (5 genes out of 10)

Blue box (downregulated):
1) Pectin methylesterase ↓ (15 members out of 20)
2) Expansin & Expansin-like ↓ (10 genes out of 17)
3) Cellulose synthase & cellulose synthase-like ↓ (11 genes out of 12)
4) Xyloglucan endotrans-glucosylase/ hydrolase ↓ (4 genes out of 9)
5) Fasciclin-like arabino-galactan ↓ (4 genes out of 4)
6) NAC-type transcription factor ↓ (5 genes out of 10)

Figure 2.7: A schematic chart showing the regulation of few gene families, annotated to GO term "cell wall organization or biogenesis", in the lateral roots of *P. euphratica* after short-term (i.e. 2 days of 150 mM NaCl exposure) and long-term (i.e. after 12 days of 150 mM NaCl exposure) salt exposure. Red lined box includes upregulated and blue lined box includes downregulated gene families. The number indicates the number of genes out of total number of DEGs from the respective gene family at that time. ↑ indicates upregulation and ↓ indicates downregulation.
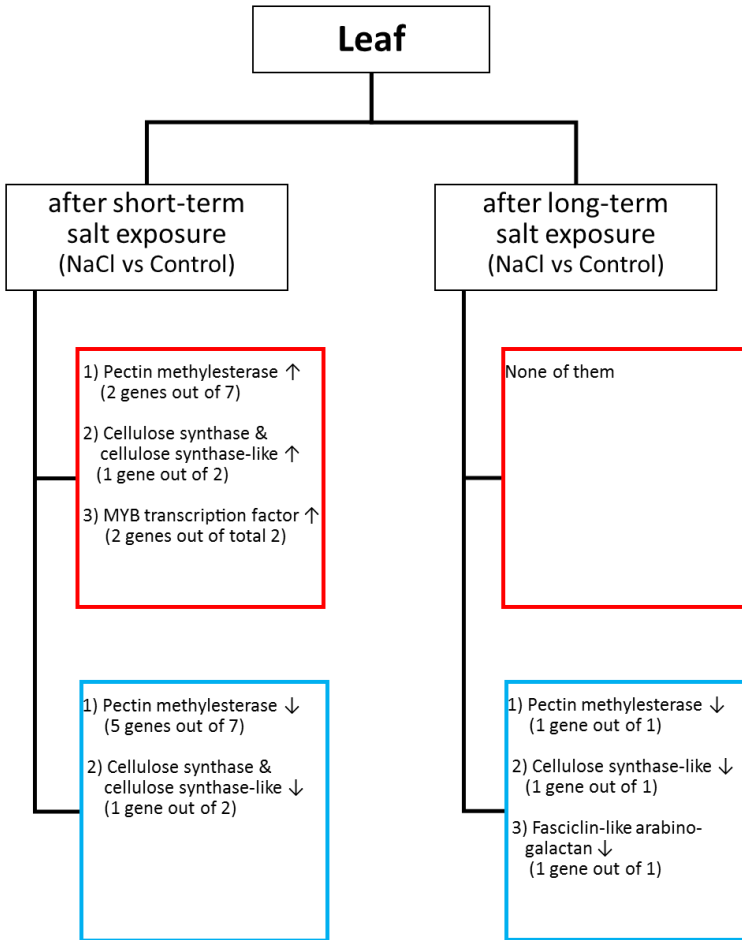
Figure 2.8: A schematic chart showing the regulation of few gene families, annotated to GO term "cell wall organization or biogenesis", in the leaf tissues of *P. euphratica* after short-term (i.e. 2 days of 150 mM NaCl exposure) and long-term (i.e. after 12 days of 150 mM NaCl exposure) salt exposure. Red lined box includes upregulated and blue lined box includes downregulated gene families. The number indicates the number of genes out of total number of DEGs from the respective gene family at that time. ↑ indicates upregulation and ↓ indicates downregulation.

and an increase in water content per unit surface area (Ayala & O'Leary, 1995; Debez et al., 2006; Akcin et al., 2017; Nguyen et al., 2017; Kherraze et al., 2018). The increase in water content per area or an increased fresh-to-dry mass ratio is considered as a hallmark of succulence. After 12 days of exposure to 150 mM NaCl, main roots (MRs) and lateral roots (LRs) of *P. euphratica* showed thickening, though thickening was much more pronounced in MRs than in LRs (Table 2.2). Longitudinal sections showed that the increased thickness in the MRs of salt-treated plants was the result of enhanced production of cortex cells (Fig 2.3D). The dry-to-fresh mass ratio

(DM/FM) indicated that thick roots of *P. euphratica* after long-term salt exposure did not develop succulence (Table 2.3). Therefore, *P. euphratica* adjusts root morphology under high salinity likely to increase the volume for deposition of salt and balancing out ion toxicity (Ottow et al., 2005; S. Chen & Polle, 2010; Hameed et al., 2010).

On the other hand, in the current study, no succulence formation in the leaf under salinity was indicated by the DM/FM of leaves (Table 2.3). The increased leaf thickness in *P. euphratica* was previously observed after 9 weeks of exposure to 150 mM NaCl (Ottow et al., 2005). Therefore, it is possible that morphological adjustments in the leaves, as a measure of protection from ion toxicity, within the period of 150 mM NaCl exposure were still too subtle to be visually detected in the present study.

2.4.3 The tissue accumulation of salt causes the morphological modifications in *P. euphratica* roots under high salinity

With increasing salinity, halophytes perform adaptations by increasing the thickness and succulence of the leaf or stem tissues (Ayala & O'Leary, 1995; Akcin et al., 2017; Nguyen et al., 2017; Kherraze et al., 2018). Debez et al. (2006) showed that higher leaf salt content in the halophyte *Cakile maritima* is associated with increased leaf thickness and succulence. The halophyte *Sesuvium portulacastrum* accumulated large amounts of sodium in both leaf and stem and showed increased leaf and shoot succulence in presence of high external Na$^+$ compared to other ions (D. Wang et al., 2012).

In the present study, salt-stressed MRs of *P. euphratica* was accumulating more Na with increasing exposure to 150 mM NaCl (Fig. 2.4A). This result suggested that long-term salt exposure caused alterations in root morphology in *P. euphratica* due to increasing internal Na content. In the LRs, there was a trend of increasing Na content with increasing exposure, but the Na level in LRs was not that high like MRs under salinity (Fig. 2.4A). This comparatively low Na level might be a reason why LRs did not show pronounce thickness in diameter as in MRs.

Salt treatment decreased K and Ca contents in the roots which can be the result of reduced root uptake under high Na$^+$ concentration in the medium (Table 2.4). However, the content of nutrients in the leaves was nearly unaffected under salinity (Table 2.5). Less negative effects of

salinity on the leaf nutrient levels of *P. euphratica* were observed earlier compared to a hybrid poplar (S. Chen et al., 2001). In a salt-susceptible poplar, the leaf levels of Ca^{2+} and Mg^{2+} were decreased under salinity and this was partially produced by a reduction in stomatal conductance and transpiration (Sharmin et al., 2021). In this study, *P. euphratica* showed the competence to maintain the nutrient levels in the leaves under higher salinity, although transpiration was decreased greatly in salt-treated plants.

2.4.4 GH3::GUS activity reveals that auxin has no evident influence on the morphological alterations of *P. euphratica* roots in response to salinity

Auxin plays a critical role in root growth and development under abiotic stresses including salinity (Korver et al., 2018; van Zelm et al., 2020). The GH3 promoter (named after the discoverer, Gretchen Hagen), first identified in soybean *Glycine max* (L.) Merr., regulates the expression of an auxin-inducible gene (Hagen et al., 1984; Hagen & Guilfoyle, 2002). Genes related to soybean (*Glycine max*) *GH3* encode enzymes that catalyze the conjugation of amino acids with the auxin indole-3-acetic acid (IAA) (Staswick et al., 2005; Q. Chen et al., 2010). Thereby, the active IAA levels are modulated and auxin homeostasis is maintained (Staswick et al., 2005; Q. Chen et al., 2010). In our study, we used *P. euphratica* transformed with the promoter-reporter construct GH3::GUS containing the β-glucuronidase (GUS) reporter gene and the promoter and 5' UTR of soybean *GH3* gene. The β-glucuronidase (GUS) gene is widely used as a gene fusion marker for analysis of gene expression in transformed plants (Jefferson, 1987; Jefferson et al., 1987; Guivarc'h et al., 1996). β-glucuronidase (GUS) functions in the hydrolysis of a wide variety of β-glucuronides such as 5-bromo-4-chloro-3-indolyl-β-D-glucuronic acid (X-Gluc) which is a commercially available histochemical substrate (Jefferson, 1987; Jefferson et al., 1987; Guivarc'h et al., 1996). The substrate X-Gluc is hydrolyzed in the presence of GUS to yield a blue color as the product (Jefferson, 1987; Jefferson et al., 1987; Guivarc'h et al., 1996). GH3::GUS construct has been used to study auxin physiology in many plants including poplar (Bierfreund et al., 2003; Pacios-Bras et al., 2003; Teichmann et al., 2008; Takanashi et al., 2011; Elobeid et al., 2012).

In the present study, GUS staining pattern in MRs and LRs indicated high free auxin levels in the root cap and root meristematic region supporting the role of auxin in promotion of the elongation of roots (Fig. 2.5). Obvious strong differences in the GUS staining pattern in response to salt stress

were not observed, suggesting that the main and lateral root development by the regulation of auxin was not affected in *P. euphratica* under higher salinity. In addition, increased root thickness after long-term salt exposure did not exhibit any changes in the GUS staining (Fig. 2.5). This result suggested no obvious role of auxin for the process of morpho-anatomical modifications of *P. euphratica* roots under salinity.

2.4.5 The regulation of several cell wall associated genes during root thickening reveals their influence in the morphological alterations in *P. euphratica* roots under salinity

During plant growth and development, the cell wall has several biological functions including regulation of cell expansion (Popper, 2008; Chebli & Geitmann, 2017). Each cell is surrounded by a primary cell wall, a structural layer composed of polysaccharides (approx. 90%) and some proteins (approx. 10%) (Doblin et al., 2010; Y. Zhao et al., 2019). The major polysaccharides in the primary cell wall are cellulose, hemicellulose and pectin. In a primary cell wall, cellulose microfibrils are linked with hemicellulose to form the cellulose-hemicellulose network which is embedded in the pectin matrix (Popper, 2008; Chebli & Geitmann, 2017; Y. Zhao et al., 2019).

The polysaccharide synthases and glycosyltransferases (GlyTs) are the key enzymes in wall biogenesis (Doblin et al., 2010). The polysaccharide synthases catalyze the transfer of glycosyl residues from a sugar nucleotide donor to construct the main backbone of wall polysaccharides such as cellulose, hemicellulose, etc. (Doblin et al., 2010). The GlyTs transfer single glycosyl residues from the donor to a polysaccharide backbone (Doblin et al., 2010). Proteins involved in cellulose synthesis are encoded by a large family of cellulose synthase (CesA) genes (Popper, 2008; Doblin et al., 2010). Cellulose synthase-like (Csl) genes encode proteins that are responsible for the synthesis of hemicelluloses (Popper, 2008; Doblin et al., 2010). The xyloglucan endotransglucosylase/hydrolases (XTHs) are enzymes involved in cell wall expansion and re-modeling, cleaving and re-joining xyloglucan (hemicellulose) chains in the xyloglucan–cellulose network (Doblin et al., 2010; Stratilová et al., 2020; De Caroli et al., 2021). Pectin mediated cell wall loosening is as an important factor during cell and tissue morphogenesis (Chebli & Geitmann, 2017). Pectin methyl-esterase (PME) removes ester bond, leading to cell wall loosening (Pelloux et al., 2007; Chebli & Geitmann, 2017).

Cell wall proteins include several enzymes, expansins, wall-associated kinases, glycoproteins etc. (Popper, 2008; Doblin et al., 2010). Expansins are wall proteins that play role in increasing cell wall extensibility (Popper, 2008; Byrt et al., 2018; Lohoff et al., 2021). Genes responsible for expansins can be grouped into four families; EXLA (expansin-like A), EXLB (expansin-like B), EXPA (α-expansins) and EXPB (β-expansins) (Popper, 2008; Lohoff et al., 2021). No enzymatic activity has been assigned to expansins and their functioning mechanism remains elusive (Byrt et al., 2018; Lohoff et al., 2021). Fasciclin-like arabinogalactan proteins (FLAs) are a subclass of arabinogalactan proteins (AGPs), have cell adhesion domains known as fasciclin domains, play role in cell adhesion, shoot development and secondary cell wall synthesis (Johnson et al., 2003; Zang et al., 2015; Hossain et al., 2020).

Moreover, several transcription factors in the NAC and MYB families act as master regulators for modulating the biosynthetic pathways of the secondary wall components cellulose, xylan and lignin, etc. (Zhong & Ye, 2007; C. Li et al., 2014; S. Wang et al., 2014; Eckert et al., 2019; Geng et al., 2020). In the current study, members from PME, EXP, EXL, CesA, Csl, XTH, FLA, MYB and NAC-type transcription factor gene families exhibited differential expressions frequently in the root and leaf tissues under salinity. After short-term salt exposure, PME, EXP, EXL, CesA, Csl, XTH, FLA, MYB and NAC-type transcription factor related genes were predominantly upregulated in MRs indicating the involvement of cell wall remodeling reactions in the modification of main root morphology (Fig. 2.6). The upregulation of cell wall related genes in the short-term salt-stressed MRs suggested that the reactions for new cell wall formation and cell wall extension were stimulated via increased gene expression to modify the root morphology. Plants likely started to increase the production of proteins responsible for manufacturing cell wall components such as cellulose, hemicellulose and regulating cell wall extensibility. However, after long-term salt exposure, genes from all these families exhibited reduced transcript levels in MRs, particularly genes related to cellulose, hemicellulose synthesis, and cellulose-hemicellulose network remodeling (Fig. 2.6). This result suggested that plants initiated adjustment in the synthesis of proteins for cell wall reactions by decreasing gene expressions as thickening of main root already happened to a good extent after long-term salt exposure.

In LRs, the cell wall associated genes showed up- and downregulation after short- and long-term salt exposure (Fig. 2.7). At both time points, genes related to MYB and NAC-type transcription factors were mostly upregulated and genes encoding CesA, Csl, XTH and FLA were mainly downregulated in the salt-stressed LRs (Fig. 2.7). The regulations of many members of all these gene families at both times suggested that modifications in LR morphology by regulating the cell wall modifying reactions was ongoing.

The regulations of the cell wall-related gene families under salinity were less affected in leaves than in roots (Fig. 2.8). This result suggested that the alteration of tissue morphology by the regulation of cell wall modifications was not activated in the leaves.

2.5 Conclusion

P. euphratica responses to higher salinity via an adjustment in root morphology. *P. euphratica* roots become thicker in diameter in response to high salinity. This study indicated that an increase in root thickness was likely stimulated by the internal tissue accumulation of Na^+. The enlarged diameter in the main roots under salinity was shaped by the increased number of cortex cells. The more cell volume in thick roots under salinity than control thin roots may help *P. euphratica* to control salt levels accumulated into the root tissues. Transcriptome analyses indicated the involvement of cell wall modifying genes in the regulation of root morphology adjustment under salinity. *P. euphratica* showed efficiency to deal with negative effects of salinity on gas exchange and repaired photosynthesis rate after salt adaptation. Though root uptake of macronutrients was reduced by salt stress, *P. euphratica* preserved the nutrient contents in the foliar tissues. Therefore, *P. euphratica* exhibits salt tolerance by adapting root morphology and retaining nutrient balance under high salinity. However, it would be interesting to investigate the contribution of this root thickening in the salt tolerance strategy of *P. euphratica* which was not possible in this study.

2.6 Declaration:

I conducted all experiments, analysed data, prepared all tables and figures and wrote the chapter. Dr. Dennis Janz and Dr. Christian Eckert did the preliminary analyses of the RNA-seq data. Prof.

2.7 References

Ahmad, P., & Prasad, M. N. V. (Eds.). (2012). *Abiotic stress responses in plants*. Springer New York. https://doi.org/10.1007/978-1-4614-0634-1

Akcin, T. A., Akcin, A., & Yalcın, E. (2017). Anatomical changes induced by salinity stress in *Salicornia freitagii* (Amaranthaceae). *Brazilian Journal of Botany*, *40*(4), 1013–1018. https://doi.org/10.1007/s40415-017-0393-0

Albert, R. (1975). Salt regulation in halophytes. *Oecologia*, *21*(1), 57–71. https://doi.org/10.1007/BF00345893

Ayala, F., & O'Leary, J. W. (1995). Growth and physiology of *Salicornia bigelovii* Torr. At suboptimal salinity. *International Journal of Plant Sciences*, *156*(2), 197–205. https://doi.org/10.1086/297241

Ben Hamed, K., Dabbous, A., El Shaer, H., & Abdely, C. (2018). Salinity responses and adaptive mechanisms in halophytes and their exploitation for producing salinity tolerant crops. In V. Kumar, S. H. Wani, P. Suprasanna, & L.-S. P. Tran (Eds.), *Salinity Responses and Tolerance in Plants, Volume 2* (pp. 1–19). Springer International Publishing. https://doi.org/10.1007/978-3-319-90318-7_1

Bierfreund, N. M., Reski, R., & Decker, E. L. (2003). Use of an inducible reporter gene system for the analysis of auxin distribution in the moss *Physcomitrella patens*. *Plant Cell Reports*, *21*(12), 1143–1152. https://doi.org/10.1007/s00299-003-0646-1

Brinker, M., Broscheé, M., Vinocur, B., Abo-Ogiala, A., Fayyaz, P., Janz, D., Ottow, E. A., Cullmann, A. D., Saborowski, J., Kangasjärvi, J., Altman, A., & Polle, A. (2010). Linking the salt transcriptome with physiological responses of a salt-resistant *Populus* species as a strategy to identify genes important for stress acclimation. *Plant Physiology*, *154*(4), 1697–1709. https://doi.org/10.1104/pp.110.164152

Burssens, S., Himanen, K., van de Cotte, B., Beeckman, T., Van Montagu, M., Inzé, D., & Verbruggen, N. (2000). Expression of cell cycle regulatory genes and morphological

alterations in response to salt stress in *Arabidopsis thaliana*. *Planta*, *211*(5), 632–640. https://doi.org/10.1007/s004250000334

Byrt, C. S., Munns, R., Burton, R. A., Gilliham, M., & Wege, S. (2018). Root cell wall solutions for crop plants in saline soils. *Plant Science*, *269*, 47–55. https://doi.org/10.1016/j.plantsci.2017.12.012

Chebli, Y., & Geitmann, A. (2017). Cellular growth in plants requires regulation of cell wall biochemistry. *Current Opinion in Cell Biology*, *44*, 28–35. https://doi.org/10.1016/j.ceb.2017.01.002

Chen, Q., Westfall, C. S., Hicks, L. M., Wang, S., & Jez, J. M. (2010). Kinetic basis for the conjugation of auxin by a GH3 family indole-acetic acid-amido synthetase. *Journal of Biological Chemistry*, *285*(39), 29780–29786. https://doi.org/10.1074/jbc.M110.146431

Chen, S., Li, J., Fritz, E., Wang, S., & Hüttermann, A. (2002). Sodium and chloride distribution in roots and transport in three poplar genotypes under increasing NaCl stress. *Forest Ecology and Management*, *168*(1–3), 217–230. https://doi.org/10.1016/S0378-1127(01)00743-5

Chen, S., Li, J., Wang, S., Fritz, E., Hüttermann, A., & Altman, A. (2003). Effects of NaCl on shoot growth, transpiration, ion compartmentation, and transport in regenerated plants of *Populus euphratica* and *Populus tomentosa*. *Canadian Journal of Forest Research*, *33*(6), 967–975. https://doi.org/10.1139/x03-066

Chen, S., Li, J., Wang, S., Hüttermann, A., & Altman, A. (2001). Salt, nutrient uptake and transport, and ABA of *Populus euphratica*; a hybrid in response to increasing soil NaCl. *Trees*, *15*(3), 186–194. https://doi.org/10.1007/s004680100091

Chen, S., & Polle, A. (2010). Salinity tolerance of *Populus*. *Plant Biology*, *12*(2), 317–333. https://doi.org/10.1111/j.1438-8677.2009.00301.x

Chen, S., Zhou, Y., Chen, Y., & Gu, J. (2018). fastp: An ultra-fast all-in-one FASTQ preprocessor. *Bioinformatics*, *34*(17), i884–i890. https://doi.org/10.1093/bioinformatics/bty560

De Caroli, M., Manno, E., Piro, G., & Lenucci, M. S. (2021). Ride to cell wall: Arabidopsis XTH11, XTH29 and XTH33 exhibit different secretion pathways and responses to heat and drought stress. *The Plant Journal*, *107*(2), 448–466. https://doi.org/10.1111/tpj.15301

Debez, A., Saadaoui, D., Ramani, B., Ouerghi, Z., Koyro, H.-W., Huchzermeyer, B., & Abdelly, C. (2006). Leaf H^+-ATPase activity and photosynthetic capacity of *Cakile maritima* under increasing salinity. *Environmental and Experimental Botany*, *57*(3), 285–295. https://doi.org/10.1016/j.envexpbot.2005.06.009

Doblin, M. S., Pettolino, F., & Bacic, A. (2010). Plant cell walls: The skeleton of the plant world. *Functional Plant Biology*, *37*(5), 357. https://doi.org/10.1071/FP09279

Eckert, C., Sharmin, S., Kogel, A., Yu, D., Kins, L., Strijkstra, G.-J., & Polle, A. (2019). What makes the wood? Exploring the molecular mechanisms of xylem acclimation in hardwoods to an ever-changing environment. *Forests*, *10*(4), 358. https://doi.org/10.3390/f10040358

Elobeid, M., Göbel, C., Feussner, I., & Polle, A. (2012). Cadmium interferes with auxin physiology and lignification in poplar. *Journal of Experimental Botany*, *63*(3), 1413–1421. https://doi.org/10.1093/jxb/err384

Estravis-Barcala, M., Mattera, M. G., Soliani, C., Bellora, N., Opgenoorth, L., Heer, K., & Arana, M. V. (2020). Molecular bases of responses to abiotic stress in trees. *Journal of Experimental Botany*, *71*(13), 3765–3779. https://doi.org/10.1093/jxb/erz532

Farquhar, G. D., & Sharkey, T. D. (1982). Stomatal conductance and photosynthesis. *Annual Review of Plant Physiology*, *33*(1), 317–345. https://doi.org/10.1146/annurev.pp.33.060182.001533

Flowers, T. J., & Colmer, T. D. (2008). Salinity tolerance in halophytes. *New Phytologist*, *179*(4), 945–963. https://doi.org/10.1111/j.1469-8137.2008.02531.x

Flowers, T. J., & Colmer, T. D. (2015). Plant salt tolerance: Adaptations in halophytes. *Annals of Botany*, *115*(3), 327–331. https://doi.org/10.1093/aob/mcu267

Flowers, T. J., Troke, P. F., & Yeo, A. R. (1977). The mechanism of salt tolerance in halophytes. *Annual Review of Plant Physiology*, *28*(1), 89–121. https://doi.org/10.1146/annurev.pp.28.060177.000513

Gene Ontology Consortium. (2004). The Gene Ontology (GO) database and informatics resource. *Nucleic Acids Research*, *32*(90001), 258D – 261. https://doi.org/10.1093/nar/gkh036

Geng, P., Zhang, S., Liu, J., Zhao, C., Wu, J., Cao, Y., Fu, C., Han, X., He, H., & Zhao, Q. (2020). MYB20, MYB42, MYB43, and MYB85 regulate phenylalanine and lignin biosynthesis

during secondary cell wall formation. *Plant Physiology*, *182*(3), 1272–1283. https://doi.org/10.1104/pp.19.01070

Gu, R., Fonseca, S., Puskás, L. G., Hackler, L., Jr., Zvara, Á., Dudits, D., & Pais, M. S. (2004). Transcript identification and profiling during salt stress and recovery of *Populus euphratica*. *Tree Physiology*, *24*(3), 265–276. https://doi.org/10.1093/treephys/24.3.265

Guivarc'h, A., Caissard, J. C., Azmi, A., Elmayan, T., Chriqui, D., & Tepfer, M. (1996). *In situ* detection of expression of the gus reporter gene in transgenic plants: Ten years of blue genes. *Transgenic Research*, *5*(5), 281–288. https://doi.org/10.1007/BF01968938

Hagen, G., & Guilfoyle, T. (2002). Auxin-responsive gene expression: Genes, promoters and regulatory factors. *Plant Molecular Biology*, *49*(3), 373–385. https://doi.org/10.1023/A:1015207114117

Hagen, G., Kleinschmidt, A., & Guilfoyle, T. (1984). Auxin-regulated gene expression in intact soybean hypocotyl and excised hypocotyl sections. *Planta*, *162*(2), 147–153. https://doi.org/10.1007/BF00410211

Hameed, M., Ashraf, M., Ahmad, M. S. A., & Naz, N. (2010). Structural and functional adaptations in plants for salinity tolerance. In M. Ashraf, M. Ozturk, & M. S. A. Ahmad (Eds.), *Plant Adaptation and Phytoremediation* (pp. 151–170). Springer Netherlands. https://doi.org/10.1007/978-90-481-9370-7_8

Hewitt, E. J., & Smith, T. A. (1975). *Plant mineral nutrition*. English Universities Press.

Hori, C., Yu, X., Mortimer, J. C., Sano, R., Matsumoto, T., Kikuchi, J., Demura, T., & Ohtani, M. (2020). Impact of abiotic stress on the regulation of cell wall biosynthesis in *Populus trichocarpa*. *Plant Biotechnology*, *37*(3), 273–283. https://doi.org/10.5511/plantbiotechnology.20.0326a

Hossain, Md. S., Ahmed, B., Ullah, Md. W., Aktar, N., Haque, Md. S., & Islam, Md. S. (2020). Genome-wide identification of fasciclin-like arabinogalactan proteins in jute and their expression pattern during fiber formation. *Molecular Biology Reports*, *47*(10), 7815–7829. https://doi.org/10.1007/s11033-020-05858-w

Janz, D., Lautner, S., Wildhagen, H., Behnke, K., Schnitzler, J.-P., Rennenberg, H., Fromm, J., & Polle, A. (2012). Salt stress induces the formation of a novel type of 'pressure wood' in

two *Populus* species. *New Phytologist*, *194*(1), 129–141. https://doi.org/10.1111/j.1469-8137.2011.03975.x

Jefferson, R. A. (1987). Assaying chimeric genes in plants: The GUS gene fusion system. *Plant Molecular Biology Reporter*, *5*(4), 387–405. https://doi.org/10.1007/BF02667740

Jefferson, R. A., Kavanagh, T. A., & Bevan, M. W. (1987). GUS fusions: β-glucuronidase as a sensitive and versatile gene fusion marker in higher plants. *The EMBO Journal*, *6*(13), 3901–3907. https://doi.org/10.1002/j.1460-2075.1987.tb02730.x

Johnson, K. L., Jones, B. J., Bacic, A., & Schultz, C. J. (2003). The fasciclin-like arabinogalactan proteins of Arabidopsis. A multigene family of putative cell adhesion molecules. *Plant Physiology*, *133*(4), 1911–1925. https://doi.org/10.1104/pp.103.031237

Junghans, U., Polle, A., Düchting, P., Weiler, E., Kuhlman, B., Gruber, F., & Teichmann, T. (2006). Adaptation to high salinity in poplar involves changes in xylem anatomy and auxin physiology. *Plant, Cell & Environment*, *29*(8), 1519–1531. https://doi.org/10.1111/j.1365-3040.2006.01529.x

Kherraze, M. E., Belhamra, M., & Grigore, M.-N. (2018). Aspects of ecological anatomy of *Traganum nudatum* Del. (Amaranthaceae) from the Northeast of the Algerian Sahara. *Acta Biologica Szegediensis*, *62*(1), 25–36. https://doi.org/10.14232/abs.2018.1.25-36

Korver, R. A., Koevoets, I. T., & Testerink, C. (2018). Out of shape during stress: A key role for auxin. *Trends in Plant Science*, *23*(9), 783–793. https://doi.org/10.1016/j.tplants.2018.05.011

Lamalakshmi Devi, E., Kumar, S., Basanta Singh, T., Sharma, S. K., Beemrote, A., Devi, C. P., Chongtham, S. K., Singh, C. H., Yumlembam, R. A., Haribhushan, A., Prakash, N., & Wani, S. H. (2017). Adaptation strategies and defence mechanisms of plants during environmental stress. In M. Ghorbanpour & A. Varma (Eds.), *Medicinal Plants and Environmental Challenges* (pp. 359–413). Springer International Publishing. https://doi.org/10.1007/978-3-319-68717-9_20

Langmead, B., & Salzberg, S. L. (2012). Fast gapped-read alignment with Bowtie 2. *Nature Methods*, *9*(4), 357–359. https://doi.org/10.1038/nmeth.1923

Leplé, J., Brasileiro, A., Michel, M., Delmotte, F., & Jouanin, L. (1992). Transgenic poplars: Expression of chimeric genes using four different constructs. *Plant Cell Reports*, *11*(3), 137–141. https://doi.org/10.1007/BF00232166

Li, C., Wang, X., Lu, W., Liu, R., Tian, Q., Sun, Y., & Luo, K. (2014). A poplar R2R3-MYB transcription factor, PtrMYB152, is involved in regulation of lignin biosynthesis during secondary cell wall formation. *Plant Cell, Tissue and Organ Culture (PCTOC)*, *119*(3), 553–563. https://doi.org/10.1007/s11240-014-0555-8

Li, H., Yan, S., Zhao, L., Tan, J., Zhang, Q., Gao, F., Wang, P., Hou, H., & Li, L. (2014). Histone acetylation associated up-regulation of the cell wall related genes is involved in salt stress induced maize root swelling. *BMC Plant Biology*, *14*(1), 105. https://doi.org/10.1186/1471-2229-14-105

Lloyd, G., & McCown, B. (1980). Commercially-feasible micropropagation of mountain laurel, *Kalmia latifolia*, by use of shoot-tip culture. *Proceedings of International Plant Propagators' Society*, *30*, 421–427. https://www.cabdirect.org/cabdirect/abstract/19830315515

Lohoff, C., Buchholz, P. C. F., Le Roes-Hill, M., & Pleiss, J. (2021). Expansin Engineering Database: A navigation and classification tool for expansins and homologues. *Proteins: Structure, Function, and Bioinformatics*, *89*(2), 149–162. https://doi.org/10.1002/prot.26001

Love, M. I., Huber, W., & Anders, S. (2014). Moderated estimation of fold change and dispersion for RNA-seq data with DESeq2. *Genome Biology*, *15*(12), 550. https://doi.org/10.1186/s13059-014-0550-8

Ma, H.-C., Fung, L., Wang, S.-S., Altman, A., & Hüttermann, A. (1997). Photosynthetic response of *Populus euphratica* to salt stress. *Forest Ecology and Management*, *93*(1), 55–61. https://doi.org/10.1016/S0378-1127(96)03943-6

Mantovani, A. (1999). A method to improve leaf succulence quantification. *Brazilian Archives of Biology and Technology*, *42*(1). https://doi.org/10.1590/S1516-89131999000100002

Metternicht, G. I., & Zinck, J. A. (2003). Remote sensing of soil salinity: Potentials and constraints. *Remote Sensing of Environment*, *85*(1), 1–20. https://doi.org/10.1016/S0034-4257(02)00188-8

Moss, D. N., & Rawlins, S. L. (1963). Concentration of carbon dioxide inside leaves. *Nature*, *197*(4874), 1320–1321. https://doi.org/10.1038/1971320a0

Mu, W., Wei, J., Yang, T., Fan, Y., Cheng, L., Yang, J., Mu, R., Liu, J., Zhao, J., Sun, W., Xu, X., Liu, X., Drmanac, R., & Liu, H. (2017). RNA extraction for plant samples using CTAB-pBIOZOL. *Protocols.Io*. https://doi.org/10.17504/protocols.io.gsnbwde

Müller, A., Volmer, K., Mishra-Knyrim, M., & Polle, A. (2013). Growing poplars for research with and without mycorrhizas. *Frontiers in Plant Science*, *4*, 332. https://doi.org/10.3389/fpls.2013.00332

Munns, R., & Gilliham, M. (2015). Salinity tolerance of crops – what is the cost? *New Phytologist*, *208*(3), 668–673. https://doi.org/10.1111/nph.13519

Nguyen, H. T., Meir, P., Sack, L., Evans, J. R., Oliveira, R. S., & Ball, M. C. (2017). Leaf water storage increases with salinity and aridity in the mangrove *Avicennia marina*: Integration of leaf structure, osmotic adjustment and access to multiple water sources. *Plant, Cell & Environment*, *40*(8), 1576–1591. https://doi.org/10.1111/pce.12962

Ottow, E. A., Brinker, M., Teichmann, T., Fritz, E., Kaiser, W., Brosché, M., Kangasjärvi, J., Jiang, X., & Polle, A. (2005). *Populus euphratica* displays apoplastic sodium accumulation, osmotic adjustment by decreases in calcium and soluble carbohydrates, and develops leaf succulence under salt stress. *Plant Physiology*, *139*(4), 1762–1772. https://doi.org/10.1104/pp.105.069971

Pacios-Bras, C., Schlaman, H. R. M., Boot, K., Admiraal, P., Mateos Langerak, J., Stougaard, J., & Spaink, H. P. (2003). Auxin distribution in *Lotus japonicus* during root nodule development. *Plant Molecular Biology*, *52*(6), 1169–1180. https://doi.org/10.1023/B:PLAN.0000004308.78057.f5

Paul, S., Wildhagen, H., Janz, D., Teichmann, T., Hänsch, R., & Polle, A. (2016). Tissue- and cell-specific cytokinin activity in *Populus × canescens* monitored by *ARR5::GUS* reporter lines in summer and winter. *Frontiers in Plant Science*, *7*. https://doi.org/10.3389/fpls.2016.00652

Pelloux, J., Rusterucci, C., & Mellerowicz, E. (2007). New insights into pectin methylesterase structure and function. *Trends in Plant Science*, *12*(6), 267–277. https://doi.org/10.1016/j.tplants.2007.04.001

Polle, A., & Chen, S. (2015). On the salty side of life: Molecular, physiological and anatomical adaptation and acclimation of trees to extreme habitats. *Plant, Cell & Environment*, *38*(9), 1794–1816. https://doi.org/10.1111/pce.12440

Popper, Z. (2008). Evolution and diversity of green plant cell walls. *Current Opinion in Plant Biology*, *11*(3), 286–292. https://doi.org/10.1016/j.pbi.2008.02.012

R Core Team. (2018). *R: A language and environment for statistical computing*. R Foundation for Statistical Computing, Vienna, Austria. https://www.r-project.org/

Sharmin, S., Lipka, U., Polle, A., & Eckert, C. (2021). The influence of transpiration on foliar accumulation of salt and nutrients under salinity in poplar (*Populus × canescens)*. *PLOS ONE*, *16*(6), e0253228. https://doi.org/10.1371/journal.pone.0253228

Staswick, P. E., Serban, B., Rowe, M., Tiryaki, I., Maldonado, M. T., Maldonado, M. C., & Suza, W. (2005). Characterization of an Arabidopsis enzyme family that conjugates amino acids to indole-3-acetic acid. *The Plant Cell*, *17*(2), 616–627. https://doi.org/10.1105/tpc.104.026690

Stratilová, B., Kozmon, S., Stratilová, E., & Hrmova, M. (2020). Plant xyloglucan xyloglucosyl transferases and the cell wall structure: Subtle but significant. *Molecules*, *25*(23), 5619. https://doi.org/10.3390/molecules25235619

Suárez, N., & Sobrado, M. A. (2000). Adjustments in leaf water relations of mangrove (*Avicennia germinans*) seedlings grown in a salinity gradient. *Tree Physiology*, *20*(4), 277–282. https://doi.org/10.1093/treephys/20.4.277

Sun, J., Chen, S., Dai, S., Wang, R., Li, N., Shen, X., Zhou, X., Lu, C., Zheng, X., Hu, Z., Zhang, Z., Song, J., & Xu, Y. (2009). NaCl-induced alternations of cellular and tissue ion fluxes in roots of salt-resistant and salt-sensitive poplar species. *Plant Physiology*, *149*(2), 1141–1153. https://doi.org/10.1104/pp.108.129494

Takanashi, K., Sugiyama, A., & Yazaki, K. (2011). Involvement of auxin distribution in root nodule development of *Lotus japonicus*. *Planta*, *234*(1), 73–81. https://doi.org/10.1007/s00425-011-1385-0

Tan, J., Ben-Gal, A., Shtein, I., Bustan, A., Dag, A., & Erel, R. (2020). Root structural plasticity enhances salt tolerance in mature olives. *Environmental and Experimental Botany*, *179*, 104224. https://doi.org/10.1016/j.envexpbot.2020.104224

Teichmann, T., Bolu-Arianto, W. H., Olbrich, A., Langenfeld-Heyser, R., Gobel, C., Grzeganek, P., Feussner, I., Hansch, R., & Polle, A. (2008). GH3::GUS reflects cell-specific developmental patterns and stress-induced changes in wood anatomy in the poplar stem. *Tree Physiology*, *28*(9), 1305–1315. https://doi.org/10.1093/treephys/28.9.1305

Tominaga, J., Shimada, H., & Kawamitsu, Y. (2018). Direct measurement of intercellular CO_2 concentration in a gas-exchange system resolves overestimation using the standard method. *Journal of Experimental Botany*, *69*(8), 1981–1991. https://doi.org/10.1093/jxb/ery044

van Zelm, E., Zhang, Y., & Testerink, C. (2020). Salt tolerance mechanisms of plants. *Annual Review of Plant Biology*, *71*(1), 403–433. https://doi.org/10.1146/annurev-arplant-050718-100005

Vijayan, K., Chakraborti, S. P., Ercisli, S., & Ghosh, P. D. (2008). NaCl induced morpho-biochemical and anatomical changes in mulberry (*Morus* spp.). *Plant Growth Regulation*, *56*(1), 61–69. https://doi.org/10.1007/s10725-008-9284-5

Wang, D., Wang, H., Han, B., Wang, B., Guo, A., Zheng, D., Liu, C., Chang, L., Peng, M., & Wang, X. (2012). Sodium instead of potassium and chloride is an important macronutrient to improve leaf succulence and shoot development for halophyte *Sesuvium portulacastrum*. *Plant Physiology and Biochemistry*, *51*, 53–62. https://doi.org/10.1016/j.plaphy.2011.10.009

Wang, M., Zhang, L., Zhang, Z., Li, M., Wang, D., Zhang, X., Xi, Z., Keefover-Ring, K., Smart, L. B., DiFazio, S. P., Olson, M. S., Yin, T., Liu, J., & Ma, T. (2020). Phylogenomics of the genus *Populus* reveals extensive interspecific gene flow and balancing selection. *New Phytologist*, *225*(3), 1370–1382. https://doi.org/10.1111/nph.16215

Wang, S., Li, E., Porth, I., Chen, J.-G., Mansfield, S. D., & Douglas, C. J. (2014). Regulation of secondary cell wall biosynthesis by poplar R2R3 MYB transcription factor PtrMYB152 in *Arabidopsis*. *Scientific Reports*, *4*(1), 5054. https://doi.org/10.1038/srep05054

Woodward, A. W., & Bartel, B. (2005). Auxin: Regulation, action, and interaction. *Annals of Botany*, *95*(5), 707–735. https://doi.org/10.1093/aob/mci083

Zang, L., Zheng, T., Chu, Y., Ding, C., Zhang, W., Huang, Q., & Su, X. (2015). Genome-wide analysis of the fasciclin-like arabinogalactan protein gene family reveals differential expression patterns, localization, and salt stress response in *Populus*. *Frontiers in Plant Science*, *6*, 1140. https://doi.org/10.3389/fpls.2015.01140

Zeng, F., Yan, H., & Arndt, S. K. (2009). Leaf and whole tree adaptations to mild salinity in field grown *Populus euphratica*. *Tree Physiology*, *29*(10), 1237–1246. https://doi.org/10.1093/treephys/tpp055

Zhao, C., Zhang, H., Song, C., Zhu, J.-K., & Shabala, S. (2020). Mechanisms of plant responses and adaptation to soil salinity. *The Innovation*, *1*(1), 100017. https://doi.org/10.1016/j.xinn.2020.100017

Zhao, Y., Man, Y., Wen, J., Guo, Y., & Lin, J. (2019). Advances in imaging plant cell walls. *Trends in Plant Science*, *24*(9), 867–878. https://doi.org/10.1016/j.tplants.2019.05.009

Zhong, R., & Ye, Z.-H. (2007). Regulation of cell wall biosynthesis. *Current Opinion in Plant Biology*, *10*(6), 564–572. https://doi.org/10.1016/j.pbi.2007.09.001

2.8 Supplementary materials – chapter 2

Supplementary Table S2.1: Table showing the changes in expressions (Fold change = NaCl/Control) of all genes obtained from transcriptome analysis of root tips (main roots), lateral roots and leaves of *P. euphratica* after short term (Tp1 = after 2 days of 150 mM NaCl exposure) and long-term (Tp2 = after 12 days of 150 mM NaCl exposure) salt exposure.

Supplementary Table S2.2: A list of all genes involved in plant "cell wall organization or biogenesis" expressed in different tissues of *P. euphratica* plant. This list was obtained after screening our study data set (Table S2.1) based on the complete gene list of the GO term "Cell Wall Organization or Biogenesis" (Accession: GO:0071554).

Supplementary Table S2.3: A list of differentially expressed genes (DEGs) involved in plant "cell wall organization or biogenesis" expressed in different tissues of *P. euphratica* plant under salt stress compared to control after short-term salt exposure (time point 1).

Supplementary Table S2.4: A list of differentially expressed genes (DEGs) involved in plant "cell wall organization or biogenesis" expressed in different tissues of *P. euphratica* plant under salt stress compared to control after long-term salt exposure (time point 2).

Chapter 3: Salt-induced root thickening contributes to salt tolerance of *Populus euphratica* by limiting Na$^+$ accumulation and maintaining ion homeostasis

3.1 Introduction

Soil salinity is a worldwide environmental challenge for agriculture and forestry because of detrimental effects on plant growth (Chen and Polle, 2010; Polle and Chen, 2015). The salt-affected areas are still expanding due to natural causes like rock weathering and human induced salinization (Rengasamy, 2006; Hassani et al., 2020). To combat land loss, the cultivation of salt-tolerant plants is crucial. Among woody species, *Populus euphratica* is equipped with a number of molecular and physiological features that enable this species to survive higher levels of salinity than many other tree species (Gu et al., 2004; Ma et al., 2013, 2015; Zhang et al., 2020b). Therefore, *P. euphratica* is widely used as model for salt tolerance in woody species.

Coping with salinity principally depends on the plants´ ability to protect their cytosol from Na$^+$ toxicity by maintaining favorable ion balances (Munns and Tester, 2008). The strategies to manage Na$^+$ levels include limiting Na$^+$ uptake, promoting Na$^+$ compartmentalization into vacuoles, extruding Na$^+$ out of the cell (Tester and Davenport, 2003; Munns and Tester, 2008; Deinlein et al., 2014) and salt dilution by development of succulent leaves (Ottow et al., 2005a). *P. euphratica* exhibits a greater restriction on the root uptake and transport of Na$^+$ than salt-sensitive poplars (Chen et al., 2002, 2003). In addition, this species keeps Na$^+$ preferentially in the apoplast rather than the vacuole, although vacuolar sequestration increases with extended salt exposure (Chen et al., 2002, 2003; Ottow et al., 2005a). A highly active Na$^+$ extrusion system in the plasma membrane (PM) benefits *P. euphratica* cells to avoid excess Na$^+$ levels (Sun et al., 2009). Na$^+$ efflux from the cell and sequestration into vacuoles are performed by SOS1 and NHX type Na$^+$/H$^+$ antiporters, respectively (Apse et al., 1999; Shi et al., 2002; Yokoi et al., 2002). Genes encoding Na$^+$/H$^+$ antiporters i.e. *PeSOS1*, *PeNHX1-6* and *PeNhaD1* were characterized in *P. euphratica* and function in salt tolerance (Ottow et al., 2005b; Wu et al., 2007; Ye et al., 2009).

Na$^+$ extrusion is an energy-dependent process, as ions have to move against their electrochemical gradient, and the proton-motive force generated by the H$^+$-ATPases or pyrophosphatases (H$^+$-PPiase) powers the action of Na$^+$/H$^+$ antiporters (Yang et al., 2007a; Zhang et al., 2020a; Blumwald et al., 2000; van Zelm et al., 2020). Increased PM H$^+$-ATPase activity and protein abundance were observed in *P. euphratica* in response to salt exposure (Zhang et al., 2007; Yang et al., 2007b; Ma et al., 2010; Yao et al., 2020).

Salt acclimation, which requires the stimulation of salt-induced PM H$^+$-coupled transport systems (H$^+$-ATPase and Na$^+$/H$^+$ antiporter), occurs via a stress signal transduction pathway involving increases in H$_2$O$_2$ production by stimulating NADPH oxidase activity (Sun et al., 2010b). NADPH oxidases, also known in plants as respiratory burst oxidase homolog (RBOH) proteins, catalyze the formation of superoxide, which is then converted to H$_2$O$_2$ by superoxide dismutase (SOD) (McCord and Fridovich, 1969; Sagi and Fluhr, 2006). Increased endogenous H$_2$O$_2$ levels subsequently mediate elevation in cytosolic Ca^{2+} concentration ([Ca^{2+}]$_{cyt}$) in salt-stressed *P. euphratica* cells (Sun et al., 2010b). The salt-induced H$_2$O$_2$ and [Ca^{2+}]$_{cyt}$ signaling contribute to salt resistance of *P. euphratica* by stimulating PM H$^+$-ATPase and Na$^+$/H$^+$ antiporter activity, and by triggering K$^+$/Na$^+$ homeostasis (Zhang et al., 2007; Sun et al., 2009, 2010a, 2010b, 2012). The stimulated PM H$^+$-ATPase activity facilitates K$^+$/Na$^+$ homeostasis by reducing NaCl-induced K$^+$ loss via depolarization-activated channels, i.e. the outward-rectifying K$^+$ channels (KORCs) and the nonselective cation channels (NSCCs) (Sun et al., 2009; Zhang et al., 2020a). Elevated [Ca^{2+}]$_{cyt}$ is also known to stimulate Na$^+$ extrusion through the SOS signaling pathway, where SOS3 senses the calcium signal and then interacts with SOS2, and finally activates SOS1, an Na$^+$/H$^+$ antiporter (Zhu, 2001, 2002, 2003; Quintero et al., 2011). Furthermore, the tonoplast Na$^+$/H$^+$ exchanger is regulated by the SOS pathway (Qiu et al., 2004). Collectively, the cellular regulation of these systems mediates K$^+$/Na$^+$ homeostasis in *P. euphratica* cells (Polle and Chen, 2015).

In higher plants, the Ca^{2+} signal can be sensed by proteins from different families: Calmodulin (CAM) (Luan et al., 2002; McCormack et al., 2005), Calmodulin-like proteins (CMLs) (McCormack et al., 2005), Calcineurin B-like proteins (CBLs) (Kudla et al., 1999; Luan et al., 2002), and calcium-dependent protein kinases (CDPKs) (Cheng et al., 2002). CBL family sensors decode the Ca^{2+} signal by interacting with CBL-interacting protein kinases (CIPKs) (Shi et al., 1999; Tang et al., 2020;

Weinl and Kudla, 2009). A well-characterized CBL-CIPK interaction complex is the SOS signaling network, formed by the SOS3/CBL4-SOS2/CIPK24 complex. CBL and CIPK candidate genes were identified in *P. trichocarpa* (Yu et al., 2007; Zhang et al., 2008). *CBL*s from *P. euphratica (PeCBLs)* were isolated as well and their upregulation under multiple abiotic stresses including salinity suggested an important role in stress resistance (Zhang et al., 2008; Li et al., 2012, 2013). Each component of the SOS pathway was functionally characterized in *P. trichocarpa* (Tang et al., 2010, 2014). SOS1 and SOS2/PeCIPK26 have also been functionally characterized in *P. euphratica,* showing interaction of PeCIPK26 with PeCBL4 (Zhang et al., 2013; Lv et al., 2014). The transcriptional responses of *PeCBL*s to salinity stress were studied in leaves (Zhang et al., 2013; Lv et al., 2014) but not in other tissues of *P. euphratica*. Very little is known about the expression patterns of other Ca^{2+} sensors, e.g., *CAM*s, under salt stress (Gu et al., 2004; Chang et al., 2006). Information on the expression patterns of *CML*s and *CDPK*s in *P. euphratica* acclimated to high salinity is not available. Overall, comprehensive expression analyses for components involved in the pathways for salt sensing, signaling, uptake and extrusion in combination with salt uptake under acute and long-term stress are still lacking.

In the present study, we aimed to characterize salt uptake in roots after short- and long-term acclimation to high salinity in combination with the transcriptional regulation of genes involved in mediating salt tolerance of *P. euphratica*. Long-term acclimation resulted in morphological changes in root anatomy leading to pronounced root thickening of the main root. We hypothesized that thick roots accumulate less salt than thin roots. We measured the enrichment of Na^+ in the thick and thin roots under salinity using the radioactive $^{22}Na^+$ tracer. Extrusion of Na^+ from both types of roots was also studied to distinguish the strategy applied by thick roots between either less Na^+ uptake or immediate discharge. The expression patterns of the molecular networks likely involved in salt signaling and ion homeostasis of *P. euphratica* cells were explored by RNA sequencing in the control and salt-exposed roots before and after thickening. We found that salt-induced thick roots contribute to Na^+ homeostasis in *P. euphratica* under salinity requiring only moderate stress regulation for stress adaptation.

3.2. Materials and methods

3.2.1 Propagation and cultivation of plant

Plantlets of *P. euphratica* (clone B2 from Ein Avdat valley in Israel) were multiplied by *in vitro* micropropagation according to Leplé et al. (1992). The stem cuttings (approximately 1 to 2 cm long), each having at least one leaf, were transferred onto Woody Plant Medium (Lloyd and McCown, 1980) under sterile conditions and incubated in a culture room under controlled conditions [16 h light / 8 h dark, 150 µmol m^{-2} s^{-1} photosynthetically active radiation (PAR) (Lamp: L 18W/840 cool white, Osram, Munich, Germany), 22 to 25 °C, 40 to 50 % relative air humidity] for five or six weeks as described by Müller et al. (2013). Afterwards, rooted plants were transferred into an aerated hydroponic culture system with Long-Ashton (LA) nutrient solution (Hewitt and Smith, 1975), which was exchanged weekly.

3.2.2 Salt treatments

For the salt treatments, LA solution was prepared with NaCl (with the concentrations indicated below) and the plants were transferred into the salt-containing solution. Controls were transferred into LA without NaCl addition. Plants (mean heights: 19 ± 3 cm) were adapted to salt by exposing them to 50 mM NaCl for 1 day followed by 100 mM NaCl for 2 days, and finally to 150 mM NaCl (Fig. 3.1A). The plants were kept in LA solution with or without 150 mM NaCl until the ^{22}Na$^+$ labelling experiments, exchanging the nutrient solution weekly (Fig. 3.1A). A total of 40 plants per treatment was used. The root system produced thin and thick root tips under elevated salinity, while the controls had only thin root tips (Fig. 3.2A, B).

3.2.3 Na$^+$ enrichment after short-term ^{22}Na$^+$ labeling

To determine short-term Na$^+$ enrichment in thick and thin roots, radioactive tracer experiments with ^{22}Na$^+$ were performed after four weeks of growth with salt-acclimated and control plants (Fig. 3.1B). The poplar plants were transferred in a climatized room [20 to 23 °C air temperature, 40 to 50 % relative air humidity, 150 µmol m^{-2} s^{-1} PAR (Lamp: 3071/400 HI-I, Adolf Schuch GmbH, Worms, Germany), 16h light per day]. Control and salt-acclimated plants were exposed to low (10 mM) or high (150 mM) NaCl in hydroponic LA solution, resulting in four treatment groups:

low salt control (thin roots), high salt-shock (thin roots), high salt-acclimated (thick roots), high salt release (plants transferred from high to low salt, thick roots) (n = 20 plants per treatment group). Inclusion of low NaCl (10 mM) concentrations in the LA solution was necessary for the ^{22}Na labelling experiments since the specific activity of Na$^+$ cannot be accurately determined in the absence of sodium. Immediately after exposure of a plant to the treatment, an attached root
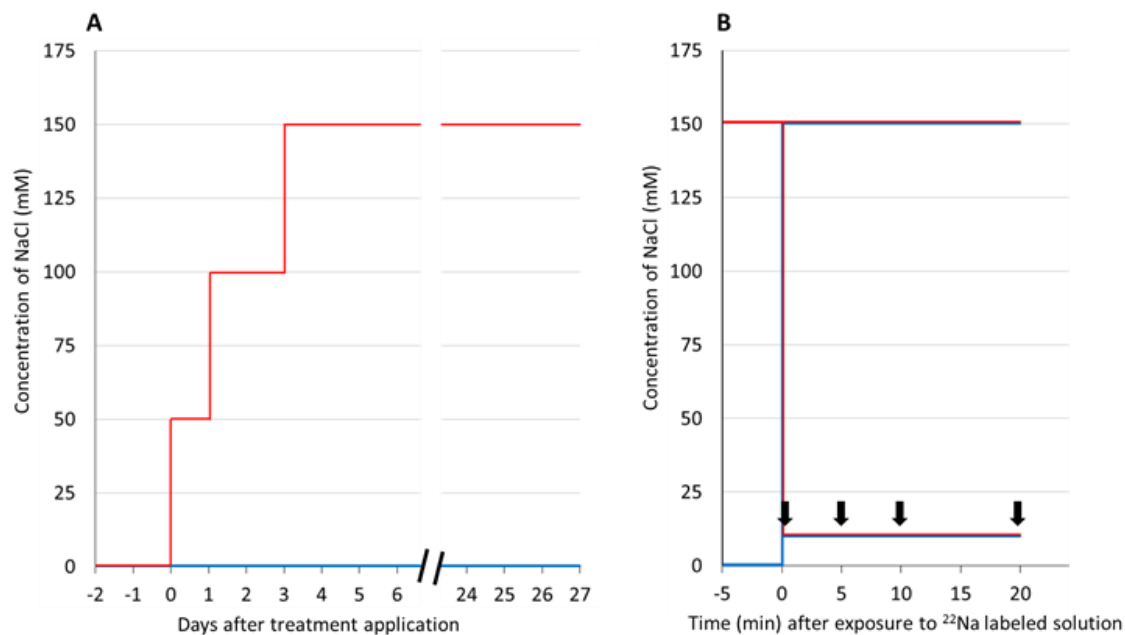

Figure 3.1: Schematic presentation of the steps of salt adaptation (A) and radioactive tracer experiment (B). During salt treatment application (A), salt-treated *P. euphratica* plants (red line) were gradually adapted to higher NaCl concentration by exposing them to 50 mM NaCl Long-Ashton (LA) solution for 1 day followed by 100 mM NaCl LA solution for 2 days and finally to 150 mM NaCl LA solution. Control plants (blue line) were grown in LA solution (no NaCl) simultaneously. After gradual salt adaptation, plants were maintained in LA solution without NaCl (Control: blue line) or with 150 mM NaCl (Salt: red line) by exchanging solution weekly (A). Radioactive tracer experiment was performed on the 27th day of salt adaptation (B). For this experiment, plants from salt and control groups were divided into two sub-groups (B). The whole root system of each plant (except a single root) from one sub-group of control (blue line) and one sub-group of salt (red line) was exposed to 10 mM NaCl LA solution (B). Similarly, the second sub-group of control (blue line) and salt (red line) was exposed to 150 mM NaCl LA solution (B). Concurrently, a single root from each plant (attached to the plant) was placed into a vessel containing 10 mM or 150 mM NaCl LA solution supplemented with ^{22}Na$^+$ (labeled solution). Root tips were exposed in the labeled solution for 0 min, 5 min, 10 min and 20 min. At the end of every exposure period, the root tip was cut off from the plant, washed with non-labeled exposure solution and collected for the radioactivity measurement.

was placed with the tip to a length of about 2 cm in a vessel (Micro tube 1.5 ml, Sarstedt, Nümbrecht, Germany) containing the treatment solution supplemented with 29 to 27 KBq $^{22}Na^+$ ml^{-1} (PerkinElmer, Waltham, USA), referred to as labeled solution. The exposed roots were harvested after 0 min, 5 min, 10 min and 20 min (arrows in Fig 3.1B). The exposure for 0 min was performed by taking roots out of labeled solution immediately after dipping. The harvested roots (length ca 5 cm) were briefly washed with non-labeled exposure solution to remove surface-bound $^{22}Na^+$ and separated into three parts, i.e., the $^{22}Na^+$ exposed part, the adjacent "intermediate" part (2 cm) and a further 2-cm-long adjacent upper part of the root. Fresh and dry mass (after drying at 60 ^{o}C for 7 days) of each root piece was measured. The dried root segments were used to quantify the radioactivity of ^{22}Na in the root tissue.

Figure 3.2: Thick and thin root tips from *P. euphratica* plants grown in Long-Ashton solution supplied with 150 mM NaCl (A; thick root) and 10 mM NaCl (B; thin root), respectively. The black bar indicates 1 cm.

3.2.4 Short term sodium extrusion analysis using $^{22}Na^+$ labeling

Poplar plants were grown for six weeks in 150 mM or 10 mM NaCl LA solution (n = 15 per treatment). The extrusion experiment was performed with thick and thin roots in two steps: 1st salt loading into the roots, 2nd Na$^+$ extrusion into LA nutrient solution (Fig 3.3). For salt loading, a thick (from 150 mM NaCl treated plants) or thin root (from 10 mM NaCl treated plants), was attached to the plant, was placed for 30 min in a vessel (Tube 5 ml, Sarstedt, Nümbrecht, Germany) containing 300 mM NaCl LA solution supplemented with 26 KBq $^{22}Na^+$ ml^{-1} (loading

solution) (Fig 3.3). Control loading (0 min loading) of single roots (n = 5 per treatment) was performed separately by removing the roots immediately after dipping into the loading solution. After loading, the exposed portion of root tip (approximately 5 cm length) was immediately cut off from the plant, washed with non-labeled 300 mM NaCl LA solution and collected to determine the Na concentration after loading.

To investigate Na^+ extrusion, five plants per treatment was used to determine Na^+ unloading (Fig 3.3). Loaded, attached roots were quickly washed with non-labeled 300 mM NaCl LA solution and then placed in a vessel (Tube 5 ml, Sarstedt, Nümbrecht, Germany) containing 4 ml of non-labeled LA solution without NaCl (collecting-solution) (Fig 3.3). Unloading was studied after exposure of loaded roots for time intervals of 0 (quick dipping), 5 min, 10 min, and 20 min in fresh unloading solution. Then, the root (approximately 5 cm length) was cut and used for Na determination. Fresh and dry mass (60 °C, 7 days) of harvested roots was determined und used to determine the relative water content as the fresh-to-dry mass ratio. Roots were used to measure element contents. The activity of ^{22}Na was determined in the collecting-solution.

Figure 3.3: A schematic model showing steps of Na^+ extrusion experiment. This experiment had two steps:- 1) loading of salt into root and 2) observation of Na^+ extrusion. In salt loading step, single root from a *P. euphratica* plant was immersed into a small tube containing 300 mM NaCl LA solution provided with 26 KBq ^{22}Na ml^{-1} (loading solution). The incubation of single roots into labeled loading solution was done for 30 min. After loading, one group of plants were proceeded to next step (step 2). Loaded root was quickly washed with non-labeled 300 mM NaCl LA solution and then dipped into small tube holding non-labeled LA solution with no NaCl (collecting-solution). The collection of ions releasing from loaded root was done over 40 min with 10 or 20 min interval starting from 0 min (quick dipping). Tube holding

collecting-solution was replaced at each interval with new tube having fresh LA solution. Root tips after salt loading and also after unloading were cut and processed for further analyses.

3.2.5 Determination of ^{22}Na in roots and exposure solutions

The signals of ^{22}Na (CPM, counts per minute) in exposure (^{22}Na labeled) solutions and dried root segments were measured in a gamma counter (Hidex Automatic Gamma Counter, Turku, Finland). A background correction value (CPM) was subtracted from all sample values, which was obtained by measuring empty vials (in case of dried root segments) or vials containing the exposure solutions without ^{22}Na. For the calculation of ^{22}Na activity (Bq) in the sample, the following formula was used:

$$\text{The activity of } ^{22}\text{Na (Bq)} = \frac{\text{CPM}}{60 \times \text{efficiency of measurement}}$$

The activity of ^{22}Na in different root parts were expressed based on dry mass of the root segment:

$$\text{Activity of } ^{22}\text{Na in root part (Bq g}^{-1}\text{ dry weight)} = \frac{\text{Activity of } ^{22}\text{Na (Bq)}}{\text{Dry mass of root part (g)}}$$

The enrichment of Na$^+$ in root segment over the exposure period was calculated based on the activity of ^{22}Na (Bq g^{-1} dry weight) in root part and the specific activity of the ^{22}Na labeled exposure solution. The specific activity of labeled solution (Bq mg^{-1} Na) was calculated from the activity of ^{22}Na (Bq L^{-1}) and Na content (mg L^{-1}) of that solution as follows:

$$\text{Specific activity (Bq mg}^{-1}\text{ Na) of labeled solution} = \frac{\text{Activity of } ^{22}\text{Na in solution (Bq L}^{-1})}{\text{Na content of solution (mg L}^{-1})}$$

$$\text{Na}^+ \text{ enrichment (mg g}^{-1}\text{ dry weight)} = \frac{\text{Activity of } ^{22}\text{Na in root part (Bq g}^{-1}\text{ dry weight)}}{\text{Specific activity (Bq mg}^{-1}\text{ Na) of labeled solution}}$$

To determine the actual enrichment of Na$^+$ over the exposure period, the mean value of Na$^+$ enrichment at control exposure (0 min; T_0) was subtracted from all values obtained at different exposure periods (T_x).

The actual Na$^+$ enrichment (mg g^{-1} dry weight) at T_x = Na$^+$ enrichment at T_x - Mean of Na$^+$ enrichment at T_0 where T denotes time and x denotes 0, 5, 10 and 20 min.

In the Na$^+$ extrusion experiments, the activity of ^{22}Na in collecting-solution was quantified in 4 ml of collecting-solution used at each interval. The amount of Na released from a root within a

specific period was calculated based on the ^{22}Na activity (Bq) in the respective aliquot. Specific activity was calculated as follows:

Specific activity of collecting-solution (Bq mg^{-1} Na) =

$$\frac{\text{Activity of } ^{22}\text{Na in collecting-solution (Bq L}^{-1}\text{)}}{\text{Total Na content of collecting-solution (mg L}^{-1}\text{) - Na content of LA solution (mg L}^{-1}\text{)}}$$

Extrusion of Na$^+$ from a root tip (mg g^{-1} dry weight) at a given period (t_x) was calculated as follows:

Extrusion of Na$^+$ (mg g^{-1} dry weight) at t_x =

$$\frac{\text{Activity of } ^{22}\text{Na (Bq) in the aliquot of collecting-solution used at } t_x}{\text{Specific activity of collecting-solution (Bq mg}^{-1}\text{ Na) × dry mass of root (g)}}$$

where t denotes time and x denotes 0, 0–10, 10–20 and 20–40 min.

3.2.6 Measurement of elements

Elements (Na, K, Ca, Mg, S, Mn, Fe and P) were determined in roots before loading, and after loading and unloading. Since the root samples were small (in the range of 4 to 21 mg), the dry tissue was extracted without further pretreatment in 2 ml of 65 % HNO_3 overnight and then digested in a microwave digestion system (ETHOS.start, MLS GmbH, Leutkirch, Germany). The microwave program used for the digestion was as follows: 2.5 min at 90 °C (power 1000 W), 5 min at 150 °C (1000 W), 2.5 min at 210 °C (1400 W) and 20 min at 210 °C (1600 W) (Sharmin et al., 2021). The resulting suspension was cooled and adjusted to 25 ml with ultrapure water (Sartorius Arium Pro, Sartorius, Göttingen, Germany). The diluted suspension was filtered (MN 640 w, 90 mm, Macherey-Nagel GmbH & Co. KG, Düren, Germany). The elements were measured in the liquid samples or the filtered root extracts by inductively coupled plasma-optical emission spectrometry (ICP-OES) (iCAP 7000 series ICP-OES, Thermo Fisher Scientific, Dreieich, Germany). The element concentrations were calculated using calibration standards (Single-element standards, Bernd Kraft GmbH, Duisburg, Germany).

3.2.7 Collection of samples for RNA analysis

P. euphratica plants were cultivated in hydroponic LA solution in a greenhouse (21 to 23 °C air temperature, 60 to 70 % relative air humidity, ambient light that was supplemented with

additional light of 150 μmol m^{-2} s^{-1} PAR (Lamp: 3071/400 HI-I, Adolf Schuch GmbH, Worms, Germany) for 16h per day). When they had reached a height of 52 ± 11 cm, they were adapted to 150 mM NaCl within 3 days are described above (Fig. 3.1A). Preliminary experiments showed that *P. euphratica* roots started thickening after 3 to 4 days of exposure to 150 mM NaCl. Therefore, we harvested roots after 2 days (time point 1 = short-term) and 12 days (time point 2 = long-term) of 150 mM NaCl exposure. The main root (approximately 5 cm long starting at the apex) was harvested from controls (no NaCl) and salt-stressed plants. The root samples (n= 5 per time point and treatment) were immediately frozen in liquid N$_2$ and stored at -80 °C until use.

3.2.8 RNA extraction and analyses

RNA extraction and library construction were conducted at Beijing Genomics Institute (BGI, Shenzhen, China). Total RNA was extracted with cetyltrimethylammonium bromide (CTAB)-pBIOZOL reagent (Plant media, Dublin, Ireland) and purified by ethanol steps according to the protocol of Mu et al. (2017). Total RNA was quantified using a NanoDrop (Thermo Fisher Scientific, Waltham, USA) and Agilent 2100 bioanalyzer (Agilent, Santa Clara, USA).

Oligo(dT)-attached magnetic beads were used to purify mRNA. Purified mRNA was fragmented, then first-strand cDNA was generated using random hexamer-primed reverse transcription, followed by a second-strand cDNA synthesis. After A-Tailing and RNA Index adapter addition, cDNA fragments were amplified by PCC and purified via Ampure XP Beads. The product was validated on the Agilent 2100 Bioanalyzer for quality control. The double stranded PCR products from the previous step were heated, denatured and circularized to get the final strand circle DNA library. Paired-end reads with a length of 100 bases were sequenced on a BGIseq-500 (BGI-Shenzhen, China) according to manufacturer's instructions.

Raw sequence data have been deposited in the ArrayExpress database at EMBL-EBI (accession number E-MTAB-8988). Processing of raw sequence data was performed with fastp (Chen et al. 2018) using default parameters. The processed sequences were mapped against the transcriptome of *Populus euphratica* (GCF_000495115.1_PopEup_1.0_rna.fna.gz, https://www.ncbi.nlm.nih.gov/genome/13265) using Bowtie 2 (Langmead and Salzberg, 2012). Depending on the sample, 88 to 92 % of all filtered reads could be mapped to a gene model.

Bowtie mapping files were summarized to count tables of the gene models in R (R Core Team 2018) (Supplemental Table S3.1). Identification of differentially expressed transcripts was conducted using the DESeq2 package (Love et al., 2014), using a generalized linear model with Benjamini and Hochberg correction to adjust p-values.

We searched the complete count table for all genes potentially related to salt stress signaling and ion homeostasis used the following categories: sodium transport, potassium transport, H^+-ATPase, cyclic nucleotide gated channel (CNGC), glutamate receptor (GLR), CAM, CAM-like, CBL, CIPK, CDPK, Respiratory burst, and SOD on the basis of literature (Chen and Polle, 2010; Polle and Chen, 2015). The Arabidopsis IDs of these genes were identified in the ARAMEMNON database (http://aramemnon.uni-koeln.de, accessed 17. July 2021, (Schwacke et al., 2003)). Using the function all "Cluster", all members of the gene family were identified. Then, the RNA seq count table with *P. euphratica* IDs and their best Arabidopsis matches was searched with the list of identified AGIs, potentially involved in stress responses. We identified the number of significantly differentially expressed genes (DEGs) in each category and visualized the expression of those genes in a heatmap (settings: rows centered, unit variance scaling applied) using ClustVis (https://biit.cs.ut.ee/clustvis/, accessed 21 September, 2021 (Metsalu and Vilo, 2015)).

3.2.9 Statistical analyses

Statistical analyses were performed with free statistical software R (version 3.5.2) and with Statgraphics XVIII (Statgraphics Technologies, Inc., The Plains, Virginia, USA). Data were analysed with General Linear Models followed by Tukey's multiple comparison test. When the same sample was used for repeated analyses, repeated measures ANOVA was employed. Normal distribution of data was tested by the plotting residuals. Data were normal distributed with few exceptions (2 or 3 outliers in the data sets of the time course experiment were included) and therefore no transformation was applied. Data shown are means ± SE. If not indicated otherwise, 5 biological replicates were investigated. Means were considered to be significantly different with p-values < 0.05.

3.3 Results

3.3.1 Thick root tips showed less Na⁺ enrichment under high salinity than thin root

P. euphratica grown in hydroponic solution supplemented with 150 mM NaCl developed thick roots (Fig. 3.2A). Plants without or with addition of 10 mM NaCl did not show root thickening (Fig. 3.2B) and contained significantly less water than thick roots (Fresh-to-dry ratio of thin versus thick roots: 6.6 ± 0.1 vs 7.9 ± 0.5 (n = $5 \pm$ SE), $p < 0.05$). The time course of Na⁺ accumulation in thin (non-acclimated) and thick (salt-acclimated) roots was analyzed under high salt (150 mM NaCl) and low salt (10 mM NaCl) treatments in three root segments, the root tip, an intermediate and an upper part (Fig 3.4A-C) using ^{22}Na⁺ to trace newly taken up sodium. The accumulation of Na⁺ in root tips, which were in contact with the tracer solution and in the intermediate (non-exposed part) showed significant time-dependent Na accumulation, whereas only very little new Na appeared in the upper root part in the time course of our study (Figure 3.4A-C, Table 3.1). Non-acclimated, thin root tips showed significantly higher Na uptake than the acclimated thick root tips, if exposed to high salt (Fig. 3.4A). Under low salt and in the intermediate root parts, no difference between thick and thin roots was observed (Fig. 3.4B, Table 3.1). Under high salt, the upper part of thin roots showed significant salt enrichment at the end of the exposure period compared with thick roots or roots exposed to low salt (Fig. 3.4C, Table 3.1).

3.3.2 Thin and thick roots show immediate Na⁺ release and Ca²⁺ replenishment in response to low salinity

We determined Na⁺ extrusion from both root types for a 40 min period. For this purpose, *P. euphratica* plants acclimated to 150 mM or 10 mM NaCl were used. The high salt-acclimated roots contained approximately 3-fold greater Na contents than the low salt roots (Fig. 3.5A). Attached roots of both types were loaded with 300 mM NaCl for 30 minutes. This treatment resulted in a significant increment in salt contents in the thin roots, whereas the Na⁺ increase in thick roots was small and not significant on the background of the high Na contents in these roots (Fig. 3.5A). After 40 min of salt release in nutrient solution without NaCl, the root Na contents were decreased and similar to those of the roots before salt loading (Fig. 3.5A). The time course of salt accumulation in the exudation medium revealed that both thin and thick roots showed

significant Na release, which was however much greater for thin than for thick roots (Fig. 3.5B, Table 3.2).
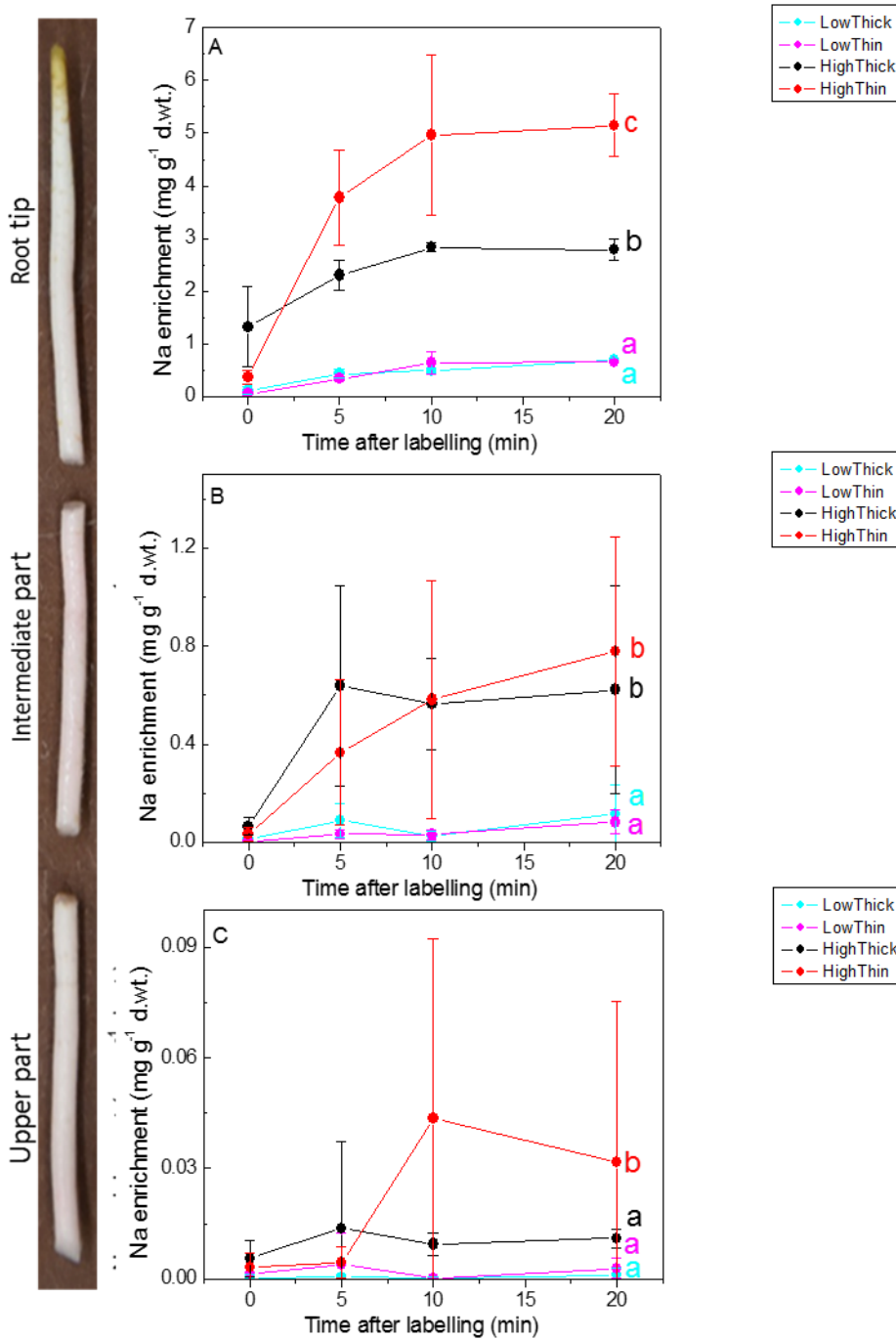

Figure 3.4: Time course of Na⁺ enrichment (mg g⁻¹ weight) in the root tip (A), the intermediate (B) and upper root part (C) of *P. euphratica* under low (10 mM NaCl) or high (150 mM) NaCl. Acclimated plants with thick root roots were tested under low (light blue), or high (black) salt conditions. Non-acclimated controls with thin roots were tested under low (pink) or high salt (red). Attached roots were exposed to

[22]Na solution with the tip (approximately 2 cm) and the translocation into the upper parts was analyzed. Data show means (n = 3 or 5, ± SE). Different letters refer differences in Na enrichment at the end of the exposure period at $p < 0.05$.
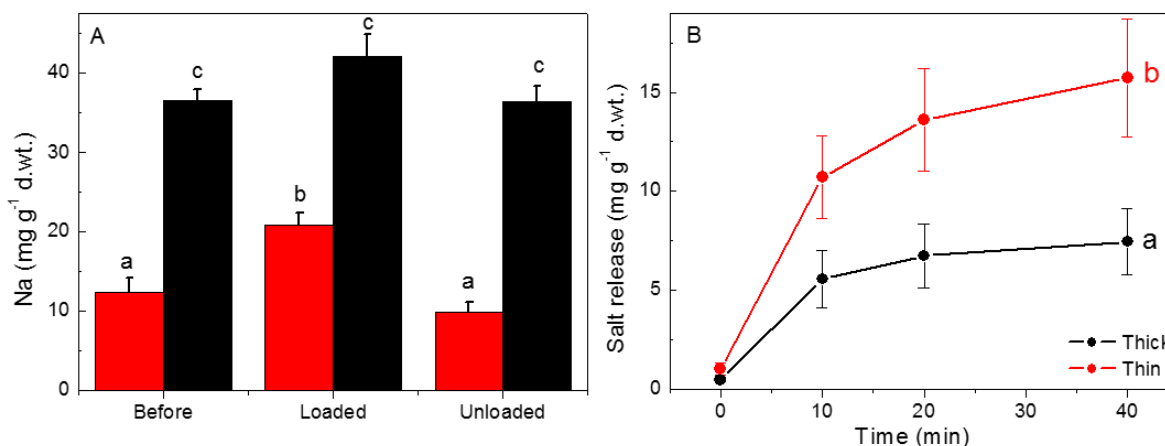
Figure 3.5: The content of Na (mg g^{-1} dry weight) in the root tips at different time points (A) and release of Na$^+$ (mg g^{-1} dry weight) from root tips during salt unloading (B). Graph A represents the content of Na (mg g^{-1} dry weight) in the thick root tips (black bars) and thin root tips (red bars) harvested after 0 min salt loading (before), after 30 min loading (loaded) and after 30 min loading followed by 40 min unloading (unloaded). For salt loading, a single thick root (from 150 mM NaCl adapted plant) or a single thin root (from 10 mM NaCl adapted plant), still attached to the plant, was placed in a vessel containing 300 mM NaCl LA solution supplemented with ^{22}Na$^+$. Bar represents means ± SE (n = 5). For Na content (A), two-way ANOVA was conducted with root type and incubation time as the main factors and homogeneous subsets were obtained using Post-hoc Tukey's HSD test. Different lower case letters in graph A indicate significant differences at $p < 0.05$. Graph B represents the extrusion (release) of Na$^+$ (mg g^{-1} dry weight) from salt loaded thin roots (red line) and thick roots (black line) over 0 min, 10 min, 20 min and 40 min of salt unloading. Data represent means ± SE (n = 5). In case of Na$^+$ release (B), repeated measures ANOVA was performed.

We also measured the responses of other nutrient elements to loading and unloading of NaCl. In thin roots, Ca^{2+} contents decreased in response to salt loading and increased in response to unloading (Table 3.3). In thick roots, salt loading did not influence Ca^{2+} contents, but unloading also caused increased Ca^{2+} contents (Table 3.3). Thick roots contained lower contents of potassium and higher contents of iron and phosphorus than the thin roots, but the loading and unloading treatments had no significant effect on any of these nutrient elements (Table 3.3). Magnesium, manganese and sulfur were unaffected by the treatments in thick and thin roots.

Table 3.1: Analyses of variance for Na enrichment in the tips, intermediate (inter) and upper parts (top) of *P. euphratica* roots. Results of GLM are shown. SoS = Sum of squares, Df = degrees of freedom, MS = Mean squares

Source	Analysis of Variance for Tip					Analysis of Variance for Inter					Analysis of Variance for Top				
	SoS	Df	MS	F-Ratio	P-Value	SoS	Df	MS	F-Ratio	P-Value	SoS	Df	MS	F-Ratio	P-Value
Model	215.0	15	14.3	12.6	0.000	5.2	15	0.3	6.0	0.000	0.011	15	0.0007	2.1	0.022
Root type	6.5	1	6.5	5.7	0.020	0.0	1	0.0	0.2	0.637	0.001	1	0.0007	1.9	0.176
Time	39.3	3	13.1	11.5	0.000	1.4	3	0.5	7.8	0.000	0.001	3	0.0004	1.2	0.307
Salt	107.6	1	107.6	94.3	0.000	2.8	1	2.8	48.4	0.000	0.003	1	0.0034	9.6	0.003
Root type*Time	8.3	3	2.8	2.4	0.075	0.1	3	0.0	0.7	0.551	0.001	3	0.0004	1.1	0.370
Root type*Salt	6.8	1	6.8	6.0	0.018	0.0	1	0.0	0.0	0.939	0.000	1	0.0004	1.0	0.314
Time*Salt	19.6	3	6.5	5.7	0.002	0.9	3	0.3	5.0	0.004	0.001	3	0.0005	1.4	0.266
RT*Time*Salt	7.4	3	2.5	2.2	0.104	0.1	3	0.0	0.5	0.682	0.001	3	0.0005	1.3	0.275
Residual	62.8	55	1.1			3.2	55	0.1			0.019	55	0.0004		
Total (corrected)	277.8	70				8.4	70				0.030	70			

Table 3.2: Repeated measures ANOVA for the time dependence of salt release (mg g^{-1} dry weight) from thick and thin roots of *P. euphratica*. The Greenhouse-Geisser (GG) correction was applied because sphericity was rejected at p <0.001 (Mauchly's Sphericity Test) and epsilon was <0.75. SoS = Sum of squares, Df = degrees of freedom, MS = Mean squares

Source	SoS	Df	MS	F-Ratio	P-Value
Model	1395.3	15	93.0	23.0	<0.001
Root type	270.9	1	270.9	6.3	0.036
ERROR (subject)	342.8	8	42.8	10.6	<0.001
Time (corrected GG)	696.9	1.03	675.6	57.4	<0.001
Time*Root type (corrected GG)	84.8	1.03	82.3	7.0	0.028
ERROR (Time)	97.1	24	4.0		
Total (corrected)	1492.4	39			

3.3.3 Regulation of genes related to salt stress signaling and Na$^+$/K$^+$ homeostasis in thin and thick roots under salinity

We searched genes involved in salt stress signaling and ion homeostasis in the whole RNA-seq count table (Supplement Table S3.1). This approach resulted in 257 genes, which we assigned to 12 functional categories, potentially mediating salt responses (Fig. 3.6, Supplement Table S3.2). We found that the majority of the selected genes showed no significant changes in transcript abundances under short- or long-term exposure to salinity (Figure 3.6, Supplement Table S3.2). This result included the genes known from Arabidopsis to mediate the SOS pathway, *SOS1*, *SOS2* and *SOS3* (Supplement Table S3.2). Among the DEGs, down-regulated genes were mainly found in the categories *CBLs*, *CIPKs* and for potassium transport (Fig. 3.6). In the other categories, down-regulated DEGs were less abundant than upregulated DEGs (Fig. 3.6). The pathways for ROS production, salt sensing and signal transduction via Calmodulin, CMLs and CDPKs as well as sodium transport and ATPases were characterized by various upregulated DEGs (Fig. 3.6, Supplement Table S3.2).

Analyses of DEGs that were responsive to salt treatments showed a significant temporal differentiation among the DEG categories (Fig. 3.7). After short-term salt exposure for 2 days, all but 1 DEG were transcriptionally upregulated, including genes putatively representing calmodulin-like (CMLs) and CDPKs, NADPH oxidases and SODs, transporters (CNGCs, potassium and sodium) and H$^+$ ATPases in the plasma and vacuolar membrane (Fig. 3.7). The salt responses

Table 3.3: Nutrient element contents in *P. euphratica* roots before loading with 300 mM NaCl, after loading and after unloading. Thin roots were collected from control plants grown with 10 mM NaCl and thick roots from salt acclimated plants grown with 150 mM NaCl. Data show means (n = 5, ± SE). Two-way ANOVA was conducted with root type and incubation time (incub.) as the main factors. Normal distribution of data was tested by plotting residuals and log transformation (for K and Fe) was used. Different letters in a column indicate significant difference among the means at $p < 0.05$ (post hoc Tukey HSD test).

Treatment	K	Ca	Mg	Mn	Fe	S	P
Thin root_(before)	8.28 ± 0.92 b	1.23 ± 0.14 b	0.69 ± 0.08 a	0.02 ± 0.00 a	0.04 ± 0.01 ab	1.69 ± 0.14 a	4.34 ± 0.41 a
Thin root_(loaded)	7.17 ± 0.64 ab	0.64 ± 0.12 a	0.51 ± 0.06 a	0.01 ± 0.00 a	0.03 ± 0.00 a	1.52 ± 0.05 a	3.81 ± 0.33 a
Thin root_(unloaded)	8.46 ± 0.91 b	1.23 ± 0.14 b	0.67 ± 0.07 a	0.02 ± 0.00 a	0.03 ± 0.00 a	1.57 ± 0.07 a	4.89 ± 0.35 ab
Thick root_(before)	5.01 ± 0.32 a	0.72 ± 0.05 a	0.62 ± 0.07 a	0.02 ± 0.00 a	0.11 ± 0.02 c	1.77 ± 0.09 a	7.08 ± 0.37 bc
Thick root_(loaded)	5.36 ± 0.24 a	0.72 ± 0.06 a	0.74 ± 0.06 a	0.02 ± 0.01 a	0.16 ± 0.05 c	1.56 ± 0.11 a	7.74 ± 0.78 c
Thick root_(unloaded)	5.18 ± 0.45 a	1.22 ± 0.12 b	0.80 ± 0.08 a	0.03 ± 0.00 a	0.09 ± 0.02 bc	1.74 ± 0.14 a	7.49 ± 0.76 c
p(incub.)	0.810	<0.001	0.283	0.192	0.464	0.208	0.631
p(root type)	<0.001	0.117	0.112	0.075	<0.001	0.267	<0.001
p(incub. × root type)	0.396	0.029	0.112	0.382	0.419	0.818	0.409

were more heterogeneous after 12d than after 2d of-salt exposure. After 12d of salt acclimation, most DEGs were down-regulated and included the main categories: signal transduction (CBLs and CIPKs), potassium transport and vacuolar H^+-ATPases (Fig. 3.7). Only few DEGs were salt responsive at both time points (2 and 12 days after salt exposure): two NADPH oxidases (up), two K^+ transporters (down) and a CML (up) (Fig. 3.7).
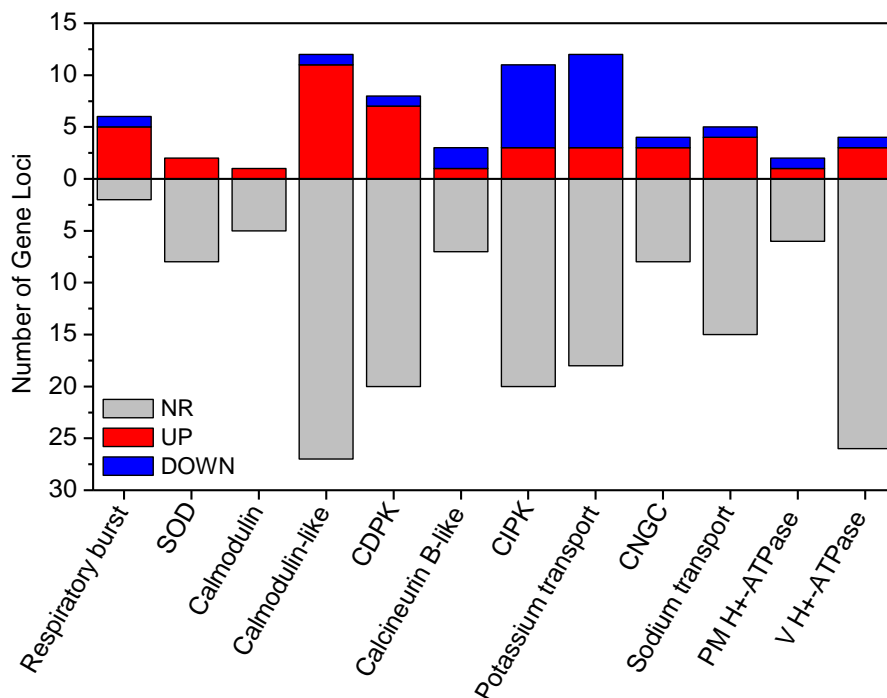
Figure 3.6: Number of genes potentially involved in salt signaling and ion homeostasis present in the transcriptomes of control and salt-exposed *P. euphratica* roots. Grey = genes which are not significantly differentially expressed, red = up and blue = down-regulated differentially expressed genes (DEGs).

3.4 Discussion

3.4.1 Thick roots limit Na⁺ in- and efflux under high salinity

In this study we exploited the ability of *P. euphratica* to form thick roots under saline conditions to investigate the importance of root features for salt tolerance. Previous studies showed that *P. euphratica* forms thick leaves under high salt, which contribute to store excess Na⁺ in the vacuole and apoplast (Ottow et al., 2005a). The formation of succulent organs such as leaf or stem succulence is well known as an adaptation to store water in arid conditions (Ogburn and Edwards,

2010; Grace, 2019) and has also been found in halophytes (Ogburn and Edwards, 2010; Flowers et al., 2015). Succulence accompanied by enhanced salt tolerance is induced by overexpression
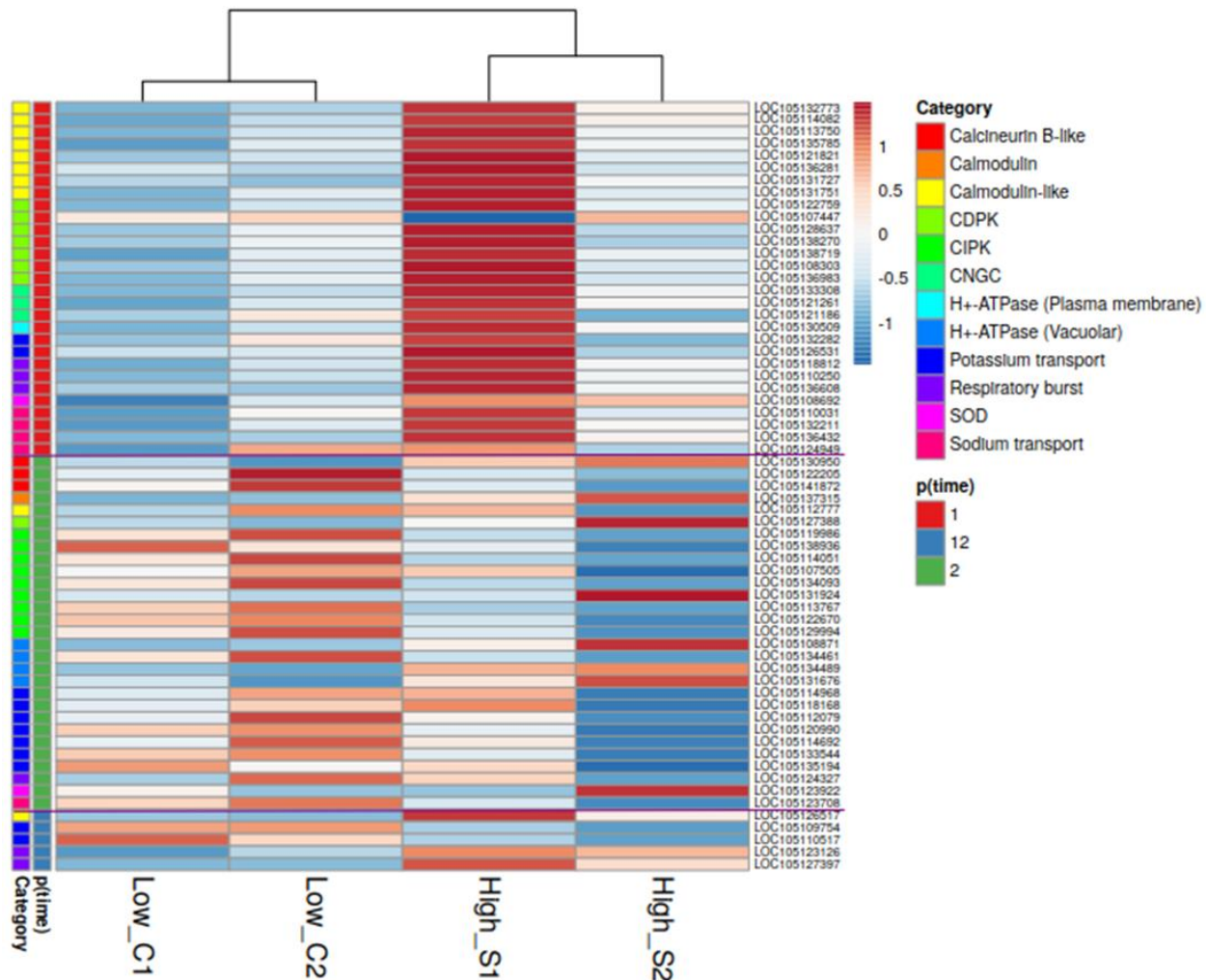
Figure 3.7: Relative expression levels of salt-responsive genes in *P. euphratica* roots in controls (C1, C2) and after salt treatment (S1, S2). C1, S1 = short-term exposure to 150 mM Na$^+$ for 2 days and C2, S2 = long term exposure for 12 days to 150 mM Na$^+$. Genes showing significant responses after short term (p(time) = 1), long term (p(time = 2) and at both time points (p(time = 12)) are shown. The original data are shown in Supplement Table S3.2.

of a cell wall loosing gene in tobacco leaves (Han et al., 2013) or by overexpression of a bZIP transcription factor in Arabidopsis roots (Lim et al., 2020). Examples for root succulence induced by salinity, as in our study, have rarely be found. An example are olive trees (*Olea europeae* L.), which show increases in diameter in response to salinity (Tan et al., 2020). Scanning electron

microscopy in combination with element analyses (EDX-TEM) revealed that salt accumulation in first order salt-exposed olive roots was lower than in higher order root branches (Tan et al., 2020). In our study we compared salt-acclimated and unacclimated first order roots and found significantly higher accumulation of Na^+ in unacclimated than in acclimated roots. EDX-TEM analyses of unacclimated *P. euphratica* plants to 300 mM NaCl showed high Na^+ accumulation in vacuoles as well as in the apoplast of roots cells (Chen et al., 2014), thus supporting the present results. The EDX-TEM study of high salt-exposed *P. euphratica* also localized high contents of Na^+ and Cl^- in the root xylem vessels, pointing to an upward transport of the ions (Chen et al., 2014). In agreement with those results, we demonstrate that upward transport of Na^+ was traceable already after short-term Na^+ exposure in unacclimated, thin roots. However, our tracer study did not reveal significant upward translocation in the acclimated thick roots. Notably, both Na^+ uptake and extrusion into the external solution were strongly reduced in the acclimated thick roots. These results underpin that acclimated roots have a higher ability to control root Na^+ levels and are relatively resistant towards changes in salt conditions.

An important question is whether these physiological results concur with transcriptional changes in pathways known to mediate salt tolerance (as outlined in the introduction). In salt sensitive plant species, activation of the SOS pathway composed of Na^+/H^+ antiporters (NHXs) and proton pumps (ATPase) drive Na^+ outward across the membrane and thus central components for plant resistance (Zhu, 2002, 2016). In addition, PeNhaD1 mediates Na^+ translocation across membranes (Ottow et al., 2005b), most likely protecting plastids from excess sodium (Müller et al., 2014). In *Arabidopsis*, SOS1 and HKT1;1 have been shown to function in controlling Na^+ transport by retrieving Na^+ from the xylem sap under severe salt stress (Shi et al., 2002; Davenport et al., 2007). Here, we found significant downregulation of *HKT1;1* after long-term salt stress, suggesting less Na^+ recovery from xylem loading in thick roots. We further detected high expression levels of PM *H^+-ATPases* and the Na^+/H^+ antiporters *SOS1* and *NhaD1* but notably no significant change under short- or long-term salinity of the most highly expressed genes of the *NHX* (including *SOS1*) and *NhaD* families. This result supports that the Na^+/H^+ antiport system is constitutively overexpressed in *P. euphratica* (Janz et al., 2010) but cannot explain higher Na^+ fluxes in unacclimated thin than in acclimated thick roots. One reason could be

posttranscriptional regulation of the SOS protein, similar as for other components of the SOS pathway (Haruta et al., 2015). Furthermore, it is possible that other members of the NHX family with lower basal expression levels than the aforementioned could be involved in mediating acclimatory salt responses since we found significantly increased transcript levels of *NHX6* and *NHX1* homologs after short-term and downregulation of an *NHX7* homolog after long-term salt exposure. Additionally, non-selective cation channels (NSCCs) such as cyclic nucleotide-gated channels (CNGCs) and glutamate receptors (GLRs) have been proposed as a major entry route of Na^+ into the roots (Demidchik and Tester, 2002; Tester and Davenport, 2003; Demidchik and Maathuis, 2007; Shabala and Cuin, 2008; Kronzucker and Britto, 2011). Here, upregulation of CNGCs after short-term and decreases of CNGCs after long-term salt exposure, together with the modulation of the antiporter system on top of high activities for high basal Na protection may be responsible for adjusting Na^+ handling during salt acclimation.

3.4.2 Salt sensing and signaling show divergent transcriptional patterns in unacclimated and acclimated roots

An essential facet of salt acclimation is Na^+ sensing and signaling via H_2O_2 and Ca^{2+} (Zhu, 2016). Our study shows transcriptional upregulation of *NADH oxidases* and *SOD,* which encode the proteins required for ROS (reactive oxygen species) production, under both short- and long-term exposure. This finding complies with accumulation of ROS, which was found in *P. euphratica* as well as in salt sensitive poplar roots under high salinity (Langenfeld-Heyser et al., 2007; Sun et al., 2010b). Here, the persistent transcriptional upregulation of ROS pathway, though initially involving more genes in acclimated roots, suggests that ROS are required to maintain sensing of elevated salinity.

In salt-stressed *P. euphratica,* increased H_2O_2 levels are facilitating Ca^{2+}-signaling by mediating a rise in cytosolic Ca^{2+} levels (Sun et al., 2010b). Ca^{2+}sensor proteins, i.e., CAMs, CMLs, CBLs and CDPKs perceive the signal by binding Ca^{2+} and trigger downstream salt stress responses (Cheng et al., 2002; Luan et al., 2002; McCormack et al., 2005). In leaves of some poplar genotypes, a correlation between CaM levels and salt resistance was found (Chang et al., 2006). In our study the DEGs, potentially required for signal transmission via Ca^{2+}, suggest a switch from strong

dominance of transcriptional activation (nine *CML* and five *CPKs* family members) after short-term salt exposure to decreases or suppression of these pathways under long salt exposure where only few members of those families remained upregulated but many showed significant reductions in transcriptional abundances, including among others eight *CIPKs*, two *CBLs*, and one *CML*.

3.4.3 Salinity acclimated roots keep K$^+$ levels and accumulate P

K$^+$ retention and homeostasis capacity are key determinants of plant salinity tolerance (Wu et al., 2018). *P. euphratica* usually maintains higher K$^+$ levels under salinity than salt-sensitive species (Chen et al., 2001, 2003; Ding et al., 2010). For example, roots of the salt-sensitive *P. x canescens* lost approximately 80% of K$^+$ after acclimation to 100 mM Na$^+$ (Sharmin et al., 2021), whereas here, the K$^+$ levels of 150 mM Na$^+$-acclimated thick roots were approximately 35% lower than in unstressed *P. euphratica* roots. The greater K$^+$ retention ability of *P. euphratica* is correlated with the transcript abundance of K$^+$ transporters and channels (Ding et al., 2010) and has also been assigned to reduction in K$^+$ loss through depolarization-activated outward rectifying K$^+$ channels (DA-KORCs) (Shabala and Cuin, 2008; Wu et al., 2018). In the current study, *SKOR,* a gene enconding a DA-KOR channel*,* maintained high transcript levels in the salt-treated roots before thickening and was downregulated in thick roots. SKOR is localized in the root stelar tissues and involved in K$^+$ release into xylem sap toward the shoots (Gaymard et al., 1998). Thus, the expression data in our study suggest that depolarization-activated K$^+$ efflux from the root stelar cells and loading into xylem via SKOR occurred at the early phase. However, in thick roots S*KOR* transcription was suppressed, possibly to reduce K$^+$ loss from the root cells and preserve K$^+$ homeostasis in the root tissue. The transcriptional regulation of K$^+$ uptake (*KUP/HAK*) transporters and channels (*AKT1* and *KAT3*) support this suggestion because high transcript abundances of these genes were found under salt stress, irrespective of short- or long-term salt exposure. In the present study, salt-stressed roots maintained high expressions for tonoplast outward-rectifiers (TPK1 and TPK5) and K$^+$ efflux antiporters (KEA1, KEA5 and KEA6) after short-term salt exposure. Among these transport systems, PeTPK1 has been shown to maintain K$^+$ homeostasis under salt stress by transferring K$^+$ from vacuole to cytosol (Wang et al., 2013), while

K$^+$ efflux antiporters (KEA) function in K$^+$ release from plastids and the Golgi apparatus into the cytosol (Tsujii et al., 2019). K$^+$ re-distribution among subcellular compartments was observed by EDX-TEM in *P. euphratica* leaves (Ottow et al., 2005a). Collectively, our data support that roots also maintained cytosolic K$^+$ levels in the face of salinity by intracellular redistribution of K$^+$ from internal storage pools and reducing K$^+$ efflux by downregulation of *DA-KORC*, *TPK5* and *KEA1* after long-acclimation.

An unexpected observation was that thick roots contained higher P and Fe contents than thin roots. The physiological significance of these results is unknown. Under salt stress, we found highly upregulated orthologs to the *Arabidopsis* P transporters *PHT1;5* and *PHT1;7,* which play major roles in P homeostasis (Smith et al., 2011). In poplar, *PHT1;5* and *PHT1;7* transcript abundances increase under P starvation and enhance P uptake (Kavka and Polle, 2016, 2017). Hence, our findings imply an enhanced P demand under salt stress. We speculate that high P contents could be required to support ATP regeneration, which may be necessary to satisfy an enhanced energy demand. However, other explanations, such as membrane restructuring to cope with high salinity (Luo et al., 2011; Sarabia et al., 2020), may also be envisaged since P is needed for the production of phospholipids.

3.5 Conclusion and outlook

P. euphratica avoids excessive Na$^+$ accumulation by limiting uptake and release. Among the genes encoding the classical constituents of the SOS pathway very little or no transcriptional changes were observed. Janz and colleagues suggested that high *SOS1* activities and loss of transcriptional regulation might be associated with the evolutionary adaptation of *P. euphratica* to salt stress (Janz et al., 2010). Genome sequencing of *P. euphratica* revealed an expansion of this gene family (Ma et al., 2013). Our results show surprising plasticity of root morphology with production of thick roots under high salinity able to buffer fluctuating Na$^+$ levels. Consequently, once restructured, only little transcriptional acclimation of the SOS pathway is required since higher cellular water contents enables dilution of excess Na$^+$. Hence, *P. euphratica* employs a specialized strategy for stress anticipation. This mechanism is probably more efficient in the natural habitats of this species, where the salt levels can rapidly change due to flooding and drying (Polle and

Chen, 2015) than up- and downregulation of protective systems, which can only follow but not anticipate stress protection.

3.6 Declaration

I conducted all experiments, analysed data, prepared the tables and graphs and wrote the chapter. Dr. Dennis Janz and Dr. Christian Eckert did the preliminary analyses of the RNA-seq data. Prof. Dr. Andrea Polle and Prof. Dr. Shaoliang Chen conceived the study, acquired funds and supervised analyses.

3.7 References

Apse, M. P., Aharon, G. S., Snedden, W. A., and Blumwald, E. (1999). Salt tolerance conferred by overexpression of a vacuolar Na^+/H^+ antiport in *Arabidopsis*. *Science* 285, 1256–1258. doi:10.1126/science.285.5431.1256.

Blumwald, E., Aharon, G. S., and Apse, M. P. (2000). Sodium transport in plant cells. *Biochim. Biophys. Acta BBA - Biomembr.* 1465, 140–151. doi:10.1016/S0005-2736(00)00135-8.

Chang, Y., Chen, S.-L., Yin, W.-L., Wang, R.-G., Liu, Y.-F., Shi, Y., et al. (2006). Growth, gas exchange, abscisic acid, and calmodulin response to salt stress in three poplars. *J. Integr. Plant Biol.* 48, 286–293. doi:https://doi.org/10.1111/j.1744-7909.2006.00194.x.

Chen, S., Diekmann, H., Janz, D., and Polle, A. (2014). Quantitative x-ray elemental imaging in plant materials at the subcellular level with a transmission electron microscope: Applications and limitations. *Materials* 7, 3160–3175. doi:10.3390/ma7043160.

Chen, S., Li, J., Fritz, E., Wang, S., and Hüttermann, A. (2002). Sodium and chloride distribution in roots and transport in three poplar genotypes under increasing NaCl stress. *For. Ecol. Manag.* 168, 217–230. doi:10.1016/S0378-1127(01)00743-5.

Chen, S., Li, J., Wang, S., Fritz, E., Hüttermann, A., and Altman, A. (2003). Effects of NaCl on shoot growth, transpiration, ion compartmentation, and transport in regenerated plants of *Populus euphratica* and *Populus tomentosa*. *Can. J. For. Res.* 33, 967–975. doi:10.1139/x03-066.

Chen, S., Li, J., Wang, S., Hüttermann, A., and Altman, A. (2001). Salt, nutrient uptake and transport, and ABA of *Populus euphratica*; a hybrid in response to increasing soil NaCl. *Trees* 15, 186–194. doi:10.1007/s004680100091.

Chen, S., and Polle, A. (2010). Salinity tolerance of *Populus*. *Plant Biol.* 12, 317–333. doi:10.1111/j.1438-8677.2009.00301.x.

Cheng, S.-H., Willmann, M. R., Chen, H.-C., and Sheen, J. (2002). Calcium signaling through protein kinases. the Arabidopsis calcium-dependent protein kinase gene family. *Plant Physiol.* 129, 469–485. doi:10.1104/pp.005645.

Davenport, R. J., Muñoz-Mayor, A., Jha, D., Essah, P. A., Rus, A., and Tester, M. (2007). The Na^+ transporter AtHKT1;1 controls retrieval of Na^+ from the xylem in *Arabidopsis*. *Plant Cell Environ.* 30, 497–507. doi:https://doi.org/10.1111/j.1365-3040.2007.01637.x.

Deinlein, U., Stephan, A. B., Horie, T., Luo, W., Xu, G., and Schroeder, J. I. (2014). Plant salt-tolerance mechanisms. *Trends Plant Sci.* 19, 371–379. doi:10.1016/j.tplants.2014.02.001.

Demidchik, V., and Maathuis, F. J. M. (2007). Physiological roles of nonselective cation channels in plants: from salt stress to signalling and development. *New Phytol.* 175, 387–404. doi:https://doi.org/10.1111/j.1469-8137.2007.02128.x.

Demidchik, V., and Tester, M. (2002). Sodium fluxes through nonselective cation channels in the plasma membrane of protoplasts from Arabidopsis roots. *Plant Physiol.* 128, 379–387. doi:10.1104/pp.010524.

Ding, M., Hou, P., Shen, X., Wang, M., Deng, S., Sun, J., et al. (2010). Salt-induced expression of genes related to Na^+/K^+ and ROS homeostasis in leaves of salt-resistant and salt-sensitive poplar species. *Plant Mol. Biol.* 73, 251–269. doi:10.1007/s11103-010-9612-9.

Flowers, T. J., Munns, R., and Colmer, T. D. (2015). Sodium chloride toxicity and the cellular basis of salt tolerance in halophytes. *Ann. Bot.* 115, 419–431. doi:10.1093/aob/mcu217.

Gaymard, F., Pilot, G., Lacombe, B., Bouchez, D., Bruneau, D., Boucherez, J., et al. (1998). Identification and disruption of a plant shaker-like outward channel involved in K^+ release into the xylem sap. *Cell* 94, 647–655. doi:10.1016/S0092-8674(00)81606-2.

Grace, O. M. (2019). Succulent plant diversity as natural capital. *PLANTS PEOPLE PLANET* 1, 336–345. doi:10.1002/ppp3.25.

Gu, R., Fonseca, S., Puskás, L. G., Hackler, L., Jr., Zvara, Á., Dudits, D., et al. (2004). Transcript identification and profiling during salt stress and recovery of *Populus euphratica*. *Tree Physiol.* 24, 265–276. doi:10.1093/treephys/24.3.265.

Han, Y., Wang, W., Sun, J., Ding, M., Zhao, R., Deng, S., et al. (2013). *Populus euphratica* XTH overexpression enhances salinity tolerance by the development of leaf succulence in transgenic tobacco plants. *J. Exp. Bot.* 64, 4225. doi:10.1093/jxb/ert229.

Haruta, M., Gray, W. M., and Sussman, M. R. (2015). Regulation of the plasma membrane proton pump (H^+-ATPase) by phosphorylation. *Curr. Opin. Plant Biol.* 28, 68–75. doi:10.1016/j.pbi.2015.09.005.

Hassani, A., Azapagic, A., and Shokri, N. (2020). Predicting long-term dynamics of soil salinity and sodicity on a global scale. *Proc. Natl. Acad. Sci.* 117, 33017–33027. doi:10.1073/pnas.2013771117.

Hewitt, E. J., and Smith, T. A. (1975). *Plant mineral nutrition*. London: English Universities Press.

Janz, D., Behnke, K., Schnitzler, J.-P., Kanawati, B., Schmitt-Kopplin, P., and Polle, A. (2010). Pathway analysis of the transcriptome and metabolome of salt sensitive and tolerant poplar species reveals evolutionary adaption of stress tolerance mechanisms. *BMC Plant Biol.* 10, 150. doi:10.1186/1471-2229-10-150.

Kavka, M., and Polle, A. (2016). Phosphate uptake kinetics and tissue-specific transporter expression profiles in poplar (*Populus × canescens*) at different phosphorus availabilities. *BMC Plant Biol.* 16, 206. doi:10.1186/s12870-016-0892-3.

Kavka, M., and Polle, A. (2017). Dissecting nutrient-related co-expression networks in phosphate starved poplars. *PLOS ONE* 12, e0171958. doi:10.1371/journal.pone.0171958.

Kronzucker, H. J., and Britto, D. T. (2011). Sodium transport in plants: a critical review. *New Phytol.* 189, 54–81. doi:10.1111/j.1469-8137.2010.03540.x.

Kudla, J., Xu, Q., Harter, K., Gruissem, W., and Luan, S. (1999). Genes for calcineurin B-like proteins in *Arabidopsis* are differentially regulated by stress signals. *Proc. Natl. Acad. Sci.* 96, 4718–4723. doi:10.1073/pnas.96.8.4718.

Langenfeld-Heyser, R., Gao, J., Ducic, T., Tachd, Ph., Lu, C. F., Fritz, E., et al. (2007). *Paxillus involutus* mycorrhiza attenuate NaCl-stress responses in the salt-sensitive hybrid poplar *Populus × canescens*. *Mycorrhiza* 17, 121–131. doi:10.1007/s00572-006-0084-3.

Langmead, B., and Salzberg, S. L. (2012). Fast gapped-read alignment with Bowtie 2. *Nat. Methods* 9, 357–359. doi:10.1038/nmeth.1923.

Leplé, J., Brasileiro, A., Michel, M., Delmotte, F., and Jouanin, L. (1992). Transgenic poplars: expression of chimeric genes using four different constructs. *Plant Cell Rep.* 11, 137–141. doi:10.1007/BF00232166.

Li, D., Song, S., Xia, X., and Yin, W. (2012). Two CBL genes from *Populus euphratica* confer multiple stress tolerance in transgenic triploid white poplar. *Plant Cell Tissue Organ Cult. PCTOC* 109, 477–489. doi:10.1007/s11240-011-0112-7.

Li, D.-D., Xia, X.-L., Yin, W.-L., and Zhang, H.-C. (2013). Two poplar calcineurin B-like proteins confer enhanced tolerance to abiotic stresses in transgenic *Arabidopsis thaliana*. *Biol. Plant.* 57, 70–78. doi:10.1007/s10535-012-0251-7.

Lim, S. D., Mayer, J. A., Yim, W. C., and Cushman, J. C. (2020). Plant tissue succulence engineering improves water-use efficiency, water-deficit stress attenuation and salinity tolerance in Arabidopsis. *Plant J.* 103, 1049–1072. doi:10.1111/tpj.14783.

Lloyd, G., and McCown, B. (1980). Commercially-feasible micropropagation of mountain laurel, *Kalmia latifolia*, by use of shoot-tip culture. in *Proceedings of International Plant Propagators' Society*, 421–427. Available at: https://www.cabdirect.org/cabdirect/abstract/19830315515 [Accessed January 31, 2020].

Love, M. I., Huber, W., and Anders, S. (2014). Moderated estimation of fold change and dispersion for RNA-seq data with DESeq2. *Genome Biol.* 15, 550. doi:10.1186/s13059-014-0550-8.

Luan, S., Kudla, J., Rodriguez-Concepcion, M., Yalovsky, S., and Gruissem, W. (2002). Calmodulins and calcineurin B-like proteins: calcium sensors for specific signal response coupling in plants. *Plant Cell* 14, S389–S400. doi:10.1105/tpc.001115.

Luo, Z.-B., Li, K., Gai, Y., Göbel, C., Wildhagen, H., Jiang, X., et al. (2011). The ectomycorrhizal fungus (*Paxillus involutus*) modulates leaf physiology of poplar towards improved salt tolerance. *Environ. Exp. Bot.* 72, 304–311. doi:10.1016/j.envexpbot.2011.04.008.

Lv, F., Zhang, H., Xia, X., and Yin, W. (2014). Expression profiling and functional characterization of a CBL-interacting protein kinase gene from *Populus euphratica*. *Plant Cell Rep.* 33, 807–818. doi:10.1007/s00299-013-1557-4.

Ma, T., Wang, J., Zhou, G., Yue, Z., Hu, Q., Chen, Y., et al. (2013). Genomic insights into salt adaptation in a desert poplar. *Nat. Commun.* 4, 2797. doi:10.1038/ncomms3797.

Ma, X., Deng, L., Li, J., Zhou, X., Li, N., Zhang, D., et al. (2010). Effect of NaCl on leaf H^+-ATPase and the relevance to salt tolerance in two contrasting poplar species. *Trees* 24, 597–607. doi:10.1007/s00468-010-0430-0.

Ma, Y., Xu, T., Wan, D., Ma, T., Shi, S., Liu, J., et al. (2015). The salinity tolerant poplar database (STPD): a comprehensive database for studying tree salt-tolerant adaption and poplar genomics. *BMC Genomics* 16, 205. doi:10.1186/s12864-015-1414-7.

McCord, J. M., and Fridovich, I. (1969). Superoxide Dismutase: AN ENZYMIC FUNCTION FOR ERYTHROCUPREIN (HEMOCUPREIN). *J. Biol. Chem.* 244, 6049–6055. doi:10.1016/S0021-9258(18)63504-5.

McCormack, E., Tsai, Y.-C., and Braam, J. (2005). Handling calcium signaling: *Arabidopsis* CaMs and CMLs. *Trends Plant Sci.* 10, 383–389. doi:10.1016/j.tplants.2005.07.001.

Metsalu, T., and Vilo, J. (2015). ClustVis: a web tool for visualizing clustering of multivariate data using Principal Component Analysis and heatmap. *Nucleic Acids Res.* 43, W566. doi:10.1093/nar/gkv468.

Mu, W., Wei, J., Yang, T., Fan, Y., Cheng, L., Yang, J., et al. (2017). RNA extraction for plant samples using CTAB-pBIOZOL. *protocols.io*. doi:10.17504/protocols.io.gsnbwde.

Müller, A., Volmer, K., Mishra-Knyrim, M., and Polle, A. (2013). Growing poplars for research with and without mycorrhizas. *Front. Plant Sci.* 4, 332. doi:10.3389/fpls.2013.00332.

Müller, M., Kunz, H.-H., Schroeder, J. I., Kemp, G., Young, H. S., and Neuhaus, H. E. (2014). Decreased capacity for sodium export out of Arabidopsis chloroplasts impairs salt

tolerance, photosynthesis and plant performance. *Plant J.* 78, 646–658. doi:https://doi.org/10.1111/tpj.12501.

Munns, R., and Tester, M. (2008). Mechanisms of salinity tolerance. *Annu. Rev. Plant Biol.* 59, 651–681. doi:10.1146/annurev.arplant.59.032607.092911.

Ogburn, R. M., and Edwards, E. J. (2010). "Chapter 4 - The ecological water-use strategies of succulent plants," in *Advances in Botanical Research*, eds. J.-C. Kader and M. Delseny (Academic Press), 179–225. doi:10.1016/B978-0-12-380868-4.00004-1.

Ottow, E. A., Brinker, M., Teichmann, T., Fritz, E., Kaiser, W., Brosché, M., et al. (2005a). *Populus euphratica* displays apoplastic sodium accumulation, osmotic adjustment by decreases in calcium and soluble carbohydrates, and develops leaf succulence under salt stress. *Plant Physiol.* 139, 1762–1772. doi:10.1104/pp.105.069971.

Ottow, E. A., Polle, A., Brosché, M., Kangasjärvi, J., Dibrov, P., Zörb, C., et al. (2005b). Molecular characterization of *PeNhaD1*: the first member of the NhaD Na^+/H^+ antiporter family of plant origin. *Plant Mol. Biol.* 58, 75–88. doi:10.1007/s11103-005-4525-8.

Polle, A., and Chen, S. (2015). On the salty side of life: molecular, physiological and anatomical adaptation and acclimation of trees to extreme habitats. *Plant Cell Amp Environ.* 38, 1794–1816. doi:10.1111/pce.12440.

Qiu, Q.-S., Guo, Y., Quintero, F. J., Pardo, J. M., Schumaker, K. S., and Zhu, J.-K. (2004). Regulation of vacuolar Na^+/H^+ exchange in *Arabidopsis thaliana* by the salt-overly-sensitive (SOS) pathway. *J. Biol. Chem.* 279, 207–215. doi:10.1074/jbc.M307982200.

Quintero, F. J., Martinez-Atienza, J., Villalta, I., Jiang, X., Kim, W.-Y., Ali, Z., et al. (2011). Activation of the plasma membrane Na/H antiporter Salt-Overly-Sensitive 1 (SOS1) by phosphorylation of an auto-inhibitory C-terminal domain. *Proc. Natl. Acad. Sci.* 108, 2611–2616. doi:10.1073/pnas.1018921108.

Rengasamy, P. (2006). World salinization with emphasis on Australia. *J. Exp. Bot.* 57, 1017–1023. doi:10.1093/jxb/erj108.

Sagi, M., and Fluhr, R. (2006). Production of Reactive Oxygen Species by Plant NADPH Oxidases. *Plant Physiol.* 141, 336–340. doi:10.1104/pp.106.078089.

Sarabia, L. D., Boughton, B. A., Rupasinghe, T., Callahan, D. L., Hill, C. B., and Roessner, U. (2020). Comparative spatial lipidomics analysis reveals cellular lipid remodelling in different developmental zones of barley roots in response to salinity. *Plant Cell Environ.* 43, 327–343. doi:10.1111/pce.13653.

Schwacke, R., Schneider, A., Graaff, E. van der, Fischer, K., Catoni, E., Desimone, M., et al. (2003). ARAMEMNON, a Novel database for Arabidopsis integral membrane proteins. *Plant Physiol.* 131, 16. doi:10.1104/pp.011577.

Shabala, S., and Cuin, T. A. (2008). Potassium transport and plant salt tolerance. *Physiol. Plant.* 133, 651–669. doi:https://doi.org/10.1111/j.1399-3054.2007.01008.x.

Sharmin, S., Lipka, U., Polle, A., and Eckert, C. (2021). The influence of transpiration on foliar accumulation of salt and nutrients under salinity in poplar (*Populus × canescens*). *PLOS ONE* 16, e0253228. doi:10.1371/journal.pone.0253228.

Shi, H., Quintero, F. J., Pardo, J. M., and Zhu, J.-K. (2002). The putative plasma membrane Na^+/H^+ antiporter SOS1 controls long-distance Na^+ transport in plants. *Plant Cell* 14, 465–477. doi:10.1105/tpc.010371.

Shi, J., Kim, K.-N., Ritz, O., Albrecht, V., Gupta, R., Harter, K., et al. (1999). Novel protein kinases associated with calcineurin B–like calcium sensors in Arabidopsis. *Plant Cell* 11, 2393–2405. doi:10.1105/tpc.11.12.2393.

Smith, A. P., Nagarajan, V. K., and Raghothama, K. G. (2011). Arabidopsis Pht1;5 plays an integral role in phosphate homeostasis. *Plant Signal. Behav.* 6, 1676–1678. doi:10.4161/psb.6.11.17906.

Sun, J., Dai, S., Wang, R., Chen, S., Li, N., Zhou, X., et al. (2009). Calcium mediates root K^+/Na^+ homeostasis in poplar species differing in salt tolerance. *Tree Physiol.* 29, 1175–1186. doi:10.1093/treephys/tpp048.

Sun, J., Li, L., Liu, M., Wang, M., Ding, M., Deng, S., et al. (2010a). Hydrogen peroxide and nitric oxide mediate K^+/Na^+ homeostasis and antioxidant defense in NaCl-stressed callus cells of two contrasting poplars. *Plant Cell Tissue Organ Cult. PCTOC* 103, 205–215. doi:10.1007/s11240-010-9768-7.

Sun, J., Wang, M.-J., Ding, M.-Q., Deng, S.-R., Liu, M.-Q., Lu, C.-F., et al. (2010b). H_2O_2 and cytosolic Ca^{2+} signals triggered by the PM H^+-coupled transport system mediate K^+/Na^+ homeostasis in NaCl-stressed *Populus euphratica* cells. *Plant Cell Environ.* 33, 943–958. doi:https://doi.org/10.1111/j.1365-3040.2010.02118.x.

Sun, J., Zhang, X., Deng, S., Zhang, C., Wang, M., Ding, M., et al. (2012). Extracellular ATP signaling is mediated by H_2O_2 and cytosolic Ca^{2+} in the salt response of *Populus euphratica* cells. *PLoS ONE* 7, e53136. doi:10.1371/journal.pone.0053136.

Tan, J., Ben-Gal, A., Shtein, I., Bustan, A., Dag, A., and Erel, R. (2020). Root structural plasticity enhances salt tolerance in mature olives. *Environ. Exp. Bot.* 179, 104224. doi:10.1016/j.envexpbot.2020.104224.

Tang, R.-J., Liu, H., Bao, Y., Lv, Q.-D., Yang, L., and Zhang, H.-X. (2010). The woody plant poplar has a functionally conserved salt overly sensitive pathway in response to salinity stress. *Plant Mol. Biol.* 74, 367–380. doi:10.1007/s11103-010-9680-x.

Tang, R.-J., Wang, C., Li, K., and Luan, S. (2020). The CBL–CIPK calcium signaling network: Unified paradigm from 20 years of discoveries. *Trends Plant Sci.* 25, 604–617. doi:10.1016/j.tplants.2020.01.009.

Tang, R.-J., Yang, Y., Yang, L., Liu, H., Wang, C.-T., Yu, M.-M., et al. (2014). Poplar calcineurin B-like proteins PtCBL10A and PtCBL10B regulate shoot salt tolerance through interaction with PtSOS2 in the vacuolar membrane: Poplar CBL10s and salt stress tolerance. *Plant Cell Environ.* 37, 573–588. doi:10.1111/pce.12178.

Tester, M., and Davenport, R. (2003). Na^+ tolerance and Na^+ transport in higher plants. *Ann. Bot.* 91, 503–527. doi:10.1093/aob/mcg058.

Tsujii, M., Kera, K., Hamamoto, S., Kuromori, T., Shikanai, T., and Uozumi, N. (2019). Evidence for potassium transport activity of Arabidopsis KEA1-KEA6. *Sci. Rep.* 9, 10040. doi:10.1038/s41598-019-46463-7.

van Zelm, E., Zhang, Y., and Testerink, C. (2020). Salt tolerance mechanisms of plants. *Annu. Rev. Plant Biol.* 71, 403–433. doi:10.1146/annurev-arplant-050718-100005.

Wang, F., Deng, S., Ding, M., Sun, J., Wang, M., Zhu, H., et al. (2013). Overexpression of a poplar two-pore K^{+} channel enhances salinity tolerance in tobacco cells. *Plant Cell Tissue Organ Cult. PCTOC* 112, 19–31. doi:10.1007/s11240-012-0207-9.

Weinl, S., and Kudla, J. (2009). The CBL–CIPK Ca^{2+}-decoding signaling network: function and perspectives. *New Phytol.* 184, 517–528. doi:10.1111/j.1469-8137.2009.02938.x.

Wu, H., Zhang, X., Giraldo, J. P., and Shabala, S. (2018). It is not all about sodium: revealing tissue specificity and signalling roles of potassium in plant responses to salt stress. *Plant Soil* 431, 1–17. doi:10.1007/s11104-018-3770-y.

Wu, Y., Ding, N., Zhao, X., Zhao, M., Chang, Z., Liu, J., et al. (2007). Molecular characterization of *PeSOS1*: the putative Na^{+}/H^{+} antiporter of *Populus euphratica*. *Plant Mol. Biol.* 65, 1–11. doi:10.1007/s11103-007-9170-y.

Yang, Y., Hu, L., Chen, X., Ottow, E. A., Polle, A., and Jiang, X. (2007a). A novel method to quantify H^{+}-ATPase-dependent Na^{+} transport across plasma membrane vesicles. *Biochim. Biophys. Acta BBA - Biomembr.* 1768, 2078–2088. doi:10.1016/j.bbamem.2007.06.028.

Yang, Y., Zhang, F., Zhao, M., An, L., Zhang, L., and Chen, N. (2007b). Properties of plasma membrane H^{+}-ATPase in salt-treated *Populus euphratica* callus. *Plant Cell Rep.* 26, 229–235. doi:10.1007/s00299-006-0220-8.

Yao, J., Shen, Z., Zhang, Y., Wu, X., Wang, J., Sa, G., et al. (2020). *Populus euphratica* WRKY1 binds the promoter of H^{+}-ATPase gene to enhance gene expression and salt tolerance. *J. Exp. Bot.* 71, 1527–1539. doi:10.1093/jxb/erz493.

Ye, C.-Y., Zhang, H.-C., Chen, J.-H., Xia, X.-L., and Yin, W.-L. (2009). Molecular characterization of putative vacuolar NHX-type Na^{+}/H^{+} exchanger genes from the salt-resistant tree *Populus euphratica*. *Physiol. Plant.* 137, 166–174. doi:10.1111/j.1399-3054.2009.01269.x.

Yokoi, S., Quintero, F. J., Cubero, B., Ruiz, M. T., Bressan, R. A., Hasegawa, P. M., et al. (2002). Differential expression and function of *Arabidopsis thaliana* NHX Na^{+}/H^{+} antiporters in the salt stress response. *Plant J.* 30, 529–539. doi:https://doi.org/10.1046/j.1365-313X.2002.01309.x.

Yu, Y., Xia, X., Yin, W., and Zhang, H. (2007). Comparative genomic analysis of CIPK gene family in *Arabidopsis* and *Populus*. *Plant Growth Regul.* 52, 101–110. doi:10.1007/s10725-007-9165-3.

Zhang, F., Wang, Y., Yang, Y., Wu, H., Wang, D., and Liu, J. (2007). Involvement of hydrogen peroxide and nitric oxide in salt resistance in the calluses from *Populus euphratica*. *Plant Cell Environ.* 30, 775–785. doi:https://doi.org/10.1111/j.1365-3040.2007.01667.x.

Zhang, H., Deng, C., Wu, X., Yao, J., Zhang, Y., Zhang, Y., et al. (2020a). *Populus euphratica* remorin 6.5 activates plasma membrane H^+-ATPases to mediate salt tolerance. *Tree Physiol.* 40, 731–745. doi:10.1093/treephys/tpaa022.

Zhang, H., Lv, F., Han, X., Xia, X., and Yin, W. (2013). The calcium sensor PeCBL1, interacting with PeCIPK24/25 and PeCIPK26, regulates Na^+/K^+ homeostasis in *Populus euphratica*. *Plant Cell Rep.* 32, 611–621. doi:10.1007/s00299-013-1394-5.

Zhang, H., Yin, W., and Xia, X. (2008). Calcineurin B-Like family in *Populus*: comparative genome analysis and expression pattern under cold, drought and salt stress treatment. *Plant Growth Regul.* 56, 129–140. doi:10.1007/s10725-008-9293-4.

Zhang, Z., Chen, Y., Zhang, J., Ma, X., Li, Y., Li, M., et al. (2020b). Improved genome assembly provides new insights into genome evolution in a desert poplar (*Populus euphratica*). *Mol. Ecol. Resour.* 20, 781–794. doi:10.1111/1755-0998.13142.

Zhu, J.-K. (2001). Plant salt tolerance. *Trends Plant Sci.* 6, 66–71. doi:10.1016/S1360-1385(00)01838-0.

Zhu, J.-K. (2002). Salt and drought stress signal transduction in plants. *Annu. Rev. Plant Biol.* 53, 247–273. doi:10.1146/annurev.arplant.53.091401.143329.

Zhu, J.-K. (2003). Regulation of ion homeostasis under salt stress. *Curr. Opin. Plant Biol.* 6, 441–445. doi:10.1016/S1369-5266(03)00085-2.

Zhu, J.-K. (2016). Abiotic Stress Signaling and Responses in Plants. *Cell* 167, 313–324. doi:10.1016/j.cell.2016.08.029.

3.8 Supplementary materials – chapter 3

Supplementary Table S3.1: The full RNA-seq count table.

Supplementary Table S3.2: Details information about the regulation of genes related to salt stress signaling and Na$^+$/K$^+$ homeostasis in *P. euphratica* roots under salt compared to control condition after short-term (T1) and after long-term (T2) salt exposure.

Chapter 4: The influence of transpiration on foliar accumulation of salt and nutrients under salinity in poplar (*Populus × canescens*)

RESEARCH ARTICLE

The influence of transpiration on foliar accumulation of salt and nutrients under salinity in poplar (*Populus × canescens*)

Shayla Sharmin, Ulrike Lipka, Andrea Polle, Christian Eckert *

Forest Botany and Tree Physiology, University of Göttingen, Göttingen, Germany

* eckert5@gwdg.de

Abstract

Increasing salinity is one of the major drawbacks for plant growth. Besides the ion itself being toxic to plant cells, it greatly interferes with the supply of other macronutrients like potassium, calcium and magnesium. However, little is known about how sodium affects the translocation of these nutrients from the root to the shoot. The major driving force of this translocation process is thought to be the water flow through the xylem driven by transpiration. To dissect the effects of transpiration from those of salinity we compared salt stressed, ABA treated and combined salt- and ABA treated poplars with untreated controls. Salinity reduced the root content of major nutrients like K^+, Ca^{2+} and Mg^{2+}. Less Ca^{2+} and Mg^{2+} in the roots resulted in reduced leaf Ca^{2+} and leaf Mg^{2+} levels due to reduced stomatal conductance and reduced transpiration. Interestingly, leaf K^+ levels were positively affected in leaves under salt stress although there was less K^+ in the roots under salt. In response to ABA, transpiration was also decreased and Mg^{2+} and Ca^{2+} levels decreased comparably to the salt stress treatment, while K^+ levels were not affected. Thus, our results suggest that loading and retention of leaf K^+ is enhanced under salt stress compared to merely transpiration driven cation supply.

Introduction

Soil salinity is one of the most severe abiotic stress that limits the distribution and productivity of crops worldwide. Salinization of arable soils can have natural causes but is mostly the consequence of unsuitable cultivation practices [1, 2]. Soils are generally classified as saline when the electrical conductivity of the saturated soil extract is 4 dS m^{-1} or more [3], equivalent to approximately 40 mM NaCl [4]. The presence of soluble salts at higher concentrations in the soil reduces water availability to roots and causes ion toxicity and nutrient deficiency in plants [1, 5, 6].

Plants acquire nutrients from the environment surrounding their root system. Under salinity, Na^+ and Cl^- can disrupt nutrient uptake of glycophytes through competitive interactions or by affecting the membrane selectivity for ions [7]. The presence of NaCl under saline conditions results in nutritional imbalances inside the plant evident as high ratios of Na^+/Ca^{2+}, Na^+/K^+ and Na^+/Mg^{2+} [8–10]. After uptake by the roots, the delivery of ions from roots to leaves

89

occurs through the vascular system of the xylem with the transpiration stream as the transport vehicle [11]. Since the movement of ions from root to shoot is influenced by the transpiration-driven water flow [12], shoot ion uptake is affected by both the ion concentration and the rate of transpiration.

Among woody plants, poplars (*Populus* spp.) have often been used to investigate the responses to salt stress [2]. These studies suggested a role of abscisic acid (ABA) in restricting salt uptake [13, 14]. It is well known that ABA is a central regulator of plant adaptation to osmotic stress [15]. ABA regulates stomatal opening [16, 17]. The levels of ABA in poplars increase in response to salinity [18–21]. Overall, higher levels of ABA in salt-tolerant compared to salt-sensitive hybrid [(*P. euphratica* versus *P. talassica* Kom × (*P. euphratica* + *Salix alba* L.)] under stress conditions suggested that ABA-induced stomatal closure may reduce root-to-shoot xylem water flow and consequently limit the total amount of salt ions transported to leaves [13]. However, enhanced salt accumulation in roots and elevated xylem loading may counteract the anticipated ameliorating effect of a reduced transpirational pull on foliar salt accumulation. It is thus still unclear, whether ABA contributes to decreasing tissue salt enrichment.

In addition to salt accumulation, exposure to enhanced NaCl causes alteration in tissue concentrations of cationic nutrients such as K^+, Ca^{2+} and Mg^{2+} [20]. For example, in a poplar hybrid NaCl treatment caused reductions in Mg^{2+} and Ca^{2+} levels in roots and leaves, while K^+ level was unaffected [13]. In some other poplar genotypes, e.g., *P. tomentosa* and *P. × canescens*, salinity caused reduction in K^+ uptake in roots but no reduction in leaves [19, 21]. Salinity induced reduction in the tissue concentrations of K^+, Ca^{2+} and Mg^{2+} nutrients was also reported in other salt-sensitive woody plants e. g. in citrus rootstocks, avocado rootstocks, cherry etc. [22–25]. These examples show that it is not known if the reduction of nutrients in tissues under salinity is predominantly due to less uptake by root or if the reduced transport via the transpiration stream plays role as well.

This study aimed to investigate the effect of reduced transpiration on nutrient accumulation in *P. × canescens* under salt stress. We hypothesize that reduced transpiration decreases accumulation of Na^+ and contributes to a favorable ion balance in leaves, thereby, protecting poplars against salinity stress. In addition, we hypothesize that accumulation of Na^+ and other cations is independent from stomatal opening and therefore, enhanced NaCl content in soils imposes Na^+ accumulation independent of transpiration. Gas exchange, growth, ion concentrations in leaves and root were measured in *P. × canescens* and the resultant effect on the growth of the plants was analyzed as well. Our results suggest that interplay between foliar ion accumulation and transpiration is moderate.

Materials and methods

Plant material

Plantlets of *P. × canescens* (clone INRA717 1-B4) were multiplied by *in-vitro* micropropagation as described by Leplé and colleagues [26]. Approximately, 1 to 2 cm long stem cuttings having at least one leaf were placed up-right into glass jars containing half strength Murashige & Skoog (MS) medium [27] under sterile conditions and incubated in a culture room [16 h light / 8 h dark, 150 μmol PAR m^{-2} s^{-1} (Osram L 18W/840 cool white, Osram, Munich, Germany), 23 to 25˚C, 40 to 60% relative air humidity] for 5 weeks as described by Müller and colleagues [28]. Afterward, rooted plants were moved into a greenhouse (Department of Forest Botany and Tree Physiology, University of Göttingen, Göttingen, Germany), acclimated to ambient conditions, and raised in aerated hydroponic culture with Long-Ashton (LA) nutrient solution [28]. The plants were grown with additional light (150 μmol m^{-2} s^{-1} PAR) (Lamp: 3071/400 HI-I, Adolf Schuch GmbH, Worms, Germany) to maintain a 16 h photoperiod and at air

90

temperatures from 21 to 24˚C and relative air humidity from 70 to 80%. The nutrient solution was exchanged weekly. After a growth phase of 5 weeks, when the plants had mean height of 29.82 ± 4.24 cm, the experimental treatments were started in September 2017. The experiment was conducted with a total of 94 plants.

Salt and ABA treatment

The total duration of the treatment period was six weeks (S1 Fig). Before applying saline stress, the plants were divided into three groups: control, low salt and ABA [(±) ABA, Duchefa Bio-chemie B.V, Haarlem, Netherlands]. The control group was supplied with LA nutrient solution as before. The low salt (Ls) group was exposed to 25 mM NaCl in the nutrient solution. The ABA group was exposed to 10 µM ABA for 1 week and then to 50 µM ABA for 2 weeks in the nutrient solution (S1 Fig).

After three weeks, groups were divided into the following experimental groups (S1 Fig): The control group was split into two groups, of which one was kept under control conditions (control) and the second was stressed with 100 mM NaCl (Hs group). The low salt group was divided into two groups, of which one was kept with 25 mM NaCl [continuous low salt (cLs) group] and the second was exposed to 100 mM NaCl (Ls+Hs group). The ABA treated group was split in four treatments, among which one group was returned to control conditions in LA nutrient solution [discontinuous ABA (dABA) group]; in the second group, 50 µM ABA treatment was continued [continuous ABA (cABA) group]; the third group was exposed to 100 mM NaCl only [discontinuous ABA plus high salt (dABA+Hs) group] and the fourth group was exposed to 100 mM NaCl together with 50 µM ABA [continuous ABA plus high salt (cABA+Hs) group]. This resulted in a total of eight different treatments (S1 Fig). The nutrient solutions with different salt or ABA amendments as well as the control solutions were exchanged weekly. The plants were randomized regularly. After three weeks of stress phase, all plants were harvested (n = 9 to 10 per treatment).

Plant growth measurements

Plant height was recorded twice a week and stem diameter was recorded once a week. The shoot height was measured from the growing tip to the base of the stem. The stem diameter was measured by a digital caliper at a marked position approximately 2 cm above from the base of the plant. Relative height increment and relative diameter increment over the stress phase i.e., last three weeks of the whole-treatment period were calculated by the following formula:

$$\text{Relative height increment} = \frac{H_{end} - H_{start}}{H_{start}}$$

$$\text{Relative diameter increment} = \frac{D_{end} - D_{start}}{D_{start}}$$

Where H_{start} and H_{end} are the shoot heights, and D_{start} and D_{end} are the shoot diameters at the time of start and end of stress phase, respectively.

Shed leaves per individual plant were collected during the six-week-long experimental period and dried at 60˚C for 7 days to determine total leaf loss.

Gas exchange measurement

Net photosynthesis, transpiration, stomatal conductance, sub-stomatal CO_2 concentration and atmospheric CO_2 concentration of mature leaves (using the 8th -10th leaf from the apex) were

measured once a week between 9:00 h and 14:00 h with an LCpro+ portable photosynthesis system (ADC BioScientific Ltd., Hoddesdon, UK). The measurements were carried out with constant irradiation of 870 µmol PAR m^{-2} s^{-1} and a temperature of 23.1 ± 0.6 °C and at 419.7 ± 11.2 µmol mol^{-1} ambient atmospheric CO_2 concentration.

Harvest

At the end of the experiment, destructive harvest was done. Leaves, stem and root of each plant were weight separately. The dry mass was determined after drying aliquots from each tissue for 7 days at 60°C. The dry mass of the whole tissue was calculated as:

$$\text{Total tissue dry mass (g)} = \frac{\text{total fresh mass of the tissue (g)} \times \text{dry mass of the aliquot (g)}}{\text{fresh mass of the aliquot (g)}}$$

For leaf area measurement, three leaves from the top, middle and bottom part of the shoot were collected, weighed, and scanned. The area of each leaf was measured from scanned pictures using ImageJ software. Leaf size and whole-plant leaf area were calculated using the following equations:

$$\text{Leaf size } (\text{cm}^2 \text{ leaf}^{-1}) = \frac{\text{leaf area of sample leaves } (\text{m}^2)}{\text{number of sample leaves}} \times 10000$$

$$\text{Whole}-\text{plant leaf area } (\text{m}^2 \text{ plant}^{-1})$$
$$= \frac{\text{leaf area of sample leaves } (\text{m}^2) \times \text{fresh mass of all leaves of the plant (g)}}{\text{fresh mass of the sample leaves (g)}}$$

Analysis of elements

Different elements were measured in the representative aliquots of leaves and fine roots of a plant (5 or 10 plants per treatment). Dried aliquots of leaf and root tissues were milled (Retsch, Haan, Germany) into fine powder before digestion. Approximately 40 to 50 mg of ground sample was digested with 2 ml of 65% HNO_3 in a microwave digestion system (ETHOS.start, MLS GmbH, Leutkirch, Germany). The microwave program used for the digestion of sample was as follows: 2.5 min at 90°C (power 1000 W), 5 min at 150°C (power 1000 W), 2.5 min at 210°C (power 1600 W) and 20 min at 210°C (1600 W). The resulting solutions were cooled and filled up to 25 ml volume with de-ionized water. The final volumes were filtered by filter paper (MN 640 w, 90 mm, Macherey-Nagel GmbH & Co. KG, Düren, Germany) and elements (Na, K, Ca, Mg, S, Mn, Fe and P) were measured in the filtered extracts by inductively coupled plasma-optical emission spectrometry (ICP-OES) (iCAP 7000 series ICP-OES, Thermo Fisher Scientific, Dreieich, Germany). The element concentrations (mg g^{-1} dry mass) were calculated using calibration standards (Single-element standards, Bernd Kraft GmbH, Duisburg, Germany) and the sample weight used for extraction.

To determine a hypothetical concentration of ions in the cellular fluid (assuming equal distribution of the ions throughout the cell), measured elements were expressed on the basis of water content of the tissue (mM). The water content and ion concentration were calculated as

92

follows:

$$\text{Water content (L g}^{-1} \text{ dry mass)} = \frac{\text{total fresh mass of the tissue} - \text{total dry mass of the tissue}}{\text{total dry mass of the tissue}}$$

Concentration of ion (mM)

$$= \frac{\text{concentration of element (mg g}^{-1} \text{ dry mass) in the tissue}}{\text{atomic mass of that element} \times \text{water content of the tissue(L g}^{-1} \text{ dry mass)}}$$

The relative changes in the concentration of major cations (K^+, Ca^{2+} and Mg^{2+}) in response to different treatments were calculated by comparing with controls as follows:

Change in the concentration of ion (%)

$$= \frac{\text{concentration of ion (mM)} - \text{mean concentration in control (mM)}}{\text{mean concentration in control (mM)}} \times 100$$

Scanning electron microscope (SEM) and energy-dispersive x-ray microanalysis (EDXA)

Electron microscopy and X-ray microanalysis were done in root tips from selected treatments (3 or 4 plants per treatment). Two to three fresh root tips (approx. 1 cm long) per plant were harvested, wrapped with aluminum foil paper and enclosed in mesh wire bags (Haver and Boecker, Oelde, Germany). A freezing mixture of propane: isopentane (2:1) was prepared in a small container at the temperature of liquid nitrogen [29]. The wire bags containing root samples were immediately dipped into the freezing mixture for 2 to 3 min. Afterwards, the bags were transferred into liquid nitrogen for further storage.

To prepare a frozen root tip for electron microscopy, a small portion of a root tip (1 mm above from root apex) was cut off and removed with a thin razor blade, and the cut surface was fixed firmly using freeze adhesive (Tissue freezing medium, Leica Biosystems, Nussloch, Germany) on the holder of the electron microscope at the temperature of liquid nitrogen. The holder and sample were then clamped in the cooling stage of the microscope (-25˚C). Samples were analyzed by a scanning electron microscope (Phenom ProX, Phenom-World B.V., Eindhoven, Netherlands) equipped with an energy dispersive spectrometer (EDS) and element identification (EID) software package. The acceleration voltage of 15 kV and magnifications of 300X, 350X and 2500X were used with an acquisition time of 55 seconds. Element distribution was analyzed across the root cell layers radially from the center of the vascular cylinder to the rhizodermis. For this purpose, line scans with 512 pixels resolution were analyzed. To obtain representative data, at least four line-scan analyses at four separate positions per sample were recorded. Relative concentration (percentage of weight) of different elements (Na, K, Ca, Mg, P, Mn, S and Cl) obtained from line scan analyses were separated based on the distribution within cortex and vascular cells for further comparison.

Statistical analysis

Statistical analyses were performed with the statistical software R (version 3.5.2). One-way and two-way analysis of variance (ANOVA) was applied followed by Fisher's test. Normal distribution of data was tested by plotting residuals and log transformation or square root transformation was used if data were not normally distributed. Data represent means ± standard error (SE). If not indicated otherwise, n = 5 biological replicates were investigated. Means were considered to be significantly different when $p \leq 0.05$.

93

Results

Gas exchange of plants decreases strongly in response to high salt and moderately in response to ABA

Poplars exposed to high salt (Hs, 100 mM NaCl) showed an about 5-fold decline in stomatal conductance and transpiration (Fig 1A and 1B) and an about 2-fold decline in net CO_2 assimilation (Fig 1C) compared to control plants. Low salt treatment (cLs, 25 mM NaCl) resulted in less pronounced decreases in gas exchange compared to high salt (Fig 1A–1C). When the low salt pretreated plants were transferred to high salt conditions (Ls+Hs), the negative impact of salt was even stronger than in absence of low salt pretreatment (Hs, Fig 1A–1C).

Exposure of poplars to 50 μM ABA (cABA) had a negative influence on gas exchange similar to that observed in response to low salt stress (cLs, Fig 1A–1C). The ABA effect was fully reversible when the poplars were transferred after an ABA pretreatment phase to control nutrient solution (dABA, Fig 1A–1C). When poplars grown in the presence of ABA were exposed to high salt (cABA+Hs), the decline in stomatal conductance, transpiration and net photosynthesis was similar to that of plants exposed to high salt after low salt pretreatment (Ls+Hs, Fig 1A–1C). These treatments had the strongest negative effects on gas exchange. Plants, which were exposed to high salt with the discontinuation of ABA application (dABA+Hs) showed a decline in gas exchange similar to that of plants exposed only to high salt (Hs, Fig 1A–1C). Overall, exposure to high salt stress resulted in a stronger decline in gas exchange than that to either low salt stress or ABA treatment.

Shoot growth reduces significantly after salt exposure but leaf area declines in all stress treatments

The influence of salinity and ABA on the growth of the plants was investigated by examining relative shoot height increment, stem diameter increment, leaf area and biomass (Fig 2). Relative shoot height and stem diameter increments were significantly lower under high salt treatments, irrespective of with or without ABA (Fig 2A and 2B). Low salt exposure reduced height growth and diameter increment significantly (Fig 2A and 2B). ABA treatments caused no significant alterations in either height or diameter increment (Fig 2A and 2B). Whole-plant leaf area decreased significantly in response to salt stress as well as to ABA application (Fig 2C). The size of individual leaves was also reduced significantly in all stress treatments (S1 Table). Whole-plant biomass (sum of root, stem and leaves) showed a significant reduction in biomass for all ABA and high salt treated plants (Fig 2D). Loss of biomass due to leaf shedding was found in non-stressed and stressed plants and there was no significant difference among the treatments (S1 Table). However, plants showed tendency towards higher leaf loss in response to high salt and ABA exposure compared to control conditions (S1 Table). The root to shoot ratio was increased marginally in the presence of high salt and ABA, though difference was not significant (S1 Table).

Basic cation concentrations are altered in roots and leaves in response to salinity and ABA

To obtain information how salt stress or ABA treatments affected the ion balance, we estimated the total cation concentrations on the basis of the water content of root or leaf tissues (Fig 3). High salt exposure caused approximately 3- to 3.5-fold increases in root cation concentrations compared to controls (Fig 3A), whereas the increase in leaves was approximately 1.5-fold (Fig 3B). The increase was caused by substantial accumulation of Na^+ and partly counterbalanced by decreases in other cations (Fig 3A and 3B). The contributions of the
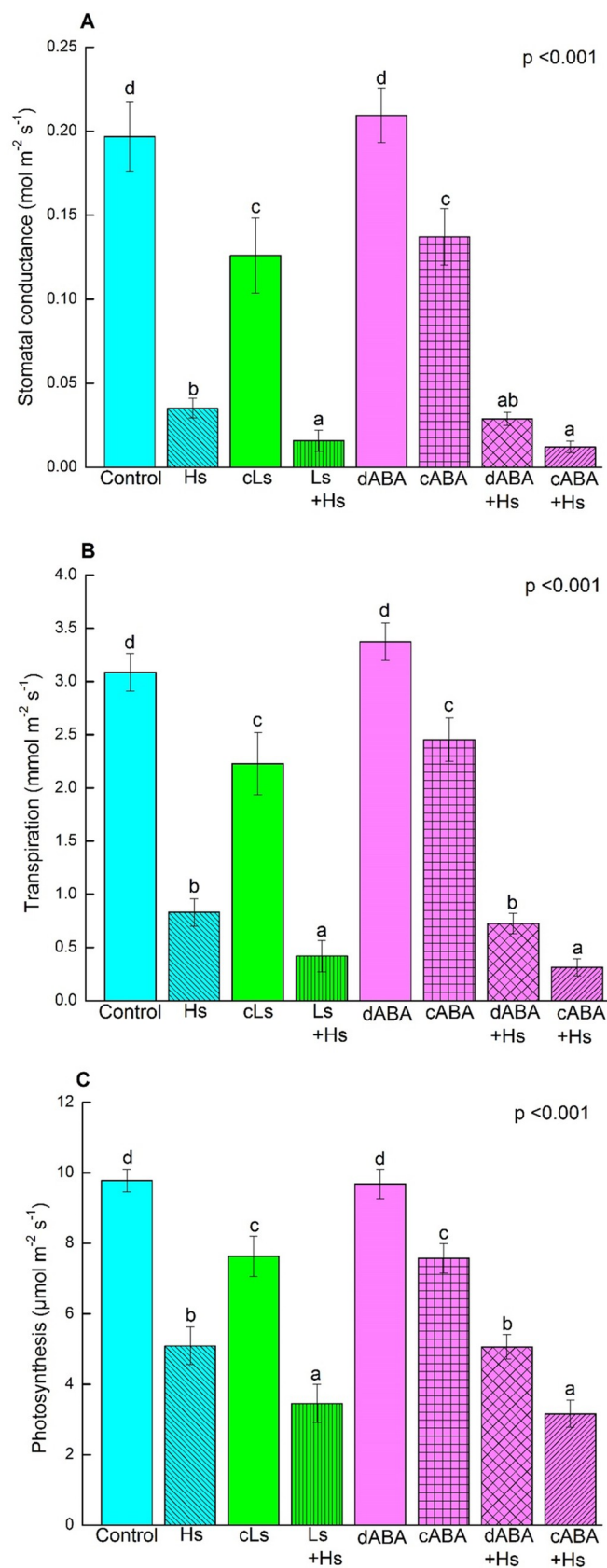
94

Fig 1. Stomatal conductance (A), transpiration (B) and photosynthetic rate (C) in the leaf of *P. × canescens* plants in response to salinity and ABA treatment. Bars indicate means ± SE. Data were obtained by analyzing all measurements from five independent plants per treatment (once a week over three weeks of stress period). One-way ANOVA was conducted. Normal distribution of data was tested by plotting residuals. Different letters obtained from Fisher's test indicate significant differences among treatments at p <0.05. ***Control*** = constantly grown with nutrient solution only; ***Hs*** = **high salt** i.e. exposed to 100 mM NaCl for three weeks of stress phase; ***cLs*** = **continuous low salt** i.e. applied with 25 mM NaCl constantly for six weeks of whole-treatment phase; ***Ls + Hs*** = **low salt plus high salt** i.e. applied with 25 mM NaCl for three weeks of pretreatment phase and then replaced with 100 mM NaCl for next three weeks of stress phase; ***dABA*** = **discontinuous ABA** i.e. treated with 50 μM ABA for three weeks of pretreatment phase and then replaced with only nutrient solution for next three weeks of stress phase; ***cABA*** = **continuous ABA** i.e. treated with 10 μM ABA in first week and then with 50 μM ABA constantly in the next five weeks of whole-treatment period; ***dABA + Hs*** = **discontinuous ABA plus high salt** i.e. treated with 50 μM ABA for three weeks of pretreatment phase and then replaced with 100 mM NaCl for next three weeks of stress phase; ***cABA + Hs*** = **continuous ABA plus high salt** i.e. 50 μM ABA was applied for three weeks of pretreatment phase and then 50 μM ABA plus 100 mM NaCl was applied for three weeks of stress phase.

https://doi.org/10.1371/journal.pone.0253228.g001
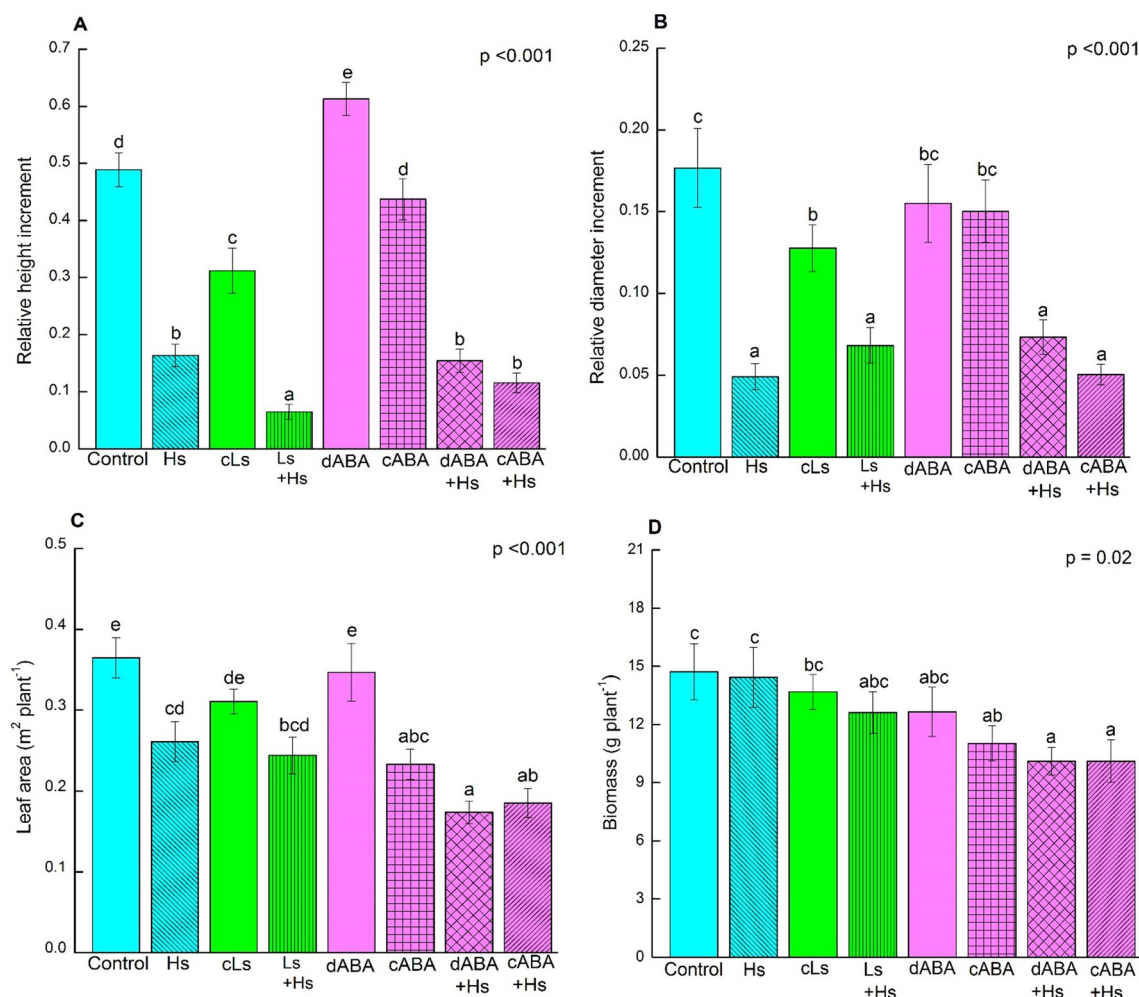
Fig 2. Relative shoot height increment (A), relative shoot diameter increment (B), leaf area (C) and biomass accumulation (D) of *P. × canescens* plants under salinity and ABA. Bars indicate means ± SE (n = 9 or 10; in case of leaf area, n = 7 or 8). One-way ANOVA was conducted. Normal distribution of data was tested by plotting residuals and square root transformation (in case of relative height increment) or log transformation (in case of biomass) was used to meet the criteria. Different letters obtained from Fisher's test indicate significant differences among treatments at p <0.05.

https://doi.org/10.1371/journal.pone.0253228.g002
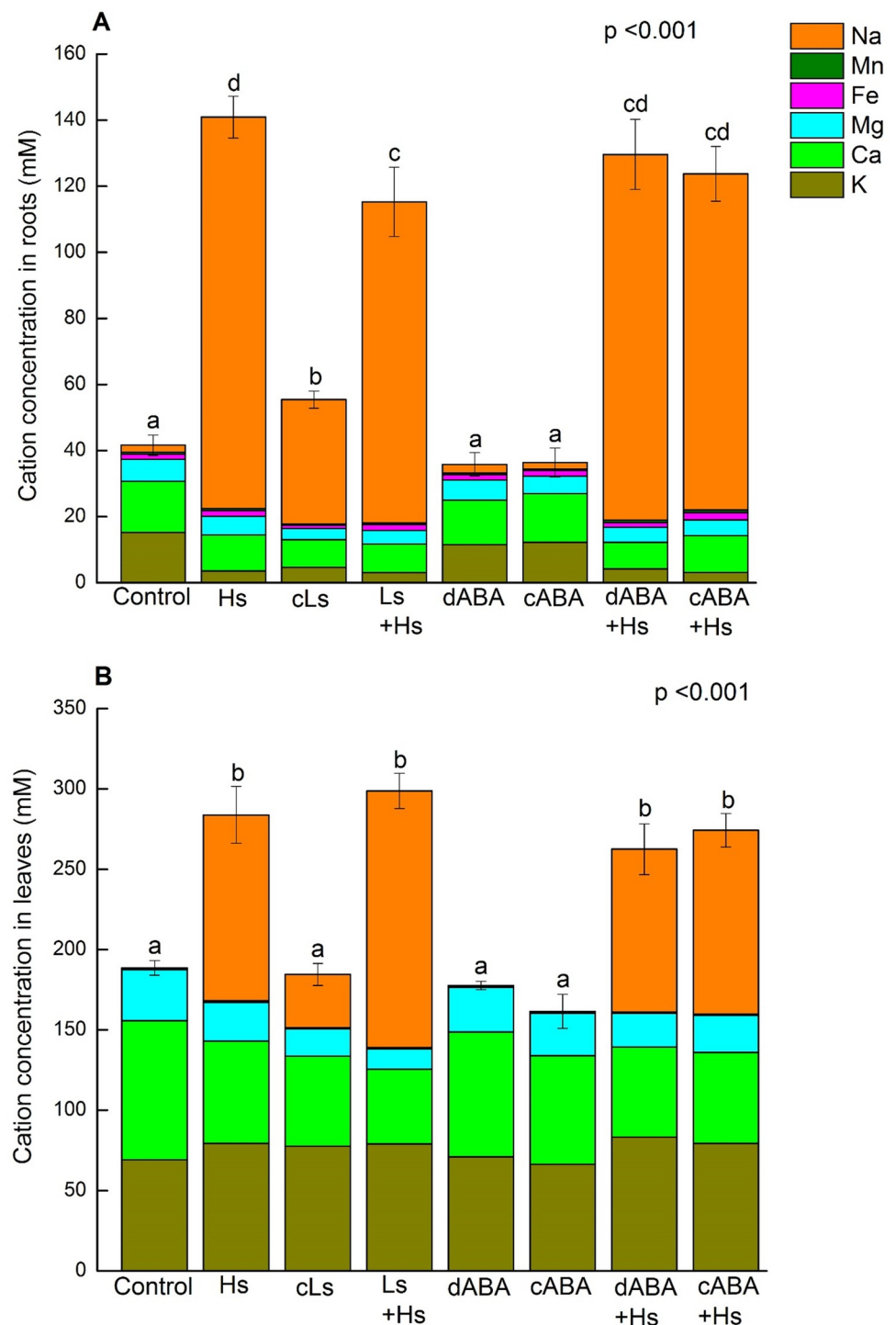
Fig 3. Concentration of cations in the root (A) and leaf tissues (B) of *P. × canescens* plants in response to salinity and ABA. Cations (mM) were calculated as sum of K^+, Ca^{2+}, Mg^{2+}, Fe^{2+}, Mn^{2+} and Na^+. Bar represents means ± SE (n = 5 or 10). Average content of specific ion is presented by specific color on the bar. One-way ANOVA was conducted. Normal distribution of data was tested by plotting residuals and log transformation was used in case of cation content in root. Different letters obtained from Fisher's test indicate significant differences among treatments at p <0.05.

micronutrient Mn and Fe to these alterations were negligible (Fig 3A and 3B). Details for all measured elements and their ratios are available in S2 and S3 Tables for root tissue and S4 and S5 Tables for leaf tissue.

To inspect the influence of salinity and ABA on the major cations K^+, Ca^{2+} and Mg^{2+} in greater details, we analyzed the relative changes in comparison to controls conditions (Fig 4). In roots, salt treatments resulted in almost 80% K^+ loss, regardless of low or high salt stress (Fig 4A), while the foliar K^+ level even showed a significant increase (Fig 4B). Interestingly, ABA treatments also resulted K^+ reduction in roots, although relatively moderate (Fig 4A), whereas no increase was observed in leaves (Fig 4B). Combined treatment of ABA und salt resulted in a K^+ level comparable to the salt only treatment.

The concentrations of Ca^{2+} were greatly decreased in response to both high salt and low salt treatments (almost -50%) in roots (Fig 4C), while leaf Ca^{2+} levels were more reduced under high salt (up to -46%) than under low salt stress (-35%) (Fig 4D). ABA treatment in the absence of salt stress caused also decline in Ca^{2+} concentrations in leaves, but not in roots (Fig 4C and 4D).

The stress treatments tended to decrease the Mg^{2+} levels in roots compared to controls but the effects were only significant for low salt stress (cLs) and low salt stress followed by high salt stress (Ls+Hs) (Fig 4E). In leaves, the negative effect of high salt on the Mg^{2+} level was more pronounced than in roots and other treatments. The concentrations of Mg^{2+} in leaves were also decreased significantly in ABA treatments (Fig 4F).

Accumulation, but not radial distribution, of cations in root cells declines in response to salinity

Restricting the radial movement of ions across the root greatly reduces the amounts loaded into xylem for delivery to upper tissues. Therefore, distribution of ions radially from outer cortex to the endodermis (denominated cortex) and the inner vascular cells of roots were analyzed by SEM-EDX (Fig 5). Root samples from salt treated plants as well as control plant were compared (Fig 5). Elemental analysis in cortex and vascular cells of fine roots revealed that relative levels of Na^+, K^+, Ca^{2+} and Mg^{2+} did not significantly vary between cortex and vasculature under any of the observed treatments (Table 1). In contrast, relative concentrations of Cl^- were moderately decreased in vascular cells compared to the cortex in response to salt stress. The relative accumulation of Na^+ and Cl^- in both cells were increased in the presence of high and low salt stress and the increases were greater in high salt stress than in low salt stress (Table 1). In contrast, the relative concentration of K^+ decreased significantly in both cortex and vascular cells in response to high and low salt exposure but the response was less pronounced for low than for high salt stress (Table 1). Ca^{2+} levels showed similar decreases, regardless of high or mild salt treatments (Table 1). Mg^{2+} levels were unaffected by any salt treatments (Table 1). The distribution of other elements (S, P and Mn) between the cortex and vascular system and their responses to salinity are shown in S6 Table.

Discussion

Salinity and ABA decreases gas exchange which eventually exerts negative effects on the growth of plant

As an immediate response to osmotic stress caused by salinity, stomatal aperture decreases in salt stressed plants [1]. Decrease in stomatal opening eventually reduces CO_2 diffusion from the atmosphere to the site of carboxylation which is an immediate cause for decreased photosynthesis under salt stress [30]. In the present study, significant reduction in stomatal
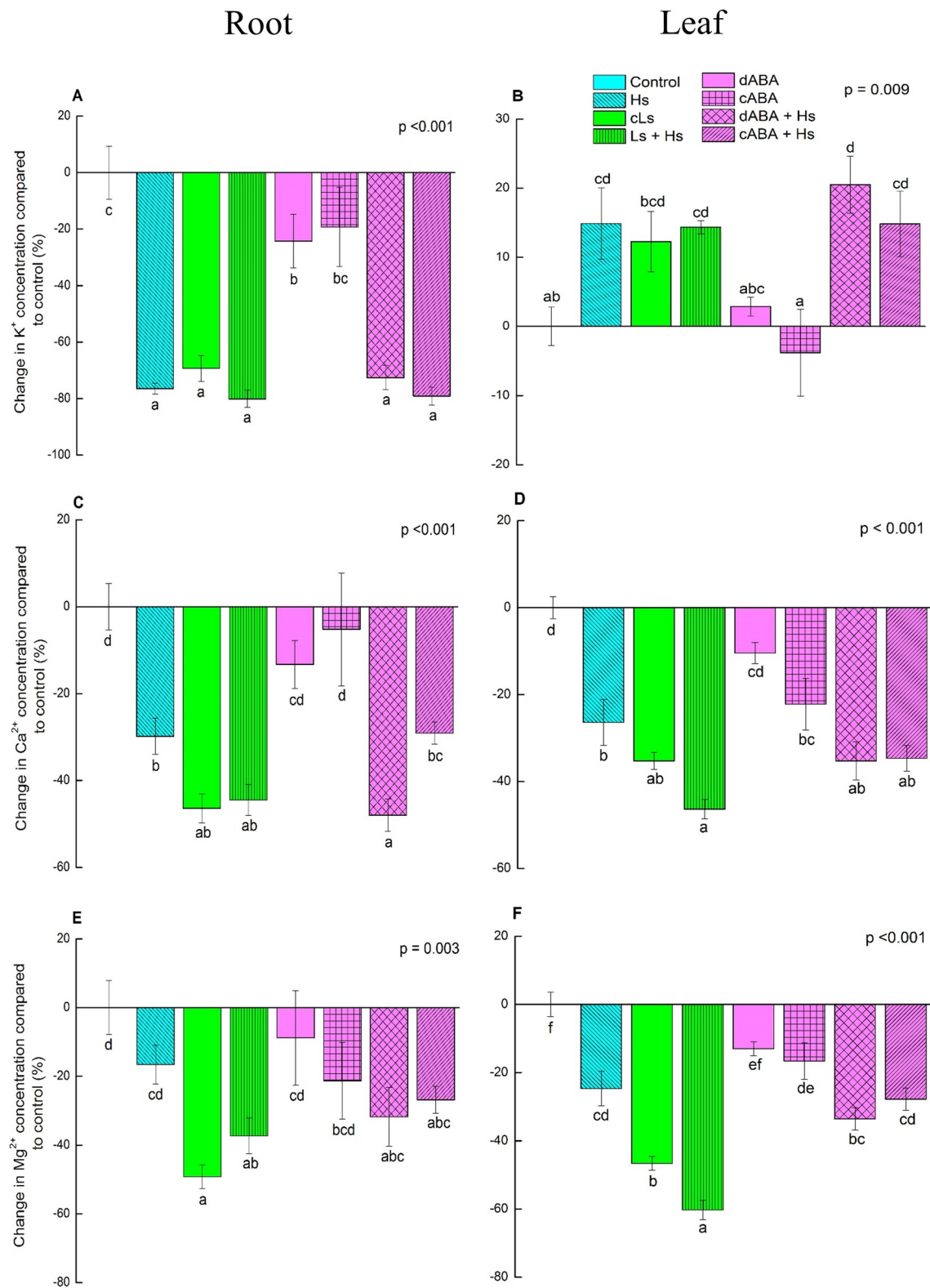
98

Fig 4. Changes in the concentration of most abundant cations (K$^+$, Ca^{2+} and Mg^{2+}) in root and leaf tissues in response to salinity and ABA. Graph A, C and E represent the changes in K$^+$, Ca^{2+} and Mg^{2+} concentrations respectively compared to control in roots. Graph B, D and F represent the changes in K$^+$, Ca^{2+} and Mg^{2+} concentrations respectively compared to control in leaves. In case of respective ion, mean value of controls was subtracted from each treatment value and then % change compared to control condition

was calculated. Bar represents means ± SE (n = 5 or 10). For statistical analysis, all treatment values got after subtracting mean value of control were subjected for one-way ANOVA. Different letters obtained from Fisher's test indicate significant differences among treatments at $p < 0.05$.

conductance was observed in response to high and low salt exposure which eventually reduced net CO_2 assimilation for photosynthesis and subsequent water loss via transpiration. Decreased gas exchange was also found in response to ABA with no salt exposure, since ABA promotes stomatal closure [31].

Significant decline in shoot height and stem diameter increment in high salt stressed plants in this study was most likely a result of reduced carbon fixation due to very low photosynthesis. Moderate reduction in photosynthesis found under low salt exposure negatively affected shoot growth as well. But the decrease in gas exchange in response to ABA treatment did not affect stem elongation significantly. However, whole-plant leaf area was negatively affected by both salt and ABA treatments. Decreased leaf size in response to salt and ABA contributed to the reduction of whole-plant leaf area here. Leaf shedding is a water-stress avoidance strategy in plants [32, 33], and is controlled by the interplay of phytohormones, including ABA [33, 34]. Besides, ABA is also involved in other morphological changes for acclimation to low water availability such as decreased shoot growth, leaf size and increased root growth [35–37]. Since the root to shoot ratio increased and loss of leaf biomass was not significant in the present study, the negative effect of salt and ABA on whole-plant biomass was moderate.

Leaf K^+ level is maintained under salt stress, whereas leaf Ca^{2+} and Mg^{2+} levels are reduced by the influence of transpiration

Accumulated Na^+ in root and leaf tissues in response to high and low salt stress eventually increased the total cation concentrations. Overall, leaves contained higher cation
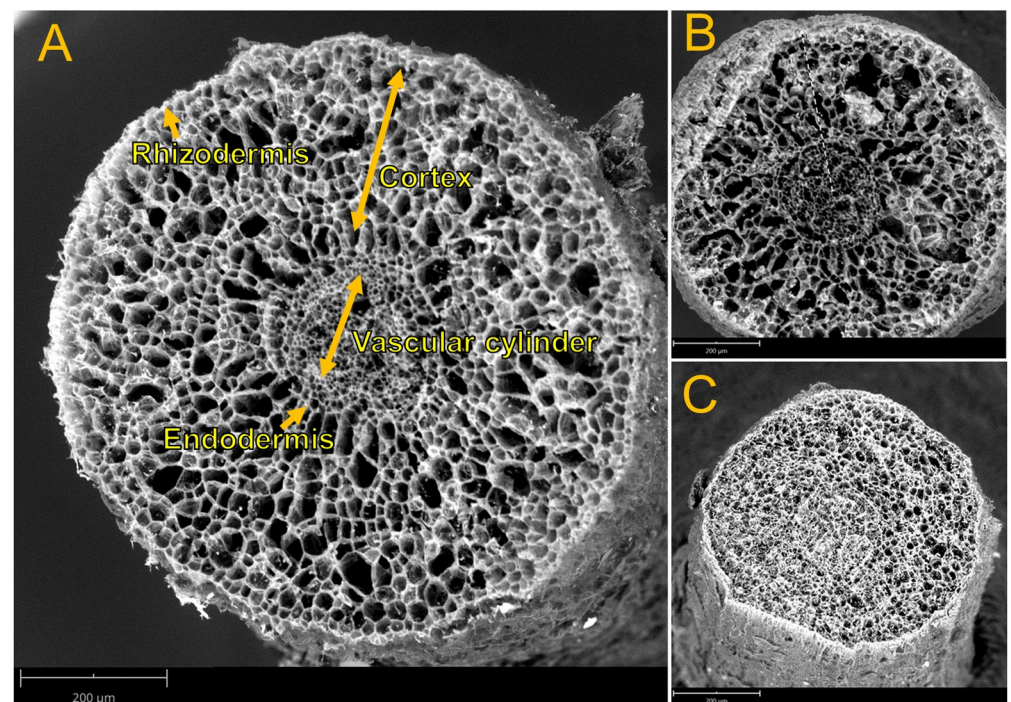
Fig 5. SEM imaging of *P. × canescens* root. Cross section (A) showing different cell layers in root. Sections of root from 100 mM NaCl treated plant (B) as well as control plant (C) are presented. Bars = 200 μm.

100

Table 1. Relative concentration of Na, K, Ca, Mg and Cl in the cortex and the vascular tissues of root of *P.* × *canescens* from EDX analysis.

Tissue	Treatment	Relative element concentration (weight %)				
		Na	K	Ca	Mg	Cl
Cortex	Control	5.59 ± 0.65 a	49.91 ± 4.02 c	8.08 ± 0.33 b	7.59 ± 0.47 abc	3.57 ± 0.41 a
	Hs	31.65 ± 4.29 d	14.91 ± 4.60 a	4.84 ± 0.27 a	6.79 ± 0.43 abc	10.06 ± 0.73 bc
	cLs	20.18 ± 3.93 bc	35.59 ± 4.79 b	5.66 ± 1.15 a	4.96 ± 1.46 a	12.01 ± 1.89 cde
	Ls + Hs	32.26 ± 3.77 d	19.70 ± 3.74 a	4.46 ± 0.57 a	5.44 ± 1.75 ab	12.42 ± 1.45 cde
	cABA + Hs	35.77 ± 4.08 d	16.96 ± 5.38 a	3.98 ± 0.41 a	4.85 ± 1.23 a	15.08 ± 2.32 e
Vascular tissue	Control	5.60 ± 0.39 a	49.52 ± 3.72 c	7.80 ± 0.34 b	8.00 ± 0.40 c	3.45 ± 0.39 a
	Hs	28.38 ± 4.32 cd	13.96 ± 4.48 a	4.94 ± 0.36 a	7.36 ± 0.33 bc	8.94 ± 0.32 b
	cLs	19.98 ± 3.59 b	34.43 ± 4.47 b	4.97 ± 1.25 a	5.35 ± 1.40 abc	9.89 ± 1.44 bc
	Ls + Hs	29.88 ± 4.24 d	18.71 ± 3.52 a	4.46 ± 0.50 a	5.76 ± 1.66 abc	10.50 ± 0.36 bcd
	cABA + Hs	34.04 ± 3.16 d	15.85 ± 4.73 a	3.97 ± 0.25 a	5.78 ± 1.61 abc	13.54 ± 2.33 de
p-value	p(treatment)	<0.001	<0.001	<0.001	0.009	<0.001
	p(tissue)	0.38	0.74	0.61	0.44	0.03
	p(treatment × tissue)	0.99	0.999	0.92	0.999	0.98

Data represent mean ± SE (n = 3 or 4) (four measurements were taken from each plant). Two—way ANOVA was conducted for each element with treatment and tissue as two main factors. Beta regression model was used for ANOVA and homogenous subsets were found using Fisher´s test. Different lowercase letters in the column of specific element for both tissues indicate significant differences among treatments at p <0.05.

https://doi.org/10.1371/journal.pone.0253228.t001

concentrations than roots under any stress conditions compared to non-stressed plants. The increased concentration may be necessary to maintain water uptake by decreasing osmotic pressure [38]. The decrease in root K^+ under salinity is most likely the outcome of competition between K^+ and Na^+ for uptake [38–40]. Na^+ competes with K^+ for the binding site of high affinity (KUP and HKT) K^+ channels as well as low affinity non-selective cation channels [41, 42]. Moreover, Na^+ influx into the cells leads to membrane depolarization resulting in leakage in voltage-gated outward-rectifying channels which leads to K^+ loss [43]. However, this reduction of K^+ content in the root has no effect on the radial transport towards the central cylinder as we did not observe any restriction in radial translocation of K^+ from cortex to vascular cells in the root under salt stress. This suggests that xylem loading of K^+ was unaffected [44]. The dramatic reduction in K^+ content in the roots did not negatively affect the K^+ content in leaves. K^+ even increased under salt stress conditions in leaves in our study. Maintaining or elevating K^+ levels in leaves is a known mechanism of halophytic plants [45] and has been reported for wheat, barley [46, 47] as well as in earlier studies for *P.* x *canescens* [19] and *P. tomentosa* [21]. Thus, we may speculate that a high leaf K^+ level is an evolutionary conserved mechanism of plants to acclimate to salt stress.

In contrast, salt exposure caused reduced concentrations of Ca^{2+} and Mg^{2+} in roots as well as in leaves, indicating a clear difference between K^+ on the one hand and Ca^{2+}/Mg^{2+}, when it comes to the translocation of these elements from the root to the shoot. ABA treatment in the absence of salt did not alter Ca^{2+} and Mg^{2+} levels in roots, but lead to a significant reduction in leaves. This observation implies that ABA did not have any negative effect on influx of Ca^{2+} and Mg^{2+} into roots, but had negative effects on the transport from root to shoot. It is known that Ca^{2+} is relatively immobile within the plant and supply to the young tissues is strongly dependent on the current acquisition from the growth medium via transpiration stream [48–50]. Moreover, both Ca^{2+} and Mg^{2+} contents in the shoots of barley seedlings (*Hordeum vulgare*) were reduced due to a decrease in transpiration rate [51]. Therefore, it is highly likely that ABA induced decrease in transpiration rate was a reason for decreased translocation of Ca^{2+} and Mg^{2+} from root to shoot resulting in reduced leaf content of these two elements.

Moreover, reduction in leaf Ca^{2+} level in ABA treated plants (cABA, -22%) was as strong as in high salt stress (Hs, -26%), although transpiration rate was comparatively higher in ABA treatments. This phenomenon suggests a strong influence of transpiration on the ion transport to the leaves under salinity. Since salt exposure increases ABA levels in the plant [13, 14, 18, 19], participation of ABA in the transpiration-based ion transport reduction might also exist in the salt treatments. Although we cannot exclude an influence of our treatments on the transport systems for these cations, our findings indicate that lower transpiration rate induced by salinity plays role in the suppression of Ca^{2+} and Mg^{2+} transport to the leaves.

In summary, reduced transpiration under salinity did not decrease the accumulation of Na^+ or K^+ in leaves, suggesting a rather transpiration independent translocation to the leaves. Ca^{2+} and Mg^{2+} levels in leaves under salt stress were at least partially dependent on reduced transpiration rate. Therefore, the present study suggests that the influence of transpiration on foliar accumulation of nutrients in *P.* × *canescens* under salinity is rather modest.

Supporting information

S1 Fig. Flow diagram showing the experimental design. *P.* × *canescens* plants (n = 94) were obtained by micropropagation and then those were grown in hydroponic culture. After five weeks of growth, treatment application was initiated and it was done in two phases: pretreatment and stress. For pretreatment, all plants were divided to grow under three different conditions:–(a) control, (b) 25 mM NaCl and (c) 50 μM ABA. After three weeks of pretreatment, groups were further divided into total 8 treatment groups (each having 9 to10 plants) to stress with NaCl (25 mM or 100 mM) and ABA in different combinations. Plants were treated for three weeks during stress phase. Abbreviated form of each treatment name is given below the respective treatment.
(TIF)

S1 Table. Leaf size, leaf biomass loss and root to shoot ratio of *P.* × *canescens* plants under different treatments. Values represent means ± SE (n = 9 or 10; except 7 or 8 in case of leaf size). One-way ANOVA was conducted for each parameter. Normal distribution of data was tested by plotting residuals. Different letters obtained from Fisher's test indicate significant differences among treatments at p <0.05.
(DOCX)

S2 Table. Concentration of different elements measured in the root of *P.* × *canescens* plant grown under different treatments. Values represent means ± SE (n = 5 or 10). One-way ANOVA was conducted in case of each element. Normal distribution of data was tested by plotting residuals and log transformation (in case of K and Ca) or square root transformation (in case of Na) was used to meet these criteria. Homogeneous subsets were found after Fisher's test. Different lowercase letters in a column indicate significant differences at p <0.05.
(DOCX)

S3 Table. Ratios of Na/K, Na/Ca, Na/Mg, Na/Mn, Na/Fe, Na/P and Na/S in the root tissues of *P.* × *canescens* plant grown under different treatments. The ratio was calculated from concentration (mg g^{-1} dry mass) values of the elements. Values represent means ± SE (n = 5 or 10). One-way ANOVA was conducted in every case. Normal distribution of data was tested by plotting residuals and log transformation was used in each case, except Na/S where square root transformation was used to meet these criteria. Homogeneous subsets were found after Fisher's test. Different lowercase letters in a column indicate significant differences at p <0.05.
(DOCX)

102

S4 Table. Concentration of different elements measured in the leaf of *P.* × *canescens* plant grown under different treatments. Values represent means ± SE (n = 5 or 10). One-way ANOVA was conducted in case of each element. Normal distribution of data was tested by plotting residuals and log transformation was used for certain cases (Na and Fe) to meet these criteria. Homogeneous subsets were found after Fisher's test. Different lowercase letters in a column indicate significant differences at p <0.05.
(DOCX)

S5 Table. Ratios of Na/K, Na/Ca, Na/Mg, Na/Mn, Na/Fe, Na/P and Na/S of in the leaf tissue of *P.* × *canescens* plant grown under different treatments. The ratio was calculated from concentration (mg g^{-1} dry mass) values of the elements. Values represent means ± SE (n = 5 or 10). One-way ANOVA was conducted in every case. Normal distribution of data was tested by plotting residuals and log transformation was used in each case to meet these criteria. Homogeneous subsets were found after Fisher's test. Different lowercase letters in a column indicate significant differences at p <0.05.
(DOCX)

S6 Table. Relative concentration of Mn, S and P in the cortex and the vascular tissues of root of *P.* × *canescens* according to EDX analysis. Data represent mean ± SE (n = 3 or 4) (four measurements were taken from each plant). Two—way ANOVA was conducted for each element with treatment and tissue as two main factors. Beta regression model was used for ANOVA and homogenous subsets were found with Fisher's test. Different lowercase letters in the column of specific element for both tissues indicate significant differences among treatments at p <0.05.
(DOCX)

Acknowledgments

Author Contributions

Conceptualization: Andrea Polle, Christian Eckert.

Data curation: Shayla Sharmin, Andrea Polle, Christian Eckert.

Formal analysis: Shayla Sharmin.

Investigation: Shayla Sharmin, Ulrike Lipka.

Methodology: Ulrike Lipka.

Project administration: Andrea Polle.

Supervision: Andrea Polle, Christian Eckert.

Writing – original draft: Shayla Sharmin.

Writing – review & editing: Andrea Polle, Christian Eckert.

References

1. Munns R, Tester M. Mechanisms of salinity tolerance. Annual Review of Plant Biology. 2008; 59: 651–681. https://doi.org/10.1146/annurev.arplant.59.032607.092911 PMID: 18444910

103

2. Polle A, Chen S. On the salty side of life: molecular, physiological and anatomical adaptation and acclimation of trees to extreme habitats. Plant, Cell & Environment. 2015; 38: 1794–1816. https://doi.org/10.1111/pce.12440 PMID: 25159181

3. US Salinity Laboratory. Diagnosis and improvement of saline and alkali soils. Agriculture Handbook No. 60. Washington DC: U.S. Government Printing Office; 1954.

4. Munns R. Genes and salt tolerance: bringing them together. New Phytologist. 2005; 167: 645–663. https://doi.org/10.1111/j.1469-8137.2005.01487.x PMID: 16101905

5. Deinlein U, Stephan AB, Horie T, Luo W, Xu G, Schroeder JI. Plant salt-tolerance mechanisms. Trends in plant science. 2014; 19: 371. https://doi.org/10.1016/j.tplants.2014.02.001 PMID: 24630845

6. Maathuis FJM. Sodium in plants: perception, signalling, and regulation of sodium fluxes. J Exp Bot. 2014; 65: 849–858. https://doi.org/10.1093/jxb/ert326 PMID: 24151301

7. Horie T, Karahara I, Katsuhara M. Salinity tolerance mechanisms in glycophytes: An overview with the central focus on rice plants. Rice. 2012; 5. https://doi.org/10.1186/1939-8433-5-11 PMID: 27234237

8. Shahzad M, Witzel K, Zörb C, Mühling KH. Growth-related changes in subcellular ion patterns in maize leaves (*Zea mays* L.) under salt stress. Journal of Agronomy and Crop Science. 2012; 198: 46–56. https://doi.org/10.1111/j.1439-037X.2011.00487.x

9. Loupassaki MH, Chartzoulakis KS, Digalaki NB, Androulakis II. Effects of salt stress on concentration of nitrogen, phosphorus, potassium, calcium, magnesium, and sodium in leaves, shoots, and roots of six olive cultivars. Journal of Plant Nutrition. 2002; 25: 2457–2482. https://doi.org/10.1081/PLN-120014707

10. Thu TTP, Yasui H, Yamakawa T. Effects of salt stress on plant growth characteristics and mineral content in diverse rice genotypes. Soil Science and Plant Nutrition. 2017; 63: 264–273. https://doi.org/10.1080/00380768.2017.1323672

11. Smith JAC. Ion transport and the transpiration stream. Botanica Acta. 1991; 104: 416–421. https://doi.org/10.1111/j.1438-8677.1991.tb00252.x

12. Pitman MG. Transpiration and the selective uptake of potassium by barley seedlings (*Hordeum vulgare* cv. bolivia). Aust Jnl Of Bio Sci. 1965; 18: 987–998. https://doi.org/10.1071/bi9650987

13. Chen S, Li J, Wang S, Hüttermann A, Altman A. Salt, nutrient uptake and transport, and ABA of *Populus euphratica*; a hybrid in response to increasing soil NaCl. Trees. 2001; 15: 186–194. https://doi.org/10.1007/s004680100091

14. Chen S, Li J, Wang T, Wang S, Polle A, Hüttermann A. Osmotic stress and ion-specific effects on xylem abscisic acid and the relevance to salinity tolerance in poplar. J Plant Growth Regul. 2002; 21: 224–233. https://doi.org/10.1007/s00344-002-1001-4

15. Popko J, Hänsch R, Mendel R-R, Polle A, Teichmann T. The role of abscisic acid and auxin in the response of poplar to abiotic stress. Plant Biology. 2010; 12: 242–258. https://doi.org/10.1111/j.1438-8677.2009.00305.x PMID: 20398232

16. Daszkowska-Golec A, Szarejko I. Open or close the gate–stomata action under the control of phytohormones in drought stress conditions. Front Plant Sci. 2013; 4. https://doi.org/10.3389/fpls.2013.00138 PMID: 23717320

17. Pantin F, Monnet F, Jannaud D, Costa JM, Renaud J, Muller B, et al. The dual effect of abscisic acid on stomata. New Phytologist. 2013; 197: 65–72. https://doi.org/10.1111/nph.12013 PMID: 23106390

18. Chen S, Li J, Wang T, Wang S, Polle A, Hüttermann A. Gas exchange, xylem ions and abscisic acid response to Na^+ -salts and Cl^- -salts in *Populus euphratica*. Acta Botanica Sinica. 2003; 561–566.

19. Escalante-Pérez M, Lautner S, Nehls U, Selle A, Teuber M, Schnitzler J-P, et al. Salt stress affects xylem differentiation of grey poplar (*Populus* × *canescens*). Planta. 2009; 229: 299–309. https://doi.org/10.1007/s00425-008-0829-7 PMID: 18946679

20. Hu Y, Schmidhalter U. Drought and salinity: a comparison of their effects on mineral nutrition of plants. Journal of Plant Nutrition and Soil Science. 2005; 168: 541–549. https://doi.org/10.1002/jpln.200420516

21. Chen S, Li J, Wang S, Fritz E, Hüttermann A, Altman A. Effects of NaCl on shoot growth, transpiration, ion compartmentation, and transport in regenerated plants of *Populus euphratica* and *Populus tomentosa*. Canadian Journal of Forest Research. 2003; 33: 967–975. https://doi.org/10.1139/x03-066

22. Zekri M, Parsons LR. Salinity tolerance of citrus rootstocks: effects of salt on root and leaf mineral concentrations. Plant and Soil. 1992; 147: 171–181. https://doi.org/10.1007/BF00029069

23. Ruiz D, Martinez V, Cerda A. Citrus response to salinity: growth and nutrient uptake. Tree Physiology. 1997; 17: 141–150. https://doi.org/10.1093/treephys/17.3.141 PMID: 14759868

24. Mickelbart MV, Melser S, Arpaia ML. Salinity-induced changes in ion concentrations of 'hass' avocado trees on three rootstocks. Journal of Plant Nutrition. 2007; 30: 105–122. https://doi.org/10.1080/01904160601055137

25. Erturk U, Sivritepe N, Yerlikaya C, Bor M, Ozdemir F, Turkan I. Responses of the cherry rootstock to salinity *in vitro*. Biologia plantarum. 2007; 51: 597–600. https://doi.org/10.1007/s10535-007-0132-7

26. Leplé J, Brasileiro A, Michel M, Delmotte F, Jouanin L. Transgenic poplars: expression of chimeric genes using four different constructs. Plant Cell Reports. 1992; 11: 137–141. https://doi.org/10.1007/BF00232166 PMID: 24213546

27. Murashige T, Skoog F. A revised medium for rapid growth and bio assays with tobacco tissue cultures. Physiologia Plantarum. 1962; 15: 473–497. https://doi.org/10.1111/j.1399-3054.1962.tb08052.x

28. Müller A, Volmer K, Mishra-Knyrim M, Polle A. Growing poplars for research with and without mycorrhizas. Front Plant Sci. 2013; 4: 332. https://doi.org/10.3389/fpls.2013.00332 PMID: 23986772

29. Jehl B, Bauer R, Dörge A, Rick R. The use of propane/isopentane mixtures for rapid freezing of biological specimens. Journal of Microscopy. 1981; 123: 307–309. https://doi.org/10.1111/j.1365-2818.1981.tb02475.x PMID: 7299814

30. Centritto M, Loreto F, Chartzoulakis K. The use of low [CO_2] to estimate diffusional and non-diffusional limitations of photosynthetic capacity of salt-stressed olive saplings. Plant, Cell & Environment. 2003; 26: 585–594. https://doi.org/10.1046/j.1365-3040.2003.00993.x

31. Mittelheuser CJ, Van Steveninck RFM. Stomatal closure and inhibition of transpiration induced by (RS)-abscisic acid. Nature. 1969; 221: 281–282. https://doi.org/10.1038/221281a0

32. Polle A, Chen SL, Eckert C, Harfouche A. Engineering drought resistance in forest trees. Front Plant Sci. 2019; 9: 1875. https://doi.org/10.3389/fpls.2018.01875 PMID: 30671067

33. Munné-Bosch S, Alegre L. Die and let live: leaf senescence contributes to plant survival under drought stress. Functional Plant Biol. 2004; 31: 203–216. https://doi.org/10.1071/FP03236 PMID: 32688892

34. Chen S, Wang S, Hüttermann A, Altman A. Xylem abscisic acid accelerates leaf abscission by modulating polyamine and ethylene synthesis in water-stressed intact poplar. Trees. 2002; 16: 16–22. https://doi.org/10.1007/s00468-001-0138-2

35. Arend M, Schnitzler J-P, Ehlting B, Hänsch R, Lange T, Rennenberg H, et al. Expression of the Arabidopsis mutant *abi1* gene alters abscisic acid sensitivity, stomatal development, and growth morphology in gray poplars. Plant Physiology. 2009; 151: 2110–2119. https://doi.org/10.1104/pp.109.144956 PMID: 19837818

36. Sharp RE, Poroyko V, Hejlek LG, Spollen WG, Springer GK, Bohnert HJ, et al. Root growth maintenance during water deficits: physiology to functional genomics. J Exp Bot. 2004; 55: 2343–2351. https://doi.org/10.1093/jxb/erh276 PMID: 15448181

37. Yu D, Wildhagen H, Tylewicz S, Miskolczi PC, Bhalerao RP, Polle A. Abscisic acid signalling mediates biomass trade-off and allocation in poplar. New Phytologist. 2019; 223: 1192–1203. https://doi.org/10.1111/nph.15878 PMID: 31050802

38. Hasegawa PM, Bressan RA, Zhu J-K, Bohnert HJ. Plant cellular and molecular responses to high salinity. Annual Review of Plant Physiology and Plant Molecular Biology. 2000; 51: 463–499. https://doi.org/10.1146/annurev.arplant.51.1.463 PMID: 15012199

39. Grattan SR, Grieve CM. Mineral element acquisition and growth response of plants grown in saline environments. Agriculture, Ecosystems & Environment. 1992; 38: 275–300. https://doi.org/10.1016/0167-8809(92)90151-Z

40. Hirsch RE, Lewis BD, Spalding EP, Sussman MR. A Role for the AKT1 Potassium Channel in Plant Nutrition. Science. 1998; 280: 918–921. https://doi.org/10.1126/science.280.5365.918 PMID: 9572739

41. Wang M, Zheng Q, Shen Q, Guo S. The critical role of potassium in plant stress response. International Journal of Molecular Sciences. 2013; 14: 7370–7390. https://doi.org/10.3390/ijms14047370 PMID: 23549270

42. Mian A, Oomen RJFJ, Isayenkov S, Sentenac H, Maathuis FJM, Véry A-A. Over-expression of an Na^+- and K^+-permeable HKT transporter in barley improves salt tolerance. Plant J. 2011; 68: 468–479. https://doi.org/10.1111/j.1365-313X.2011.04701.x PMID: 21749504

43. Chen Z, Newman I, Zhou M, Mendham N, Zhang G, Shabala S. Screening plants for salt tolerance by measuring K^+ flux: a case study for barley. Plant, Cell & Environment. 2005; 28: 1230–1246. https://doi.org/10.1111/j.1365-3040.2005.01364.x

44. Wu H, Zhang X, Giraldo JP, Shabala S. It is not all about sodium: revealing tissue specificity and signalling roles of potassium in plant responses to salt stress. Plant Soil. 2018; 431: 1–17. https://doi.org/10.1007/s11104-018-3770-y

45. Percey WJ, Shabala L, Wu Q, Su N, Breadmore MC, Guijt RM, et al. Potassium retention in leaf mesophyll as an element of salinity tissue tolerance in halophytes. Plant Physiology and Biochemistry. 2016; 109: 346–354. https://doi.org/10.1016/j.plaphy.2016.10.011 PMID: 27810674

46. Wu H, Shabala L, Barry K, Zhou M, Shabala S. Ability of leaf mesophyll to retain potassium correlates with salinity tolerance in wheat and barley. Physiologia Plantarum. 2013; 149: 515–527. https://doi.org/10.1111/ppl.12056 PMID: 23611560

47. Wu H, Zhu M, Shabala L, Zhou M, Shabala S. K$^+$ retention in leaf mesophyll, an overlooked component of salinity tolerance mechanism: A case study for barley. Journal of Integrative Plant Biology. 2015; 57: 171–185. https://doi.org/10.1111/jipb.12238 PMID: 25040138

48. White PJ, Broadley MR. Calcium in plants. Annals of Botany. 2003; 92: 487–511. https://doi.org/10.1093/aob/mcg164 PMID: 12933363

49. Biddulph O, Cory R, Biddulph S. Translocation of calcium in the bean plant. Plant Physiol. 1959; 34: 512–519. https://doi.org/10.1104/pp.34.5.512 PMID: 16655264

50. Hanger BC. The movement of calcium in plants. Communications in Soil Science and Plant Analysis. 1979; 10: 171–193. https://doi.org/10.1080/00103627909366887

51. Lazaroff N, Pitman MG. Calcium and magnesium uptake by barley seedlings. Aust Jnl Of Bio Sci. 1966; 19: 991–1006. https://doi.org/10.1071/bi9660991

106

Chapter 5: Overall conclusion and outlook

As stated earlier, the understanding of the tactics of salt tolerant plant to cope with saline environments will assist in the better management of salt-affected lands. That is why in this thesis, I explored the strategies of the salt tolerant *P. euphratica* in response to salinity by investigating the morphological adaptations, salt and nutrient accumulation, physiological and molecular responses under salt stress.

I found that, *P. euphratica* undergoes changes in root morphology in response to salinity. The roots of *P. euphratica* became thicker when plants were exposed to high salinity for long-term. The first order root (main root) of *P. euphratica* showed almost two-fold increase in diameter under salinity than control thin roots after long-term salt exposure. The lateral roots showed thickening as well after long-term salt exposure, but in less magnitude than main roots. The increased number of cortex cells which was observed in the thick main roots may provide *P. euphratica* more room to store salt ion and possibly to dilute salt. The increased thickness of main roots accompanied by increased internal Na levels after long-term salt exposure indicated that thickening was likely induced by salt accumulation. It was shown that the dry-to-fresh mass ratio of thick main roots and control thin roots did not differ significantly, but there was a tendency of decrease in the dry-to-fresh mass ratio of thick main roots after long-term salt exposure. Moreover, significant increase in water content in thick roots was observed compared to thin roots considering only long-term salt exposure time (chapter 3). Therefore, it could be that the effect of 12 days exposure to 150 mM NaCl was at the threshold level to develop succulence in the thick roots which needs to be experimentally validated.

It was shown that salt-induced thick roots contribute to salt tolerance of *P. euphratica* by reducing Na^+ acquisition and Na^+ release out of the cell under salinity. High transcript abundances for Na^+/H^+ antiporter system (*SOS1*, *NHX*, *NhaD* and *ATPases*), which control Na^+ levels, was observed in both thin and thick roots. Less additional activation in the Na^+ level regulating systems under salinity indicated the constant readiness of *P. euphratica* towards changes in soil salinity. Transcriptional analyses also suggested that *P. euphratica* roots can retain K^+ levels under salinity by restricting K^+ loss and redistributing internally.

In *P. euphratica*, gas exchange was reduced in response to salinity. But after getting adapted to high salinity, *P. euphratica* showed the ability to recover CO_2 assimilation. Although the supply of CO_2 from outside was reduced due to decreased stomatal conductance, *P. euphratica* consumed intercellular CO_2 with more efficiency and increased photosynthesis rate. In salt-susceptible poplar *P. × canescens*, gas exchange was decreased strongly when plants were exposed to high salt (100 mM NaCl) after low salt pretreatment. Application of ABA also decreased gas exchange in this species by promoting stomatal closure. High salt exposure caused increase in Na content in roots and leaves of *P. × canescens.* In the context of nutrient accumulation under salinity, *P. euphratica* showed greater performance. In *P. euphratica* and *P. × canescens*, leaf K^+ levels were maintained under salt stress, whereas root K^+ levels were reduced. Thus, maintaining high leaf K^+ levels in leaves in response to salinity may be an evolutionary conserved mechanism of these species. Ca^{2+} and Mg^{2+} levels were reduced in roots and leaves in *P. × canescens* under salinity. ABA treatment without salt reduced Ca^{2+} and Mg^{2+} levels in *P. × canescens* leaves without causing significant reduction in root levels. Therefore, the reduced translocation of Ca^{2+} and Mg^{2+} to the *P. × canescens* leaves under ABA treatment indicated the influence of decreased transpiration on the leaf supply of these cations. However, *P. euphratica* maintained the leaf levels of Ca^{2+} and Mg^{2+} under salinity, though stomatal conductance and transpiration was reduced significantly. Besides, increased P and Fe contents were observed in the high salt-acclimated thick roots compared to non-acclimated (in chapter 2) or low salt-acclimated thin roots (chapter 3) of *P. euphratica*. The investigation on the physiological importance of this results would be interesting. The transcriptome analysis revealed several genes that participate in the salt tolerance strategies of *P. euphratica.* There is a worthy chance that among these genes, some could function as marker genes for salt tolerance in trees and based on this marker genes, a preselection of individuals can be made that are more fit for planting in salt-affected lands. In addition, it needs to be studied if other plant species produce thicker roots under salinity and if this trait can also be exploited as a criterion to select salt tolerant plant.

Acknowledgments

Curriculum Vitae

Personal Information:

Name: Shayla Sharmin
Date of birth: 31.05.1988
Place of birth: Chandpur, Bangladesh
Nationality: Bangladeshi

Education and work experiences

2016 - 2021   PhD student, Doctoral degree programme "Forest Sciences and
                   Forest Ecology",
                   Department of Forest Botany and Tree Physiology, University of
                   Göttingen, Germany
                   Dissertation: Physiological, morphological and molecular
                   acclimation of *Populus* spp. to high salinity

2014 - 2021   Assistant Professor, Department of Biochemistry and Molecular
                   Biology, Bangladesh Agricultural University, Mymensingh-2202,
                   Bangladesh

2012- 2014   Lecturer, Department of Biochemistry and Molecular Biology,
                   Bangladesh Agricultural University, Mymensingh-2202,
                   Bangladesh

2011 - 2012   Master of Science (M.S.) in Biochemistry,
                   Department of Biochemistry and Molecular Biology, Bangladesh
                   Agricultural University, Mymensingh-2202, Bangladesh

                   Thesis title: Saline induced changes in growth parameters,
                   enzymatic activity and free amino acid content of rice (*Oryza
                   sativa*) plant

2007 - 2010   Bachelor of Science in Agriculture (Honours),
                   Bangladesh Agricultural University, Mymensingh-2202,
                   Bangladesh

2004 - 2006   Higher Secondary Certificate (H.S.C)

B C I C college, Mirpur, Dhaka, Bangladesh

1999 - 2004   Secondary School Certificate (S.S.C)
                       B C I C college, Mirpur, Dhaka, Bangladesh

1994- 1998   Primary School
                       Chiriakhana Botanical High School, Mirpur, Dhaka, Bangladesh